Prepared for submission to JHEP MIT-CTP/5958

Classifying Fibers and Bases in Toric Hypersurface Calabi-Yau Threefolds

Fatima Abbasi, Richard Nally, and Washington Taylor

Center for Theoretical Physics
Department of Physics
Massachusetts Institute of Technology
77 Massachusetts Avenue
Cambridge, MA 02139, USA

E-mail: fabbasi at mit.edu, rnally at mit.edu, wati at mit.edu

Abstract: We carry out a complete analysis of the toric elliptic and genus-one fibrations of all 474 million reflexive polytopes in the Kreuzer-Skarke database. Earlier work with Huang showed that all but 29,223 of these polytopes have such a fibration. We identify 2,264,992,252 distinct fibrations, and determine the fiber and base structure in each case; after accounting for automorphisms of the ambient polytope, these fibrations furnish 2,250,744,657 equivalence classes. We summarize generic features and identify exotic special cases among these fibrations. These fibrations illustrate many features that have been explored in the context of 6D F-theory, including gauge groups hosted on non-toric divisors, automatic enhancement of gauge groups, and implicit non-toric bases and high-rank 6D SCFTs associated with non-flat fibers, as well as novel geometric features such as singular bases for genus-one fibrations with multisections. This analysis illustrates the power of elliptic and genus-one fibrations, and the geometro-physical language of F-theory as a tool for understanding the structure of Calabi-Yau threefolds.

Contents

---

1 Introduction

Calabi-Yau manifolds have been a central subject of study in theoretical physics and in mathematics since the realization over 40 years ago that these spaces can be used to construct a variety of compactifications of string theory [1]. Despite a tremendous amount of work in this area, it remains unknown whether the number of distinct topological types of Calabi-Yau threefolds is finite or infinite. Nonetheless, an important class of Calabi-Yau threefolds are those that admit an elliptic or genus-one fibration, and it is known that there exist a finite number of topological types of such geometries [2, 3]. Elliptic Calabi-Yau manifolds play a central role in the approach to string theory known as F-theory [4–6], which connects the geometry of an elliptic Calabi-Yau to a physical theory of gravity, gauge fields, and matter. A systematic approach can in principle be taken to constructing and classifying all elliptic Calabi-Yau threefolds, by first classifying allowed bases and then classifying possible "tunings" of Weierstrass models over each base. While there are a number of technical complications and subtleties in realizing a complete enumerated classification using this approach, it is clear that combining physical insights from F-theory with the mathematical structure of elliptic fibrations gives a powerful set of tools and perspectives with which to analyze Calabi-Yau threefolds (and fourfolds). Moreover, in recent years a growing body of evidence has shown that most known Calabi-Yau manifolds have the form of an elliptic or genus-one fibration (or at least lie in an extended Kähler cone that has a chamber with such a fibration) [7–12], and there are general arguments for why this should be the case [13].

The largest known set of Calabi-Yau threefolds are the toric hypersurfaces in reflexive 4D polytopes [14]. A complete classification of the 473,800,776 reflexive 4D polytopes was made some time ago by Kreuzer and Skarke (KS) [15]. This represents the richest database of examples of Calabi-Yau threefolds available; it remains unclear, however, precisely how many distinct Calabi-Yau threefolds can be built from these polytopes [16–19].

Considering toric hypersurface Calabi-Yau threefolds from the perspective of elliptic fibrations can give a useful framework for systematically studying this large set of geometries. In previous work [20], Huang and one of the authors of this work showed that, of the 474 million reflexive 4D polytopes, all but 29,233 contain at least one reflexive 2D subpolytope, indicating that at least one flop phase of each of the associated Calabi-Yau threefolds has an elliptic (or genus-one) fibration structure. Almost 15 years ago, Braun [21] identified and classified all such toric elliptic fibrations over the simplest 2D base $\mathbb{P}^2$. In this work, we extend these earlier analyses by performing a complete classification of all 2D reflexive subpolytopes of 4D polytopes in the KS database, along with the 2D toric base polytopes to which the associated elliptic Calabi-Yau threefolds project along the fiber. In this paper, we summarize the results of this classification, including a statistical analysis of typical fibers and bases, along with an examination of some more exotic structures that are found in these fibrations. Data files containing the full results of the analysis, as well as the software used to do the analysis, are included in an associated Zenodo archive [22].

The structure of this paper is as follows: in §2, we review some known facts about toric fibers and bases for elliptic Calabi-Yau threefolds. In §3, we describe the algorithm and approach used to perform the complete analysis of fibrations in the KS database. In §4, we describe general features of the statistics of the 2.25 billion fiber/base pairs found in the analysis. In §5, we go into more detail on some interesting examples and features found in the analysis. §6 contains some concluding remarks.

2 Toric Bases, Fibers, and Fibrations

In this section, we recall some key background for our work. We begin with some general comments to provide perspective on how the analysis of this paper fits into the framework of a broader research agenda.

Two of the most powerful approaches known for constructing large classes of Calabi-Yau threefolds are: (a) as hypersurfaces (or, more generally, complete intersections) in toric varieties, (b) through elliptic (or, more generally, genus-one) fibrations. For (a), the KS database of 474 million polytopes provides the richest set of concrete examples of Calabi-Yau threefolds available, which has been used in many contexts in the physics and mathematics literature. For (b), the finite nature of the set of fibered CY threefolds, the fact that almost all known Calabi-Yau threefolds have an elliptic or genus-one-fibered phase, the possibility of direct construction through tuned Weierstrass models, and the geometric interpretation from F-theory make this a very powerful framework for understanding the structure of CY threefolds. The goal of this paper is to combine these perspectives and show that almost all of the many Calabi-Yau threefolds that can be constructed from polytopes in the Kreuzer-Skarke database live in families (defined by the extended Kähler cone) that contain an elliptic or genus-one fibered representative, and that this allows us to classify and understand the structure of these spaces.

One motivation for this work is to explore the range of possible fibration structures that arise in this large class of Calabi-Yau threefolds, and how they fit into the full set of possible F-theory models. A second motivation is to illustrate how the geometric/physical language of F-theory provides a powerful tool for understanding and identifying most known Calabi-Yau threefolds. In general, a toric hypersurface Calabi-Yau is defined by a suitable triangulation of one of the 474 million reflexive polytopes in the Kreuzer-Skarke list; as reviewed in e.g. [17, 18], such a geometry is characterized topologically as a real manifold by its "Wall data," consisting of its Hodge numbers, triple intersection numbers, and second Chern class, and as a complex manifold by its Mori cone. These data are somewhat opaque, in the sense that they do not convey much intuitive understanding of the structure of a given Calabi-Yau, or enable us to easily classify structures or connect related Calabi-Yau threefolds. On the other hand, the F-theory language for Calabi-Yau threefolds provides a rich set of insights into the structure of these varieties. In particular, from this perspective, rather than identifying an elliptic Calabi-Yau in terms of its Wall data and Mori cone, we can characterize it by features with physical and geometric significance; in this language, a given polytope may correspond to a family of Calabi-Yau threefolds organized into a toric extended Kähler cone that have several different fibered phases, each of which can be described in F-theory language as, e.g., an elliptic fibration over the base Hirzebruch $\mathbb{F}_3$, with a gauge factor SU(3) over the base curve of self-intersection -3 and a gauge factor E_6 tuned over the base curve of self-intersection $+3$. The latter geometric language provides a powerful framework for understanding not only the structure of individual Calabi-Yau threefolds, as fibration data reflects key information about the intersection numbers, Hodge numbers, and Mori cone of the Calabi-Yau, but also, because all elliptic Calabi-Yau threefolds are connected by a combination of geometric transitions with physical interpretation, provides a way of understanding how different Calabi-Yau threefolds are connected. These geometric transitions include tensor transitions corresponding to blowing up points in the base, Higgs transitions in which the Hodge number $h^{1,1}(X)$ decreases representing a reduction in the physical gauge group, and more obscure matter transitions [23], in which the gauge group and base structure remain invariant.

In the remainder of this section, we will introduce the background necessary to pursue those goals. Heuristically, an elliptic threefold is one that can be viewed as a torus varying over the points of a two-dimensional base; we begin in §2.1 with basic definitions of elliptic curves and elliptic fibrations to make this intuition precise before describing the toric technology we use throughout the paper. In §2.2 and §2.3, we describe the set of 61,539 toric bases and 16 toric fibers that serve as the building blocks for toric elliptic fibrations, which are described in §2.4. In §2.5, we clarify the distinction between genus-one fibered and elliptically fibered Calabi-Yau threefolds, and in §2.6, we describe Nagell's algorithm, a unified framework for analyzing the geometry of all elliptic and genus-one fibrations. We conclude in §2.7 with an overview of 6D F-theory, which essentially provides a dictionary between structures in 6D supergravity theories and the geometry of elliptic and genus-one fibrations.

2.1 Elliptic curves and elliptic fibrations

Fix a field F; we call a genus-one curve E defined over F an *elliptic curve* if it admits at least one point over F. This is because the points of E furnish a group under a geometrically defined addition law; any group must have an identity element, so to be an elliptic curve E must have at least one point. For instance, because by the adjunction formula quartic hypersurfaces in

$\mathbb{P}^{1,1,2}$ are Calabi-Yau onefolds, i.e. complex tori, the curve

$$x^4 + y^4 = z^2 \tag{2.1}$$

has genus one, but over the rational numbers $\mathbb{Q}$, this polynomial has no nonzero solutions, so its graph does not furnish an elliptic curve over $\mathbb{Q}$. It is a general fact that the geometry of an elliptic curve can be summarized in terms of two invariants, j and Δ. The distinguishing characteristic of the discriminant Δ is that E is smooth unless $\Delta = 0$, in which case we also necessarily have $j \to i\infty$.

Our primary interest is not in elliptic curves themselves, but rather in elliptic fibrations. We call a complex manifold X torus-fibered over a d-dimensional base B_d if there exists a map $\pi : X \to B_d$ such that the preimage of a generic point $b \in B_d$ is a torus. In analogy to the requirement that an elliptic curve has a point over its field of definition, we say that a torus-fibered manifold X is *elliptically fibered* if this fibration admits a section, and *genus-one fibered* if it does not. In fact, this is more than an analogy; an elliptic fibration can equivalently be viewed as an elliptic curve whose field of definition is the function field of B_d, with the group of points being realized by the group of sections of the fibration.

The geometry of elliptically fibered Calabi-Yau threefolds (CY3s) is strongly constrained. As summarized in the introduction, elliptic CY3s can in principle be systematically classified by first classifying all compact complex Kähler surfaces B_2 that can support an elliptic or genus-one fibered Calabi-Yau threefold, and then classifying all possible fibrations over each base. We review here briefly some aspects of this classification in the context of toric bases and toric hypersurface fibers. We focus first on elliptic fibrations; genus-one fibrations are defined and discussed in more detail in §2.5.

It is a classical fact, which we review in §2.6, that an elliptic fibration over a base B_2 can be described as a Weierstrass model

$$y^2 = x^3 + fx + g\,, \tag{2.2}$$

where f, g are sections of the line bundles $\mathcal{O}(-4K), \mathcal{O}(-6K)$, where $-K$ is the anticanonical class of the base. In terms of f and g, the discriminant Δ is given by

$$\Delta = -16\left(4f^3 + 27g^2\right). \tag{2.3}$$

Tuning f, g to vanish to various orders over curves (divisors) and points in the base thus gives singularities in the fibration. The codimension one singularities were classified by Kodaira [24]; when the orders of vanishing of (f, g) do not exceed $(4, 6)$, the singularity is associated with a Dynkin diagram and can be resolved to give a smooth elliptic Calabi-Yau threefold. A key insight of F-theory is that the Dynkin diagram associated with the singularity corresponds to the Lie algebra of the gauge group in the associated 6-dimensional supergravity theory [4–6, 25].

Over any base B_2, there are a finite number of distinct topological types of elliptic Calabi–Yau threefolds that can be "tuned" by choosing special values of the Weierstrass coefficients

Type	Singularity	ord(f)	ord(g)	ord(Δ)	Gauge algebra
I_0	$\emptyset$	≥ 0	≥ 0	0	$\emptyset$
I_0^*	D_4	≥ 2	≥ 3	6	$\mathfrak{so}(8)$, $\mathfrak{so}(7)$, or $\mathfrak{g}_2$
I_n	A_{n-1}	0	0	$n \geq 2$	$\mathfrak{su}(n)$ or $\mathfrak{sp}(\lfloor n/2 \rfloor)$
I_n^*	D_{n-2}	2	3	$n \geq 7$	$\mathfrak{so}(2n-4)$ or $\mathfrak{so}(2n-5)$
II	$\emptyset$	≥ 1	1	2	$\emptyset$
II^*	E_8	≥ 4	5	10	$\mathfrak{e}_8$
III	A_1	1	≥ 2	3	$\mathfrak{su}(2)$
III^*	E_7	3	≥ 5	9	$\mathfrak{e}_7$
IV	A_2	≥ 2	2	4	$\mathfrak{su}(2)$ or $\mathfrak{su}(3)$
IV^*	E_6	≥ 3	4	8	$\mathfrak{e}_6$ or $\mathfrak{f}_4$

Table 1: The Kodaira classification of singularities in elliptic fibrations. For each Kodaira class, we give the ADE type of the singular fiber, the orders to which f, g, and Δ vanish, and the possible nonabelian gauge algebras that the singularity can give rise to in F-theory. For the classes with more than one gauge algebra, additional monodromy information is needed to specify a gauge group.

f, g [3, 26]. Roughly, each such tuning corresponds to an algebraic subvariety of the full moduli space of Weierstrass models, and by the Hilbert Basis Theorem, there are a finite number of distinct such strata. In the language of F-theory, which we describe in further detail in §2.7, and as reviewed in e.g. [27], various physical features correspond to increasingly subtle aspects of the fibration. Nonabelian gauge groups are associated with codimension one singularities; to understand these gauge groups for 6D theories, one must generalize the Kodaira classification to include nontrivial monodromy for non-simply laced groups [25]. The vanishings that can appear in F-theory, i.e. those for which the orders of vanishing of (f, g) do not exceed $(4, 6)$, and their associated gauge algebras are listed in Table 1. Note that for any base that is not weak Fano, where there are curves of self-intersection $C \cdot C \leq -3$, the curvature of the normal bundle over such curves forces an automatic Kodaira singularity associated in the F-theory picture with a geometrically rigid non-Higgsable gauge group, or "non-Higgsable cluster" (NHC) [28]. Codimension two singularities encode local matter fields, and are relatively well understood, at least for matter charged under nonabelian gauge fields (see, e.g., [25, 29–31]). Global aspects of the fibration, in particular the Mordell-Weil group and Tate-Shafarevich/Weil-Chatalet groups, correspond to abelian U(1) and discrete gauge factors, respectively, and are not understood in a completely systematic way for either $\mathrm{U}(1)^k$ beyond $k = 2$ [32], or $\mathbb{Z}_m$ structures (see, e.g., [33] for recent progress in this direction).

2.2 Toric bases for elliptic Calabi-Yau threefolds

We next discuss the possible bases for toric elliptic fibrations. From [2, 3], it is known that all bases B_2 that support elliptic or genus-one fibered Calabi-Yau threefolds can be described as complex 2D projective space $\mathbb{P}^2$, Hirzebruch surfaces $\mathbb{F}_m$ with $m \leq 12$, blowups of one of these surfaces at one or more points, or the Enriques surface. For the Enriques surface, the anticanonical class of the base $-K$ is nonzero only up to torsion, and is of limited interest in this context, so we focus on the other cases.

Starting with $\mathbb{P}^2$ and $\mathbb{F}_m$, which are all toric, one can systematically blow up toric points in all possible ways in an iterative fashion, constrained by the condition that a curve C of self-intersection $C \cdot C \leq -13$ forces a Kodaira type $(4, 6)$ singularity in the fibration, which does not have a good resolution. Thus, bases containing such curves cannot support smooth elliptic Calabi-Yau threefolds, and the systematic blowup process must stop when such curves are encountered. In [34], this approach was used to construct a comprehensive list of 61,539 toric bases that support elliptic Calabi-Yau threefolds. It is natural to expect that this set corresponds to the set of bases found from toric projections of elliptic Calabi-Yau threefolds in the Kreuzer-Skarke database, and indeed we find that this is the case; every base in this list appears as the base of a fibration in the KS database, and all bases found from explicit elliptic fibrations in the database are either in this list or a blow-down of a base in the toric list. The singular cases with blowdowns are discussed further in §4.3.2.

Note that in constructing this list, any toric points where the Weierstrass coefficients f, g are forced to vanish to orders (4, 6) are blown up; such points can be interpreted in F-theory as corresponding to strongly coupled superconformal field theories (SCFTs) coupled to the 6D supergravity theory [35, 36]. However, some bases, particularly those containing curves of self-intersection $-9, -10, -11$ (such as, e.g., $\mathbb{F}_9, \mathbb{F}_{10}, \mathbb{F}_{11}$) contain non-toric (4, 6) points in generic Weierstrass models over these bases. We will discuss similar situations further in §5.3, where the SCFT appears only for certain fibrations over a base that does not force (4, 6) points in generic Weierstrass models; this can occur even for the simplest base $\mathbb{P}^2$. In all these cases, blowing up the (4, 6) point on the base, corresponding to going onto the tensor branch of the SCFT, gives a fibration over a non-toric base without the SCFT.

While there is not yet a complete list of all possible non-toric bases B_2 that support elliptic or genus-one fibered Calabi-Yau threefolds, some progress has been made in this direction. In [37], a complete list of 162,404 semi-toric bases, i.e. bases that are invariant under a single $\mathbb{C}^*$ action, was compiled. Moreover, in [38], Wang and one of the present authors systematically identified all non-toric bases where either $h^{1,1}(B_2) < 8$ or the base supports an elliptic Calabi-Yau threefold X with $h^{2,1}(X) \geq 150$. Completing the classification of non-toric bases presents some technical complications that provide an interesting challenge for further research. As discussed below, while our analysis is based on toric structures, resolving singularities in these toric fibrations can provide insight into the structure of some non-toric bases.

2.3 Toric fibers

Next we proceed to discuss toric fibers. In the fibrations we consider here, the fibers will be hypersurfaces in toric varieties, and so are defined by two-dimensional reflexive polytopes. To understand the structure of the fibers more explicitly, it is helpful to review the basics of the construction of Calabi-Yau varieties as anticanonical hypersurfaces in toric varieties. For a more detailed review of toric geometry and this construction, see [39, 12]. Briefly, given a reflexive polytope ∇ in dimension $d+1$, and an associated fan giving a compact ambient toric variety V, the adjunction formula guarantees that an anticanonical hypersurface in V gives a Calabi-Yau variety of dimension d. This reduces the construction of a large class of Calabi-Yau varieties to a combinatorial problem [14, 15]. Specifically, the defining polynomial P_∇ of a Calabi-Yau hypersurface in a reflexive polytope ∇ is given in terms of its points p_i, as well as the points q_j of the polar dual polytope ∇°, as

$$P_\nabla = \sum_{q_j \in \nabla^\circ} a_j \prod_{p_i} x_i^{<p_i, q_j>+1}, \tag{2.4}$$

where the coefficients a_j are generically complex, the x_i are formal (redundant) quasi-homogeneous variables whose vanishing loci are the prime toric divisors, and the product is taken only over points on the boundary of ∇ not interior to its facets.

Just as four dimensional reflexive polytopes give rise to Calabi-Yau threefolds, two dimensional reflexive polytopes give rise to Calabi-Yau one-folds, i.e. complex tori. There are sixteen 2D reflexive polytopes; we show these 16 polytopes, in the coordinates we use throughout the paper, in Figure 1. Hypersurfaces in these 16 polytopes correspond to 16 distinct fiber types, which were systematically analyzed in [40].

In this paper, we study toric elliptic fibrations, where the fiber is encoded in a 2D reflexive subpolytope of a 4D reflexive polytope. Each fiber type can be thought of as a particular class of restricted Weierstrass models (2.2), where f, g are tuned to take a specific form.[1] Thus, these 16 fiber types can be thought of as describing particular subclasses of the full finite set of elliptic fibration types over any given base. Each of these subclasses generically has certain kinds of singularities and global structures associated with nonabelian, abelian, and discrete gauge groups in the F-theory context. One of the goals of this study is to understand what range of such structures arise naturally in this simple class of constructions, and to understand what more exotic features might go outside this class of constructions.

2.4 Toric elliptic fibrations

We are interested here in understanding elliptic fibrations that are explicit in the structure of a toric hypersurface Calabi-Yau threefold through torically fibered polytopes [41, 42, 39]. A 4D reflexive polytope ∇ is fibered by a 2D reflexive subpolytope ∇_2 when ∇_2 is contained in ∇ along a 2D sublattice containing the origin. It was argued in [20] that any polytope fibration of this kind can be associated with at least one triangulation giving a toric cone structure that is compatible with the toric morphism that projects out the 2D reflexive subpolytope, and hence provides an elliptic fibration structure for the resulting Calabi-Yau threefold. Note that when the toric base onto which this fibration is projected contains curves of self-intersection -3 or below, this triangulation is in general not a standard (i.e. fine, regular, and star) triangulation,

[1] Technically, for three of the toric hypersurface fiber types, the fibration does not have a section and is a genus-one fibration; in these cases there is a closely related Weierstrass model associated with the Jacobian fibration, as discussed further in §2.5, §2.6.

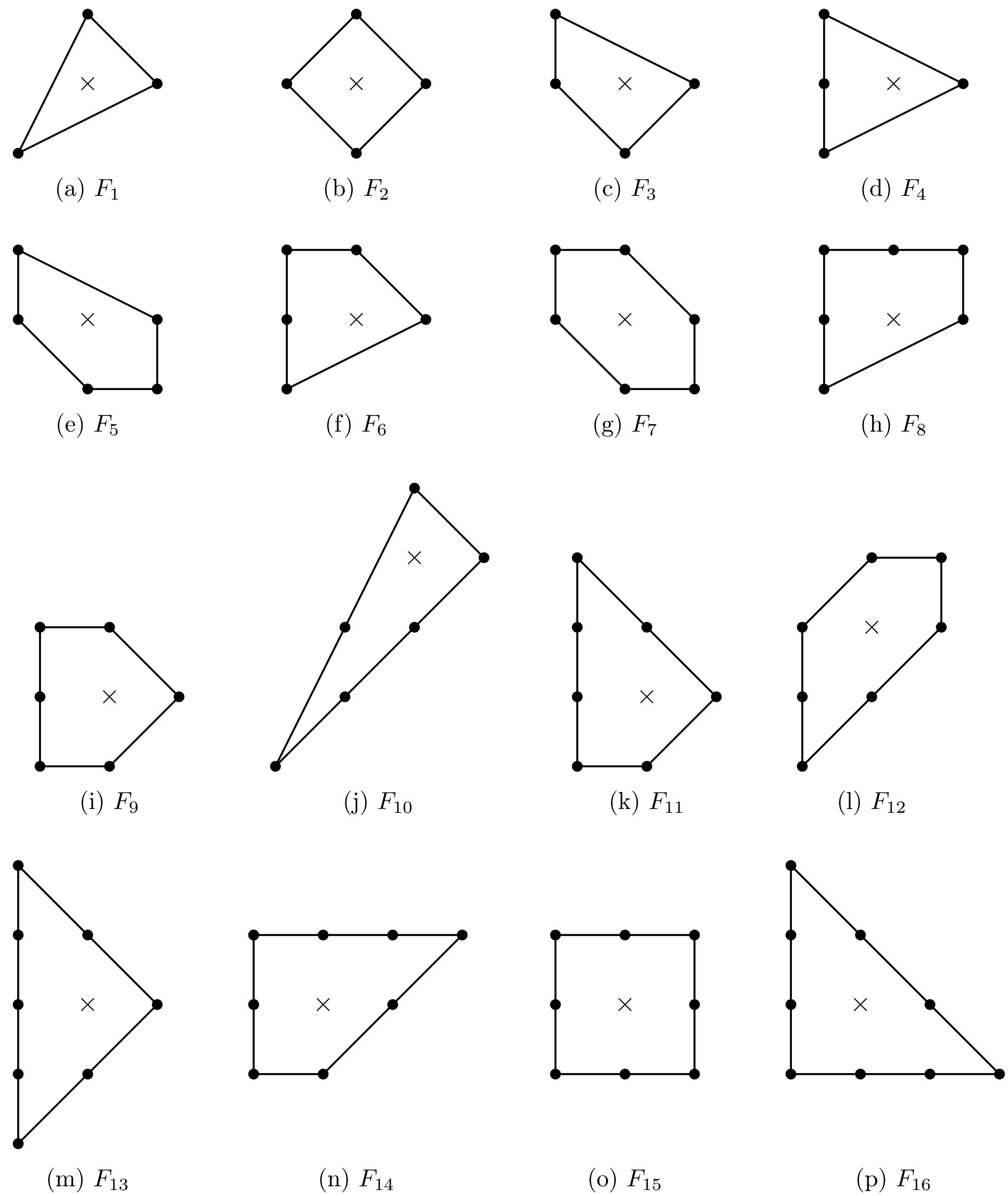

Figure 1: The sixteen two-dimensional reflexive polytopes. Vertices are connected by black lines, the origin is indicated by a cross, and all other points are indicated by a black dot.

but rather in the class studied in [43], i.e. of a type that is often referred to as a "vex" triangulation. The standard analysis of Batyrev [14] generalizes straightforwardly to this kind of triangulation. Note, however, that in most of the analysis of this paper, we do not deal with explicit triangulations; rather, we reformulate the hypersurface defining equation (2.4) in terms of a Weierstrass model, relying implicitly on the existence of a triangulation compatible with the toric morphism.

The relationship between toric structure and Weierstrass model is easiest to illustrate in the case of a "standard stacking" with the fiber $\mathbb{P}^{2,3,1}$ (fiber F_{10}), associated with the generic elliptic fibration over a given base B_2, where B_2 is described as a 2D toric variety having rays v_i. The details of this correspondence and further references are spelled out in detail in [44, 39, 12]; we summarize the story very briefly here. In the simplest case, where the base is weak Fano (and therefore also one of the 16 polytopes in Figure 1), the polytope is defined by the vertices $(1, 0; 0, 0)$, $(0, 1; 0, 0)$ and $\{(-2, -3; v_i), v_i \in B_2\}$. In this situation, the defining equation (2.4) becomes the long Weierstrass form, sometimes also called *Tate form*,

$$y^2 + a_1xyz + a_3yz^3 = x^3 + a_2x^2z^2 + a_4xz^4 + a_6z^6, \tag{2.5}$$

where x, y, z are coordinates on $\mathbb{P}^{2,3,1}$ and the a_i are determined by the sets of monomials $(j, k; m)$ in the dual polytope ∇°; for instance, points $(0, 0; m)$ correspond to monomials in a_1, points $(1, -1; m)$ correspond to monomials in a_2, and so on. Note that in this correspondence, a key insight is that the existence of a subpolytope $\nabla_2 \subset \nabla$ corresponds in the dual polytope ∇° to a projection to the 2D polytope that is dual to the fiber, $\nabla^\circ \to \nabla_2^\circ$. Building on this basic construction, related polytopes associated with tuned gauge group factors can be realized by removing monomials from the a_i so that these line bundle sections vanish to various degrees over the base toric divisors (so-called "Tate tunings," tables of which with increasing precision can be found in [25, 30, 12]; this corresponds in the original polytope ∇ to adding points associated with a "top" characterizing the associated gauge group. Similarly, for non-weak Fano bases, there is an analogous procedure but to get a reflexive polytope one must take the "dual of the dual" of this construction,[2] which automatically includes additional points in ∇ associated with non-Higgsable (rigid) gauge factors [28] lying over curves in the base of self-intersection -3 or below.

Note that the (when necessary, dual of the dual of the) "standard stacking" with fiber F_{10}, i.e. a fibration where the base is stacked over the point $(-2, -3)$ of the fiber, in general gives the generic elliptic fibration over a given base. A fibration with a different fiber or different F_{10} structure will in general involve tuning additional nonabelian or abelian gauge factors. Thus, for bases with large $h^{1,1}(B_2)$ and many toric curves of self-intersection $C \cdot C \ll -2$ that support large rigid/non-Higgsable gauge factors, where such tunings are difficult or impossible, we expect standard stacking F_{10} fibrations to dominate.

[2] To be precise, stacking F_{10} over a non-Fano base yields a non-reflexive polytope, whose dual contains rational (rather than integral) points; taking the dual of only the integral points yields a reflexive enhancement of the initial polytope, which is the correct analogue of the standard stacking for non-weak-Fano bases.

Nonabelian gauge factors in standard stackings of F_{10} are well understood through Tate tunings or equivalently through the study of polytope tops. However, for other fibers besides F_{10}, or indeed for nonstandard stackings of F_{10}, these analyses fall short. To use tops, for instance, one would need to derive new tops for each fiber type. Instead, we find it convenient to use a more unified framework, in which the different fiber types can all be analyzed with just the Kodaira classification in Table 1. We turn to this more detailed analysis in §2.6 after first briefly discussing genus-one fibrations.

2.5 Genus-one, elliptic, and Jacobian fibrations

The existence of a section in a fibration by fiber F_n can immediately be seen from the presence of a curve C of self-intersection $C \cdot C = -1$ in the fiber.[3] Torically, such a curve is realized by a ray that is the sum of the neighboring rays. From this, it is easy to see that all fibers other than F_1, F_2, and F_4 give an elliptic fibration with at least one section. For these three fibers, however, there is not a global section, rather there is a k-fold *multi-section*. For example, following the same logic as above for F_{10}, the defining equation for a Calabi-Yau threefold arising from a toric variety with a toric fiber F_1 is a general cubic, which is well known to have a 3-section, associated with 3 rational points in each fiber that may be connected by nontrivial monodromy around the base. Such a fibration is called a *genus-one* fibration, since the fiber is still geometrically a torus (i.e., a genus-one Riemann surface), but lacks the single rational section needed to make a consistent fibration by elliptic curves with related marked points. The fibers F_2 and F_4 generically provide 2-sections.

Genus-one fibrations with k-sections are related in F-theory to discrete abelian gauge groups. In general, genus-one fibrations with k-sections live in Tate-Shafarevich or Weil-Chatalet groups $\mathbb{Z}_k$ that share a common τ function describing the fibration locally, but with different monodromy structure; the *Jacobian* fibration, corresponding to the identity element of the group, is a true elliptic fibration. F-theory on the Jacobian fibration gives a 6D supergravity theory with gauge group $\mathbb{Z}_k$; compactification of this theory on a circle S^1 with a nontrivial Wilson line gives a 5D theory that can be described as M-theory compactified on the other elements of the Tate-Shafarevich group [45, 46]. To understand general elliptic and genus-one fibered Calabi-Yau threefolds with any fiber F_n in a parallel fashion to the description above of F_{10} standard stackings with tops and Tate models, we follow a standard approach to the construction of Weierstrass models for the Jacobian fibration of any genus-one or elliptically fibered CY3.

2.6 Weierstrass models and Nagell's algorithm

Any elliptic curve E over a field K can be written in *long Weierstrass form* (2.5). If the characteristic of K is not 2 or 3[4], we can complete the square in x and complete the cube in

[3] This follows from the Riemann-Roch formula for surfaces: $-K \cdot C = C \cdot C + 2 = 1$, so the anticanonical hypersurface contains a point in each fiber.

[4] We work in characteristic zero throughout. For recent work on F-theory and related string vacua in positive characteristic, see e.g. [47–50].

y to pass to *(short) Weierstrass form*,

$$y^2 = x^3 + fxz^4 + gz^6, \tag{2.6}$$

where f, g are given in terms of the a_i by

$$b_2 = a_1^2 + 4a_2 \tag{2.7a}$$
$$b_4 = a_1 a_3 + 2a_4 \tag{2.7b}$$
$$b_6 = a_2^3 + 4a_6 \tag{2.7c}$$
$$b_8 = b_2 a_6 - a_1 a_3 a_4 + a_2 a_3^2 - a_4^2 \tag{2.7d}$$
$$f = -\frac{1}{48}\left(b_2^2 - 24b_4\right) \tag{2.7e}$$
$$g = -\frac{1}{864}\left(-b_2^3 + 36b_2 b_4 - 216b_6\right). \tag{2.7f}$$

Note that the map from long Weierstrass form to short Weierstrass form is many-to-one, and hence is generically not invertible. Furthermore, note that the point $(1:1:0)$, which (largely for historical reasons) is usually called the point at infinity, satisfies Eq. (2.6) for any f, g. Thus, E must be an elliptic, rather than a genus-one, curve to be put into Weierstrass form. The complex structure of E is encoded in its j-invariant and discriminant Δ, which are given in terms of the Weierstrass coefficients f, g as

$$\Delta = -16\left(4f^3 + 27g^2\right) \tag{2.8a}$$
$$j = 1728\frac{4f^3}{4f^3 + 27g^2}. \tag{2.8b}$$

There exists an algorithm, called Nagell's algorithm, for rewriting an arbitrary elliptic curve E, equipped with a zero point p_0, in Weierstrass form; this algorithm is implemented in e.g. Sage [51].

The same procedure of going from an arbitrary defining polynomial to short Weierstrass form can be carried out for an elliptic fibration (with section); this is because elliptic fibrations can equivalently be viewed as elliptic curves whose field of definition is the function field of the base B_2. The basic idea, as described succinctly in [45], following Deligne, is that given a rational section z of $\mathcal{O}(-K_{B_2})$, one can use the Riemann-Roch theorem to compute the numbers of independent sections of multiples of $-K_{B_2}$; the number of polynomials in the generating sections at degrees below 6 exceed the number of sections at this degree, and a linear relation follows, which is the Weierstrass equation. Nagell's algorithm depends crucially on the choice of p_0, and hence does not apply if E does not have a point over K, i.e. if E is a genus-zero curve rather than an elliptic curve; however, in the genus-one context, it is quite natural to instead apply Nagell's algorithm to the Jacobian $J(E)$. This is done explicitly in [52] for the cases of 2-, 3-, and 4-sections. To analyze fibrations of the 16 toric fibers in a uniform way, therefore, one can use Nagell's algorithm to write the defining polynomial of the fibration in Weierstrass form, where the zeroes of the discriminant can be read off straightforwardly from Eq. 2.8a. This strategy was used in [40] to give explicit Weierstrass forms for elliptic and (the Jacobians of) genus-one fibrations for all 16 of the 2D toric fiber types.

The most relevant results of this general analysis are summarized in Appendix A. We give one specific example here and outline the application of Nagell's algorithm to the case of general F_{10} fibrations (i.e., including nonstandard stackings). This completes the discussion of §2.4, describing a fully general toric fibration with fiber F_{10}, and will be useful in describing specific fibrations in which F-theory gauge groups are tuned over non-toric divisors, as will be studied in §5.2. In a general toric fibration, the defining polynomial of F_{10} takes a more general form than that given in Eq. 2.5, namely

$$\alpha y^2 + a_1 xyz + a_3 yz^2 = \beta x^3 + a_2 x^2 z^2 + a_4 xz^4 + a_6 z^6. \tag{2.9}$$

Nagell's algorithm allows this to be rewritten in a standard short Weierstrass form as in Eq. 2.6, where f, g depend on the coefficients α, β as well as the a_i, and are given explicitly in Eq. A.8. From the form of f, g, we find that

$$\Delta \sim \alpha^3 \beta^2 \tilde{\Delta}, \tag{2.10}$$

where $\tilde{\Delta}$ is a generic polynomial in α, β, a_i. Importantly, neither $\tilde{\Delta}$ nor the Weierstrass coefficients f, g vanish automatically when α or β do. Thus, on $\alpha = 0$ we have $\text{ord}(f, g, \Delta) = (0, 0, 3)$; comparing to Table 1, we see that this corresponds to an I_3 singularity, and accordingly we expect an $SU(3)$ gauge group whenever α can vanish, i.e. when it consists of more than one monomial. Similarly, on the $\beta = 0$ locus we have $\text{ord}(f, g, \Delta) = (0, 0, 2)$, and we expect an $SU(2)$ gauge group. This is the origin of the "generic" $SU(2) \times SU(3)$ gauge group listed for F_{10} in Table 2, as originally identified in [40]. Note that, as in the discussion of §2.4, when the fiber F_{10} is put in standard form in the first two coordinates of the polytope, the monomials in α, β correspond to points in the dual lattice of the form $(-1, 1; m)$ and $(2, -1; m)$, respectively.

A similar analysis applies to the remaining fiber types. In general, the set of monomials over the dual 2D polytope to a given fiber type will automatically give rise to some additional structure that can include nonabelian gauge factors, U(1) factors, and discrete factors. A full list of the properties of the 16 fiber types, including whether there is a section and the generic gauge group, is given in Table 2. For more details on the specific Weierstrass models for each fiber, see Appendix A.

2.7 6D F-Theory Models

We have described so far various aspects of the geometry of elliptically fibered CY3s. The physics of F-theory essentially provides a dictionary that allows us to relate geometric features of elliptic CY3s to aspects of the 6D supergravity theories that one obtains by compactifying F-theory on these geometric spaces. In this subsection, we will describe this relationship in a little more detail; for a much more detailed review, see e.g. [27]. The material in this subsection is particularly relevant for some of the specific examples that we explore in §5.

Polytope	Dual	n_v	n_p	Section?	Weierstrass model	Gauge group [40]
F_1	F_{16}	3	4	No	A.2	$\mathbb{Z}_3$
F_2	F_{15}	4	5	No	A.4	$U(1) \times \mathbb{Z}_2$
F_3	F_{14}	4	5	Yes	A.2, $a_{003} = 0$	$U(1)$
F_4	F_{13}	3	5	No	A.6	$SU(2) \times \mathbb{Z}_4$
F_5	F_{12}	5	6	Yes	A.2, $a_{030} = a_{003} = 0$	$U(1)^2$
F_6	F_{11}	4	6	Yes	A.2, $a_{012} = a_{003} = 0$	$U(1) \times SU(2)$
F_7	F_7	6	7	Yes	A.2, $a_{300} = a_{030} = a_{003} = 0$	$U(1)^3$
F_8	F_8	4	7	Yes	A.2, $a_{030} = a_{012} = a_{003} = 0$	$SU(2)^2 \times U(1)$
F_9	F_9	5	7	Yes	A.2, $a_{030} = a_{102} = a_{003} = 0$	$SU(2) \times U(1)^2$
F_{10}	F_{10}	3	7	Yes	A.8	$SU(2) \times SU(3)$
F_{11}	F_6	4	8	Yes	A.8, $a_6 = 0$	$(SU(2) \times SU(3) \times U(1))/\mathbb{Z}_6$
F_{12}	F_5	5	8	Yes	A.2, $a_{120} = a_{030} = a_{102} =$ $a_{003} = 0$	$SU(2)^2 \times U(1)^2$
F_{13}	F_4	3	9	Yes	A.6, $a_{310} = a_{130} = a_{201} =$ $a_{021} = 0$	$SU(4) \times SU(2)^2/\mathbb{Z}_2$
F_{14}	F_3	4	9	Yes	A.2, $a_{210} = a_{120} = a_{030} =$ $a_{102} = a_{003} = 0$	$SU(3) \times SU(2)^2 \times U(1)$
F_{15}	F_2	4	9	Yes	A.2, $a_{300} = a_{120} = a_{030} =$ $a_{102} = a_{003} = 0$	$SU(2)^4/\mathbb{Z}_2 \times U(1)$
F_{16}	F_1	3	10	Yes	A.2, $a_{210} = a_{120} = a_{201} =$ $a_{102} = a_{021} = a_{012} = 0$	$SU(3)^2/\mathbb{Z}_3$

Table 2: Properties of the 16 two-dimensional reflexive polytopes and "generic" elliptic fibrations with each fiber. For each polytope, we give its dual polytope, the numbers n_v and n_p of vertices and points, respectively, whether the generic elliptic fibration admits a section or only a multi-section, the Weierstrass model of the elliptic fibration, and the generic gauge group, as computed in [40]. Note that some of these gauge groups may have a quotient by a discrete center, not indicated here.

F-theory can be thought of as a nonperturbative version of type IIB string theory, in which the axiodilaton encodes a complex structure for an auxiliary torus that can vary over the base space. For compactification to 6D, we must have a compact complex Kähler surface B (4 real dimensions) with an effective anticanonical class; supersymmetry imposes the condition that the total space forms an elliptic fibration over the base B, such that the total space of the fibration is an elliptic Calabi-Yau threefold X.

Physically, such a compactification gives rise to a 6D supergravity theory with $(1, 0)$ supersymmetry. The basic building blocks for such a theory are supergravity multiplets, which include the gravity multiplet, vector multiplets, tensor multiplets, and hypermultiplets. There is always one gravity multiplet, and we write the numbers of the other multiplets in the effective theory as V, T, and H, respectively. As usual in string compactifications, these numbers are determined by the topology of the compactification manifold. For instance, the number of tensor multiplets is fixed straightforwardly by the Hodge numbers of the base:

$$T = h^{1,1}(B) - 1. \tag{2.11}$$

As described above, the gauge group of the compactification is determined by the details of the fibration; the nonabelian gauge group is controlled by the singular fibers by means of the Kodaira classification in Table 1 and its refinement to include monodromy data, and the number of $U(1)$ gauge factors is given by the rank of the Mordell-Weil group of the fibration. For a given structure of the (continuous) gauge group G, the number V of vector multiplets is given by the dimension of G:

$$V = \dim(G). \tag{2.12}$$

The gauge group dimension is related to the topological data of the fibration through the Shioda-Tate-Wazir (STW) formula [53],

$$h^{1,1}(X) = h^{1,1}(B) + 1 + \mathrm{rk}\,\mathrm{MW(X)} + \mathrm{rk}\,G_{\mathrm{nonabelian}}, \tag{2.13}$$

which, geometrically, states that a basis of divisors for the threefold can be formed from the divisors on the base, the zero-section, Mordell-Weil sections, and the components of fibral divisors giving rise to Cartan elements of a nonabelian gauge group.

We next turn to the matter content of the theory, which is controlled by codimension two singularities in the elliptic fibration, as mentioned above (and in some cases by the topology of the divisor supporting the nonabelian gauge group). We can classify the hypermultiplets of the theory by whether they are charged or neutral under the gauge group. The total number H of hypermultiplets and the numbers H_{neutral} and H_{charged} of neutral and charged hypermultiplets, respectively, are controlled by the topological data of the fibration and the gauge group by a powerful set of gravitational, gauge-gravitational, and pure gauge anomaly cancellation constraints [54]. The simplest constraints are those that involve only the numbers of charged and uncharged matter fields:

$$h^{2,1}(X) = H_{\mathrm{neutral}} - 1 \tag{2.14a}$$

$$H - V = 273 - 29T \tag{2.14b}$$

$$h^{2,1}(X) = 272 + V - 29T - H_{\mathrm{charged}}. \tag{2.14c}$$

The anomaly constraints on charged matter fields are slightly more intricate, and play a key role in the F-theory/geometry dictionary. For a simple nonabelian gauge group G, these can be written as [26]

$$a \cdot a = 9 - T\,, \tag{2.15a}$$

$$a \cdot b = -\frac{1}{6}\lambda\left(\sum_R x_R A_R - A_{\rm Adj}\right)\,, \tag{2.15b}$$

$$0 = \sum_R x_R B_R - B_{\rm Adj}\,, \tag{2.15c}$$

$$b \cdot b = \frac{1}{3}\lambda^2\left(\sum_R x_R C_R - C_{\rm Adj}\right)\,, \tag{2.15d}$$

where x_R is the number of matter hypermultiplets transforming in representation R of G, λ is a constant depending on the type of gauge factor (e.g. $\lambda = 1$ when $G = SU(N)$), and the group theory coefficients A_R, B_R, and C_R are defined by

$$\mathrm{T}r_R F^2 = A_R \mathrm{T}r F^2\,, \quad \mathrm{T}r_R F^4 = B_R \mathrm{T}r F^4 + C_R \left(\mathrm{T}r F^2\right)^2\,. \tag{2.16}$$

A key aspect of the physics-geometry dictionary of F-theory is that the anomaly coefficients a, b, which are certain terms appearing in the 6D supergravity action, are mapped one-to-one to the divisor classes K, Σ in the F-theory base B corresponding to the canonical class and the divisor class supporting the gauge factor G, respectively; the inner product here becomes the intersection product in the F-theory base. For semi-simple groups, similar equations hold, with separate anomaly coefficients b_i for each simple factor G_i of $(G = \prod_i G_i)/\Gamma$.

For a given geometry, these anomaly equations are almost completely sufficient to determine the matter content of a given theory. For a given gauge factor G, knowing the anomaly coefficients a, b fixes a unique set of *generic* [25, 55] matter representations for hypermultiplet matter fields in the theory. For example, for SU(N), generic matter fields are those in the fundamental, two-index antisymmetric, and adjoint representations. Similarly, generic matter charged under a pair of gauge factors $G_i \times G_j$ arises at the intersection point between the divisors b_i, b_j, such as SU(N) $\times$ SU(M) bifundamental fields $(\mathbf{N}, \bar{\mathbf{M}})$. While more exotic representations can arise in special contexts (see, e.g., [31]), in this paper we encounter only constructions with generic matter content. Tables of the generic matter fields associated with specific gauge group factors (and pairs of factors) on base curves with given intersection numbers can be found in, e.g., [56].

For abelian factors, a similar set of anomaly equations to those above constrains the matter content (see, e.g., [57–59]); in this case, for a single U(1) factor, generic matter has charges ± 1 and ± 2. Abelian factors have an anomaly coefficient b that plays an analogous role to that of nonabelian factors; for multiple abelian factors, this becomes a two-index object b_{ij}. In the cases we encounter here, where the abelian factors arise from sections associated with -1 curves in the fiber, the anomaly coefficient for U(1) factors is essentially the canonical class K, and we can think of the matter content as simply that of a U(1) factor that arises from an SU(2) factor tuned on the genus-one divisor $-K$, broken on the single associated adjoint field.

Finally, there can be a discrete gauge group in the theory. This is harder to see directly from the structure of an elliptic CY3, but ties into the role of genus-one fibered Calabi-Yau threefolds. Physically, as discussed above, genus-one fibered threefolds have a multisection, and live in a group $\mathbb{Z}_k$ containing the Jacobian fibration, a genuine elliptic fibration; they are associated with the geometry of F-theory models compactified to 5D with a Wilson line that breaks the discrete gauge group. We will not go deeply into this structure here, but see [45, 46, 60, 61] for more on this subject.

3 Fiber and Base Analysis

In this section we give an overview of the methods and classification schemes used here for analyzing the toric fibration structures in the KS database. Subsection 3.1 describes the algorithm for identifying fibers and bases, subsection 3.2 describes the methodology for identifying fibrations that are equivalent under automorphisms of the ambient polytope, subsection 3.3 gives some details on the implementation and computation, and in subsection 3.4 we explain the format of our ancillary data files.

3.1 Overview of the algorithm for identifying fibers and bases

Let $L = \nabla \cap \mathbb{Z}^4$ be the set of lattice points of a 4D reflexive polytope, and V be the set of vertices of the dual polytope ∇° given by:

$$\nabla^\circ = \{w : \langle w, p\rangle \geq -1 \ \forall p \in \nabla\}$$

Following the approach developed in [20], for each point $p \in L$, we define the function $s(p) = \max_{v\in V} \langle p, v\rangle$ and define sets $S_i = \{p \in L : s(p) = i\}$. Then, ∇ contains a 2D reflexive subpolytope if and only if it satisfies one of the following conditions:

$$\begin{aligned}
&(1)\quad \exists x, y \in S_1 : x \neq -y \text{ and } -x, -y \in S_1\\
&(2)\quad \exists x, y \in S_2 : -(x+y) \in S_1 \text{ or } -(x+y) \in S_2\\
&(3)\quad \exists x, y \in S_3 : -\frac{(x+y)}{2} \in S_1
\end{aligned}$$

In order to find subpolytopes, we look for a plane spanned by two rays x and y which satisfy one of the above conditions. For any such x and y, we can then solve a set of linear equations to find all points of ∇ that are linear combinations of x and y. This yields all points in the subpolytope. To identify which specific fiber is realized by each such subpolytope, we can use the sets S_i. The sizes of the sets S_1, S_2, S_3, calculated in Table 3, distinguish all 2D reflexive polytopes except fibers 6 and 10 from Figure 1. But these polytopes have different numbers of points and since we have all the points in the subpolytope, a quick check on the number of points allows us to completely identify all the different fiber types.

For a given polytope, we can scan over all pairs of rays x, y to identify all possible fibers. Each fiber is one of the 16 toric fibers reviewed in §2.3. For each distinct fiber, we then wish to identify the corresponding base.

Polytope	$(\lvert S_1\rvert, \lvert S_2\rvert, \lvert S_3\rvert)$		Polytope	$(\lvert S_1\rvert, \lvert S_2\rvert, \lvert S_3\rvert)$
F_1	$(0, 3, 0)$		F_9	$(4, 2, 0)$
F_2	$(4, 0, 0)$		F_{10}	$(2, 2, 1)$
F_3	$(2, 2, 0)$		F_{11}	$(4, 2, 1)$
F_4	$(2, 0, 2)$		F_{12}	$(6, 1, 0)$
F_5	$(4, 1, 0)$		F_{13}	$(4, 2, 2)$
F_6	$(2, 2, 1)$		F_{14}	$(6, 2, 0)$
F_7	$(6, 0, 0)$		F_{15}	$(8, 0, 0)$
F_8	$(4, 1, 1)$		F_{16}	$(6, 3, 0)$

Table 3: The sizes of sets $|S_i|$ used to identify each fiber [20].

To find the base, we want to project out the 2D reflexive subpolytope. Let x, y be two rays that span the fiber. We find a $GL(4, \mathbb{Z})$ transformation M such that $Mx \to (1, 0, 0, 0)$. Finding this transformation requires repeated applications of the Euclidean algorithm. In this basis, projecting onto the latter three coordinates is equivalent to throwing away one dimension of the subpolytope. We repeat this procedure one more time. Starting with a 3D polytope, we find a $GL(3, \mathbb{Z})$ transformation N such that $N\tilde{y} \to (1, 0, 0)$ where $\tilde{y}$ is the projection of the vector y in the 3D polytope. Projecting onto the final two coordinates returns the base rays.

This projection gives a set of 2D rays from which we can identify the base. First, we reduce any non-primitive rays that are multiples of an integer 2D vector to the associated primitive ray; this gives a set of primitive rays $v_i = (x_i, y_i), i = 1, \ldots, k$. Next, we order the rays by angle and check to confirm that the base is smooth by checking whether $x_i y_{i+1} - x_{i+1} y_i = 1$ (imposing cyclicity, so subscripts are taken mod k). When the base constructed from the projected rays is not smooth, we identify an associated smooth base by adding all rays in the convex hull.

We identify the resulting smooth base using the set of intersection numbers of the toric divisors. After ordering the rays in the convex hull by angle, we calculate the sequence of intersection numbers $(c_1, \ldots, c_k)$ using the equation (mod k):

$$c_i(x_i, y_i) + (x_{i-1}, y_{i-1}) + (x_{i+1}, y_{i+1}) = 0 \tag{3.1}$$

In all cases, the resulting sequence of intersection numbers corresponds precisely to one of the Morrison-Taylor (MT) bases identified in [34].

The result of this analysis for a given polytope in the KS database is a list of fibrations, where each fibration can be identified by a fiber with fiber ID 1–16 (as summarized in §2.3), and a base with base ID 1–61,539 (as summarized in §2.2), where in some cases a subset of the base divisors have been blown down, indicated by a list of true-false values describing the set of base divisors that are still present.

3.2 Identifying equivalence of fibrations under polytope automorphisms

In general, a polytope ∇ might enjoy nontrivial *automorphisms*, i.e. linear transformations $\Lambda \in \mathrm{SL}(4,\mathbb{Z})$ that map the vertices of ∇ into each other. The automorphisms of ∇ form a group, $\mathrm{Aut}(\nabla)$, whose elements can be efficiently computed in e.g. CYTools [62]. For instance, it is straightforward to verify that the polytope whose vertices are given by the columns of the matrix

$$\begin{pmatrix} 1 & 0 & -2 & 0 & 0 & 0 \\ 0 & 1 & -3 & 0 & 0 & 0 \\ 0 & 0 & 0 & 1 & 0 & -2 \\ 0 & 0 & 0 & 0 & 1 & -3 \end{pmatrix}, \tag{3.2}$$

i.e. the combination of two copies of fiber F_{10} on orthogonal two-planes, has a $\mathbb{Z}_2$ group of automorphisms generated by exchanging the axes pairs containing the two F_{10} fibers. While the computation of polytope automorphisms is by now standard, to the best of our knowledge, no systematic study of their properties has appeared in the literature. Some statistics of polytope automorphisms which we collected in the course of our work and which we found helpful to its completion are presented in Appendix B.

If ∇ has nontrivial automorphisms and contains multiple 2D reflexive subpolytopes, in general the subpolytopes might be mapped into each other by automorphisms of the ambient polytope. For instance, the polytope given in Eq. 3.2 contains (along with an additional F_2 fiber) two F_{10} subpolytopes, which by construction are mapped into each other by the polytope's unique nontrivial automorphism. We call two subpolytopes *automorphism equivalent* if there exists an automorphism of the ambient polytope that exchanges them, and *automorphism inequivalent* otherwise.

Not all pairs of two subpolytopes can even potentially be mapped into each other by automorphisms; clearly, two subpolytopes can only be automorphism-equivalent if they have the same fiber type. In fact, more is true; two subpolytopes can only be automorphism equivalent if their associated fibrations have the same base as well. In what follows, it will be convenient to consider *fibration structures*, groupings of subpolytopes with the same fiber type and base type that can potentially be automorphism equivalent. Note that in general, different subpolytopes of a fixed polytope whose fiber type and base type are the same, i.e. different representatives of the same fibration structure, need not be automorphism equivalent. We therefore have the bounds

$$\#\,(\text{fibration structures}) \leq \#\,(\text{automorphism inequivalent fibrations}) \leq \#\,(\text{total fibrations})\,. \tag{3.3}$$

Fix a 4D reflexive polytope ∇. For fibrations with a smooth base, the data defining a fibration structure are simply the fiber type, in the conventions of Table 2, and the base type, i.e. the member of the MT list [34] with the same toric intersection structure as the base of the fibration. For fibrations with singular bases, in addition to the topological type of the resolved base, we also include a classification of the curves which are blown down to yield the singular base. Thus, in total, a fibration structure is identified by five pieces of information: the ambient polytope, the fiber type, the base type, whether the base is smooth, and a (possibly empty) list of curves that have been blown down.[5]

Geometrically, automorphism-equivalent fibrations should be identified. Furthermore, from the physics perspective, as emphasized in [21], because compactifying F-theory on elliptic fibrations defined by automorphism equivalent subpolytopes gives identical physical theories, it is also natural in this context to count the number of automorphism equivalence classes of fibrations, rather than the total number of fibrations. Thus, given a 4D reflexive subpolytope ∇, once we have identified the fibers and bases of all of its elliptic fibrations using the algorithm above, we also compute the automorphisms of ∇ and check whether any subpolytopes are mapped into each other by those automorphisms. In practice, we first sort the subpolytopes into fibration structures, and only compute automorphisms if at least one fibration structure has more than one representative.

3.3 Computational details

In the last two subsections, we have spelled out an algorithm for completely classifying the automorphism-inequivalent toric elliptic fibrations of a 4D reflexive polytope ∇ from the Kreuzer-Skarke list. We have applied this algorithm, which we have implemented in both CYTools [62] and Julia [63], to all 473,800,776 4D reflexive polytopes to obtain a complete classification of all toric elliptic fibrations. Before presenting the results of our analysis in §4, we briefly outline the technical details of this computation, which was carried out on MIT's subMIT cluster [64].

The KS database [65] classifies polytopes by the number of vertices of their dual polytope. Thus, the file v05.gz contains the 1,561 polytopes whose duals have five vertices each.[6] We have kept this organizational scheme throughout our analysis, including in the database accompanying this publication, but have split the vn.gz files into more manageable files of (up to) one million polytopes each, labeled vn-1.txt and so on, when appropriate.

Our analysis proceeds in three steps. Given a list of input polytopes as described above, we begin by using the PALP package to preprocess the raw KS 4D polytope files to include some additional information about each polytope. We then find all 2D reflexive subpolytopes and classify them into fibration structures. This is accomplished by means of a Julia script which implements the algorithm in §3.1, and which we have included as an ancillary file in the associated Zenodo archive. Once the fibration structures and their representatives have

[5]An additional complication arises when the base of the fibration is singular and the resolved base itself has nontrivial automorphisms, as then the specification of blowdowns becomes ambiguous. In this rare occurrence, we resolve this ambiguity by selecting the lexicographically minimal representative of the specification of blown down curves under the base automorphisms.

[6]One immediate way to verify that the KS database organizes its files by the number of vertices of the dual, rather than the number of vertices of the polytope itself, is to query it for polytopes with $h^{1,1} = 1, h^{2,1} = 101$; doing so returns the vertices of the mirror quintic rather than those of the quintic itself.

been specified, we select all polytopes with at least one fibration structure with more than one representative. These polytopes are input into CYTools, where we compute the number of automorphism inequivalent representatives of each fibration structure; the CYTools script used for this calculation is again included as an ancillary file. Finally, we merge the outputs of the Julia and CYTools analyses to create our final output files, which contain counts of the fibration structures, inequivalent fibrations, and total fibrations for all 473,800,776 4D reflexive polytopes.

3.4 Organization of results and nomenclature

The results of the analysis are organized in a set of data files that are publicly available at [22]. The details of the formatting of the files are described in more detail in the README.txt file associated with the archive, but we give a broad description here.

In the remainder of this paper and the Zenodo database, we refer to a given polytope using the syntax "vxx-yyy," where (following the format used in the KS database [65]), xx denotes the number of vertices of the dual polytope (2 digits, ranging from 05–36) and yyy denotes indexing in the order of the KS database for polytopes with that number of vertices (varying numbers of digits). Fibers 1–16 are ordered as in [40] and Figure 1, and bases 1–61,539 are ordered canonically as in the database associated with [34], i.e. they are ordered first by $h^{1,1}(B_2)$, and entries at each value of $h^{1,1}$ are ordered canonically according to (the negatives of the) intersection numbers of the toric base divisors, so e.g. bases $1, 2, \ldots, 13$ correspond to $\mathbb{P}^2, \mathbb{F}_0, \ldots, \mathbb{F}_{12}$). For convenience, that database is also included in the Zenodo archive.

With these conventions set, we can explain the format of the files in the database. Each 4D reflexive polytope appears in the database as a single line, which begins with some basic topological data specifying the polytope, namely its label (vxx-yyy, as specified above, which for machine-readability we specify as [xx,yyy]) and Hodge numbers, in the form $[h^{1,1}, h^{2,1}]$. Next we give the total number of 2D subpolytopes, before proceeding to specify how these fibrations are broken up into fibration structures, etc.

Fibration structures are presented as a list, where each structure is specified first by base, and then within each base by fiber types. We specify the base as follows:

`[base singular?, base ID,` $h^{1,1}(B)$`, [blown down curves],...`

We then specify the different fiber types that appear and the number of subpolytopes of that type as

`[fiber ID, #(total fibrations in this structure), #(inequivalent fibrations)]`

Putting it all together, the full database entry for a single polytope takes the form

`[[xx,yyy],[`$h^{1,1}(X)$`,`$h^{2,1}(X)$`],#(total fibrations),`
`[[base 1 singular?, base 1 ID,` $h^{1,1}$`(base 1), [blown down curves in base 1],`
`[[fiber 1 ID, #(total fibrations with base 1-fiber 1),`
`#(inequivalent fibrations)],`
`[fiber 2 ID, #(total fibrations with base 1-fiber 2),`

```
    #(inequivalent fibrations)],...]],
 [base 2 singular?, base 2 ID, h^{1,1}(base 2), [blown down curves in base 2],
  [[fiber 1 ID, #(total fibrations with base 2-fiber 1),
    #(inequivalent fibrations)],
   [fiber 2 ID, #(total fibrations with base 2-fiber 2),
    #(inequivalent fibrations)],...]]]  ,...]
```

Let us see how this works for a particular example. Consider the polytope with vertices given by the columns of the matrix

$$\begin{pmatrix} -1 & -1 & -1 & -1 & 2 \\ -1 & -1 & -1 & 2 & -1 \\ 1 & 1 & 3 & -1 & -1 \\ 0 & 4 & 0 & -1 & 0 \end{pmatrix}, \tag{3.4}$$

which has Hodge numbers $h^{1,1}(X) = h^{2,1}(X) = 19$. The database entry corresponding to this polytope is

```
[[5, 724], [19, 19], 3, [[0, 150, 6, [], [[10, 2, 1]]],
 [1, 4162, 14, [1, 1, 0, 0, 1, 0, 0, 1, 0, 0, 1, 0, 0, 1, 1, 1], [[1, 1, 1]]]]].
```

From this line, we see that its label (as specifed above) is v05-724, it has Hodge numbers $h^{1,1}(X) = h^{2,1}(X) = 19$, as expected, and it has three total elliptic fibrations, coming from two different fibration structures:

1. F_{10} fibered over base 150, which has $h^{1,1}(B) = 6$, with no blowdowns. There are two fibrations with this structure, and they are related by an automorphism.

2. F_1 fibered over base 4162, which has $h^{1,1}(B) = 14$, with blowdowns. The (negative) intersection form of this base is

$$[6, 1, 2, 2, 2, 2, 2, 2, 2, 2, 2, 2, 2, 1, 6, 0], \tag{3.5}$$

and the string specifiying the blowdowns is

$$[1, 1, 0, 0, 1, 0, 0, 1, 0, 0, 1, 0, 0, 1, 1, 1]. \tag{3.6}$$

A zero in this string indicates that the corresponding curve in the intersection sequence has been blown down, and a one indicates that it has not. Thus, to construct the base of this of this fibration, we have blown down eight curves of self-intersection -2. There is a single fibration in this structure.

4 Distributions of Fibers and Bases

From the complete analysis of all toric 2D subpolytopes in the KS database, we identify 2,264,992,252 fibrations, with 2,177,857,036 distinct "structures," i.e. combinations of base, fiber, and ambient polytope as defined above. After accounting for automorphism equivalence, the number of inequivalent fibrations is 2,250,744,657.

In this section, we describe some general aspects of the statistics of these fibrations. In Subsection 4.1 we organize top-level statistics in terms of polytopes, in subsection 4.2 we describe statistics of fiber types, and in subsection 4.3 we describe some statistics in terms of the bases.

4.1 Fibrations per polytope

The average number of fibrations per polytope is 4.78, of which 4.75 are automorphism-inequivalent. It is interesting to compare this with the average number of "obvious" fibrations for CICYs, which was found to be 9.85 in [9].

The polytope with the most fibrations has 362 fibrations. This is realized for polytope v08-242 (in the nomenclature of Section 3.4), which gives CY3's with Hodge numbers $(h^{1,1}(X), h^{2,1}(X)) = (68,\ 4)$. These fibrations furnish ten fibration structures and, after accounting for polytope automorphism, each fibration structure has a single equivalence class of representatives.

We plot the average number of total (automorphism inequivalent) fibrations on a polytope with a given $h^{1,1}$ and $h^{2,1}$ in Figure 2(a); plots of the maximum and minimum number of (again, automorphism equivalent) fibration structures that a polytope with a given Hodge pair can host appear in Figures 2(b, c).

In general, we see that the polytopes with many fibrations tend to have small $h^{2,1}(X)$, and the number of fibrations for polytopes with small $h^{2,1}(X)$ peaks at intermediate values of $h^{1,1}(X)$. The plot of the maximum number of fibrations at fixed Hodge numbers has an interesting structure; when both Hodge numbers are large, there is generally only a single fibration. A second fibration generally appears below a boundary with a peak around $(140, 140)$ and a slope that cuts off polytopes with large $h^{2,1}(X)$, but continues out to large $h^{1,1}(X)$; an example of an interesting polytope with two fibrations is the polytope with maximum $h^{1,1}(X) = 491$, discussed in §5.6. [7] A further boundary that more closely approximates a diagonal line separates out polytopes with at most three fibrations, and so on. It would be interesting to understand in more detail the structures responsible for this pattern.

[7] From the structure of this maximal polytope, the analyses of [66, 9], and the related structure of other polytopes with large $h^{1,1}(X)$, it seems plausible that this second fibration is often associated with structures that are natural in a dual $\mathrm{Spin}(32)/\mathbb{Z}_2$ heterotic theory, while the first, upper class of fibrations corresponds more naturally with an $E_8 \times E_8$ heterotic dual.

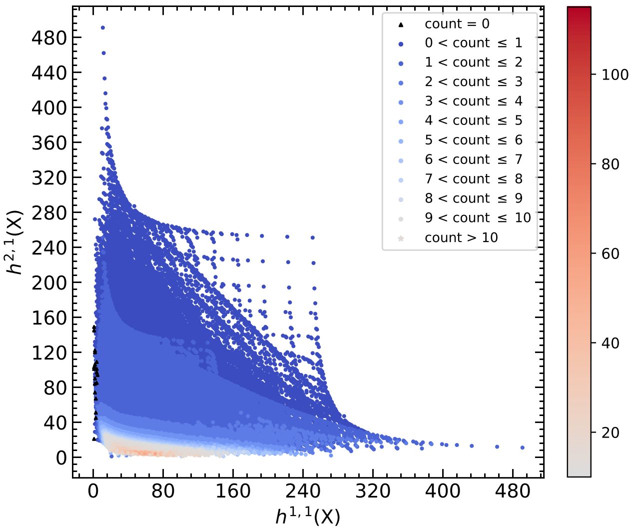

(a) Mean fibrations

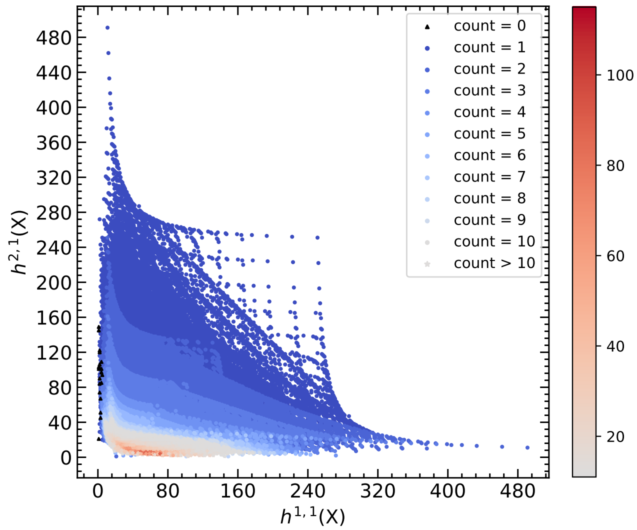

(b) Max fibrations

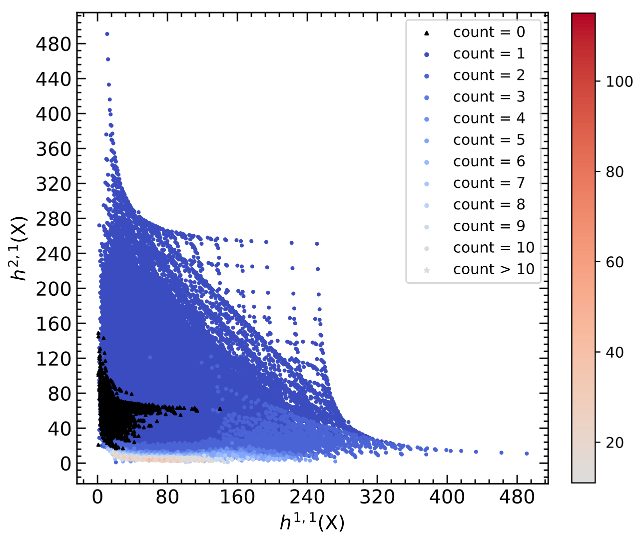

(c) Min fibrations

Figure 2: The average (a), maximum (b), and minimum (c) number of automorphism-inequivalent fibrations over a polytope giving Calabi-Yau threefolds X with Hodge numbers $h^{1,1}(X)$ and $h^{2,1}(X)$ are plotted. The black triangles indicate zero structures, the blue colors indicate smaller number of structures, up to 10, and the color bar on the right indicates the color corresponding to larger number of fibrations (more red means larger number of structures).

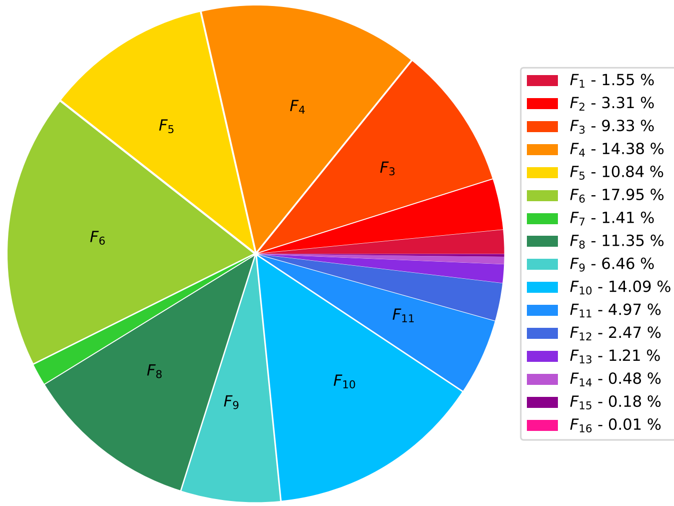

Figure 3: The density of inequivalent fibrations by each of the sixteen fiber types.

4.2 Fiber types

We find fibrations with each of the sixteen fibers. This is guaranteed since for any pair of fibers F, F' we can construct a reflexive 4D polytope as a product (with rays $(v \in F, v' \in F')$) or a "sum" (with rays $(v \in F, 0), (0, v' \in F')$) of these two fibers. [8] The distribution of fiber types is given in Table 4 and illustrated graphically in Figure 3. We find that F_6 is the most common fiber ($\sim 18\%$), with 403,991,733 automorphism-inequivalent fibrations, while F_{16} is the least common fiber ($\sim 0.01\%$), with only 182,915 inequivalent fibrations. On the other hand, for polytopes with large $h^{1,1}(X)$, F_{10} dominates, as can be seen in Figure 4; the highest $h^{1,1}$ of a polytope that has no F_{10} fibers is $h^{1,1} = 227$. The dominance of fiber F_6 was to us somewhat unexpected; because every base admits at least one fibration with fiber F_{10} (the standard stacking, §2.4), and this fiber is closest to the generic Weierstrass model, one might have expected F_{10} to dominate. Indeed, much of the previous analysis of fibrations focused implicitly on F_{10} fibers. We explore the geometry of fibrations with fiber F_6 in further detail in §5.4.

We find that genus-one fibrations, i.e. those with fiber F_1, F_2, or F_4, are common: 19.3% (436,311,489 total, 432,982,773 inequivalent) of all fibrations are genus-one, rather than elliptic. Amongst genus-one fibrations, fiber F_4 is by far the most common, representing 74.6% (325,373,736 total, 323,559,047 inequivalent) of all genus-one fibrations.

4.3 Bases

We find that each of the 61,539 toric bases on the MT list appears as the base for at least one fibration; 625 bases appear exactly once. This is unsurprising; as explained in §2.4, one can

[8] A detailed analysis of these polytopes and their behavior under mirror symmetry will be given in [67].

Fiber	Fibration Structures	Inequivalent Fibrations	Total Fibrations
F_1	34,339,236	34,990,811	35,461,473
F_2	70,340,325	74,432,915	75,476,280
F_3	201,064,783	210,042,410	212,128,020
F_4	316,154,156	323,559,047	325,373,736
F_5	222,330,801	244,004,671	246,317,835
F_6	392,614,430	403,991,733	406,116,680
F_7	30,158,692	31,807,255	32,177,670
F_8	249,141,445	255,482,339	256,753,239
F_9	140,262,167	145,501,972	146,510,508
F_{10}	314,373,356	317,175,553	317,945,412
F_{11}	111,071,735	111,917,349	112,327,098
F_{12}	53,880,209	55,577,013	55,975,484
F_{13}	27,213,569	27,275,196	27,349,323
F_{14}	10,750,057	10,798,598	10,859,072
F_{15}	3,979,255	4,004,880	4,035,646
F_{16}	182,820	182,915	184,776

Table 4: Summary statistics for fibrations of each fiber type. For each fiber, we have indicated the number of fibration structures, the number of inequivalent fibrations, and the total number of fibrations with that fiber type.

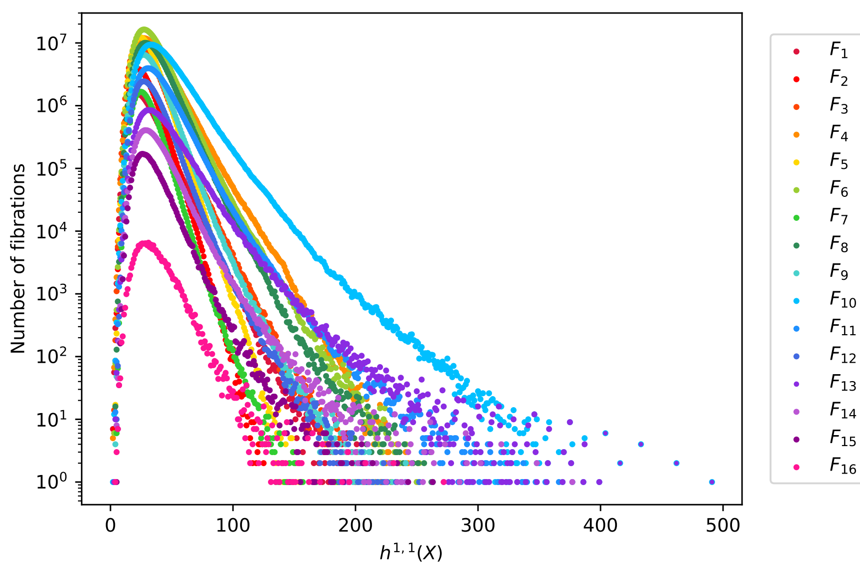

Figure 4: The total number of automorphism-inequivalent fibrations of each fiber type as a function of $h^{1,1}(X)$. Note that at large $h^{1,1}(X)$, above $h^{1,1}(X) \sim 400$, all polytopes with a fiber F_{13} also have a fiber F_{10}.

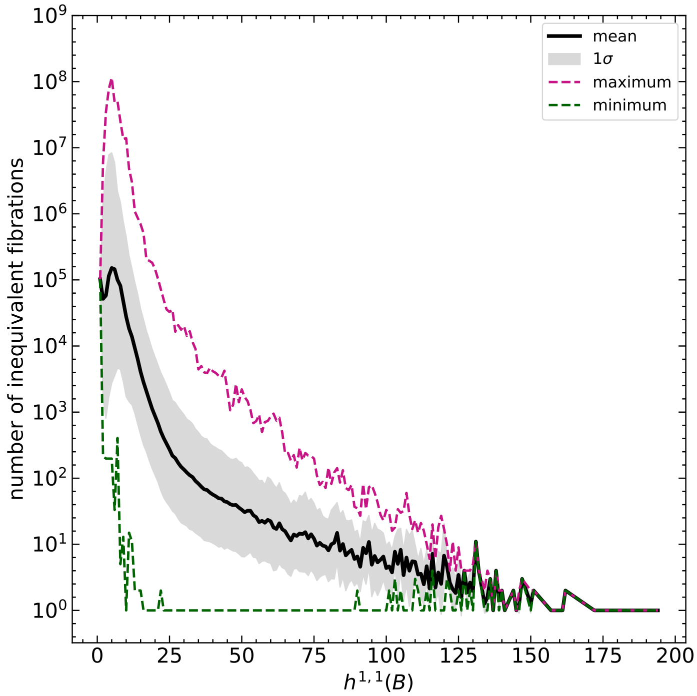

Figure 5: The mean, minimum, maximum and 1σ deviation of the number of inequivalent fibrations over a base B with a given $h^{1,1}(B)$ are plotted. Note that there are more structures fibered over bases with small $h^{1,1}(B)$.

construct the generic elliptic fibration over any toric base by taking (the dual of the dual of) the standard stacking of F_{10} over that base.

While all bases appear, there is a marked statistical preference towards bases with small $h^{1,1}(B)$. As discussed in more detail in §5.4.1, this is likely because bases with larger $h^{1,1}(B)$ have a large number of non-Higgsable clusters that strongly constrain the possibility of additional tuned gauge factors. The most common base, which is entry 72 on the MT list, is a generalized del Pezzo surface gdP_4, with $h^{1,1}(B) = 5$, and is the base for 5.1% (114,961,701 total, 114,019,846 inequivalent) of all fibrations; this is a weak Fano base, and is the toric variety defined by the F_{12} polytope, as in Figure 1. Plotting the number of fibrations over a base as a function of $h^{1,1}(B)$, as shown in Figure 5, we find a distinct peak at small $h^{1,1}(B)$. In particular, 82.5% (1,868,680,827 total, 1,857,694,025 inequivalent) of fibrations have $h^{1,1}(B) \leq 10$, and 99.4% (2,251,269,536 total, 2,237,134,428 inequivalent) have $h^{1,1}(B) \leq 25$. We have plotted the Hodge numbers of all elliptic fibrations over a number of specific bases with small $h^{1,1}(B)$ in Figure 6.

Moreover, as we see in Fig. 7, the only fiber type that appears fibered over a base with $h^{1,1}(B_2) > 100$ is F_{10}. This corroborates the expectation (c.f. §2.4) that for bases with large $h^{1,1}(B_2)$, the only available elliptic fibration is the generic elliptic fibration, associated with the standard stacking of the fiber F_{10}.

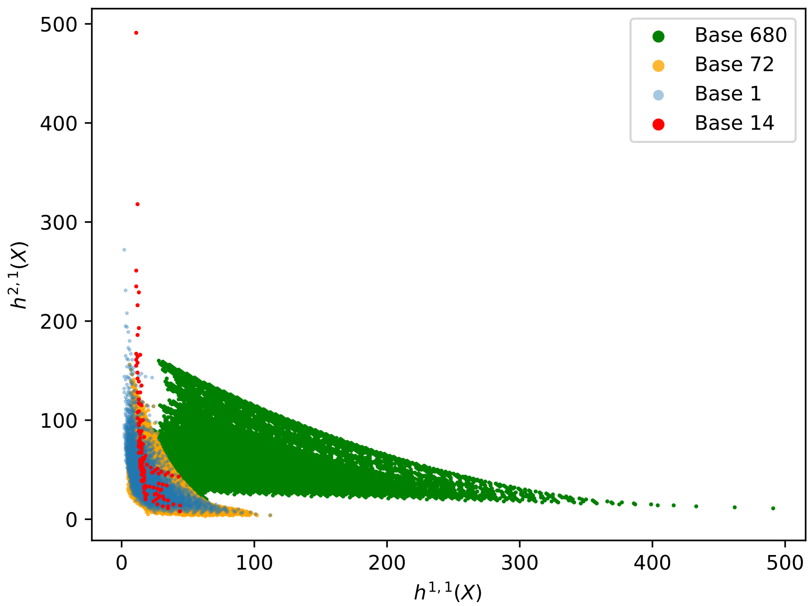

Figure 6: The Hodge numbers of fibrations over base 1, i.e. $\mathbb{P}^2$, discussed in §5.1–5.2), base 14, Hirzebruch $\mathbb{F}_{12}$ which supports the elliptic CY with the largest $h^{2,1}(X) = 491$), base 72, a gdP$_4$ which is the most common base, and base 680, which appears universally in fibrations with extremely large gauge groups, as discussed in §4.4.

4.3.1 Weak Fano and non-weak-Fano bases

As discussed in §2.4, of the 61,539 toric bases, 16 are weak Fano; these exactly correspond to the 16 toric fibers. Some summary statistics of fibrations with weak Fano bases are given in Table 5. We find that fibrations with weak Fano bases are disproportionately common, comprising 26% (588,457,836 total, 584,970,461 inequivalent) of all fibrations. In particular, the four most common bases are all weak Fano. Intuitively, this makes sense; weak Fano bases lack NHCs, and so one has additional freedom to tune gauge groups over weak Fano bases relative to non-weak-Fano bases. We show the distribution of fiber types in fibrations over the sixteen weak Fano bases in Figure 8a.

The other 61,523 bases are non-weak Fano, and contain NHCs hosted on toric divisors. non-weak-Fano bases comprise the remaining 74% (1,676,534,416 total, 1,665,774,196 inequivalent) of fibrations; 96.5% (457,234,463 total) of all polytopes admit at least one fibration with a smooth, non-weak-Fano base, and correspondingly an NHC. The most common non-weak-Fano base is base 215 on the MT list, which has $h^{1,1}(B) = 7$ and (negative) intersection form

$$[2, 2, 1, 4, 1, 2, 1, 1, 1], \tag{4.1}$$

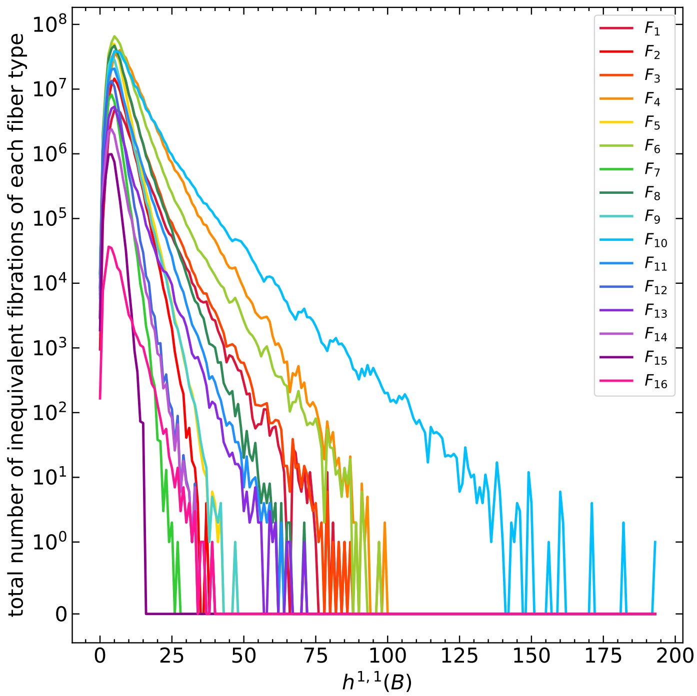

Figure 7: The number of inequivalent fibrations of each fiber type as a function of $h^{1,1}(B)$. Note that at large $h^{1,1}(B)$, only fibrations with fiber F_{10} are seen.

and thus is only non-weak-Fano because of the presence of one curve with self-intersection -4; this appears as the base in 2.2% (50,802,116 total, 50,472,765 inequivalent) of fibrations. We show the distribution of fiber types in fibrations over the sixteen most common non-weak-Fano bases in Figure 8b.

4.3.2 Singular Bases

As mentioned in Section 3, it is possible for a smooth fibration to have a singular base. We find that this occurs rarely, in only 0.5% (11,184,662 total, 11,136,035 inequivalent) of fibrations. Moreover, singular bases occur only in genus-one, rather than elliptic, fibrations. Some summary statistics of the fiber types of fibrations with singular base are given in Table 7. F_4 remains the most common fiber type in genus-one fibrations over singular bases, appearing in 80.8% (9,029,636 total, 9,002,823 inequivalent) of all such fibrations.

The singular bases have a very specific structure. In all cases, the singular bases correspond to smooth bases in the MT list with a set of -2 curves blown down. Blown down -2 curves can either appear alone or in adjacent pairs, corresponding to a local $\mathbb{C}^2/\mathbb{Z}_2$ or $\mathbb{C}^2/\mathbb{Z}_3$ singularity in the base. No other combinations occur in our dataset; furthermore, any given singular base has only one or the other type of singularity. Those with a $\mathbb{Z}_3$ singularity always have fiber F_1, while those with a $\mathbb{Z}_2$ singularity have fiber F_2 or F_4. Since these singularities corresponds precisely to the type of multisection of those genus-one fibrations, it seems that

Base ID	Fiber type	$h^{1,1}(B)$	Fibration Structures	Inequivalent Fibrations	Total Fibrations
1	F_1	1	102,563	102,581	102,600
2	F_2	2	1,975,645	2,005,188	2,020,060
3	F_3	2	5,332,362	5,415,109	5,435,366
4	F_4	2	6,031,392	6,072,869	6,084,817
15	F_5	3	28,767,691	29,917,327	30,066,698
16	F_6	3	34,433,015	34,821,744	34,879,206
27	F_7	4	19,074,969	20,268,222	20,465,927
28	F_9	4	63,835,026	67,391,516	67,765,284
49	F_8	4	74,437,389	77,408,588	77,673,426
50	F_{10}	4	32,326,443	32,432,358	32,453,682
72	F_{12}	5	98,635,610	114,019,846	114,961,701
73	F_{11}	5	82,902,723	87,426,934	87,830,312
116	F_{15}	6	26,802,481	29,288,912	29,657,220
117	F_{14}	6	45,560,240	48,889,834	49,350,175
118	F_{13}	6	25,955,132	26,745,791	26,910,622
212	F_{16}	7	2,700,198	2,763,642	2,800,740

Table 5: Summary statistics for fibrations with weak Fano bases. We specify the weak Fano bases both with their labels in the MT list and their labels as fiber types, as in Table 2. For each base, we have indicated the Hodge number $h^{1,1}(B)$ and the number of fibration structures, the number of inequivalent fibrations, and the total number of fibrations with that base.

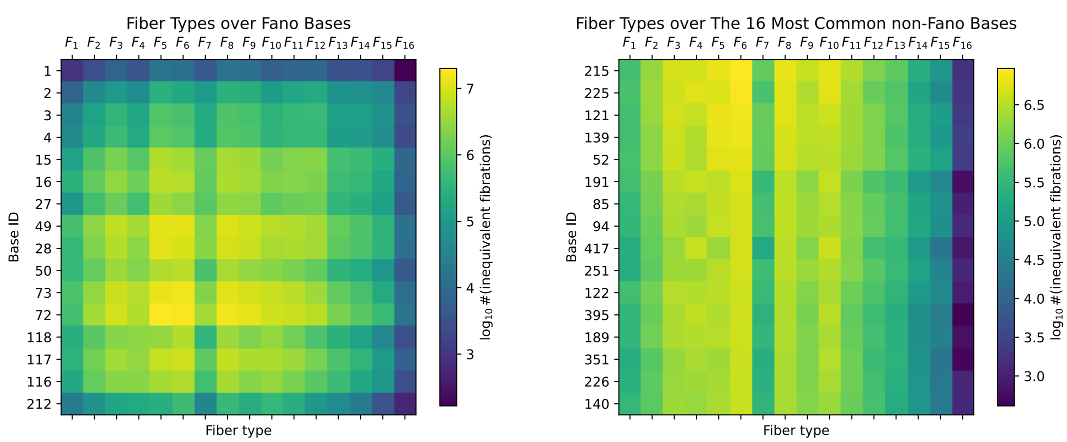

(a) (b)

Figure 8: The distribution of fiber types in irredundant fibrations over (a) the sixteen weak Fano bases and (b) the sixteen most common non-weak-Fano bases.

Base ID	$h^{1,1}(B)$	Int Form	Fib. Structs.	Ineq. Fibs.	Total Fibs.
215	7	[2,2,1,4,1,2,1,1,1]	47,759,092	50,472,765	50,802,116
225	7	[3,1,2,2,1,2,1,2,1]	40,376,100	45,551,690	46,149,521
121	6	[2,1,3,1,2,1,1,1]	41,485,826	44,448,022	44,787,034
139	6	[3,1,2,2,1,1,1,1]	38,213,080	40,125,864	40,428,279
52	5	[1,2,1,3,1,1,0]	36,711,081	37,673,030	37,807,613
191	7	[2,1,3,1,4,1,2,1,0]	28,570,661	29,257,553	29,336,318
85	6	[1,2,1,4,1,2,1,0]	27,158,061	27,660,887	27,748,385
94	6	[1,2,2,1,4,1,1,0]	26,151,001	26,804,201	26,902,391
417	8	[4,1,2,2,2,1,2,1,2,1]	23,597,546	25,187,371	25,507,833
251	7	[4,1,2,2,2,1,1,1,1]	24,163,813	24,818,246	24,951,266
122	6	[2,1,3,1,3,1,1,0]	23,937,142	24,426,767	24,498,388
395	8	[3,1,3,1,4,1,2,1,1,1]	23,166,420	23,778,385	23,883,798
189	7	[2,1,3,1,3,1,2,1,1]	22,293,631	23,307,742	23,467,491
351	8	[2,2,1,4,1,3,1,2,1,1]	20,013,295	20,764,018	20,904,914
226	7	[3,1,2,2,2,1,2,1,1]	19,097,689	19,995,395	20,217,713
140	6	[3,1,2,2,2,1,1,0]	19,439,118	19,948,414	20,068,453

Table 6: Summary statistics for fibrations with the sixteen most common non-weak-Fano bases. We specify the bases by their labels in the MT list. For each base, we have indicated the Hodge number $h^{1,1}(B)$ and the (negative of) its intersection form, as well as the number of fibration structures, the number of inequivalent fibrations, and the total number of fibrations with that base. Note that the first five most common bases in the list differ from weak Fano by containing only a single curve of self-intersection -3 or -4.

Fiber	Singularity	Sing. Fib. Structures	Ineq. Sing. Fibs.	Total Sing. Fibs.
F_1	$(\mathbb{Z}_3)$	614,963	617,188	627,149
F_2	$(\mathbb{Z}_2)$	1,508,437	1,516,024	1,527,877
F_4	$(\mathbb{Z}_2)$	8,982,183	9,002,823	9,029,636

Table 7: Summary statistics for fibrations of each fiber type over singular bases with a given local singularity structure. We list only the genus-one fibers; elliptic fibrations with singular bases do not occur. For each fiber, we have indicated the characteristic singularity structure, the number of fibration structures, the number of inequivalent fibrations, and the total number of fibrations with that fiber type.

these fibrations have nontrivial discrete monodromy around the singularities. We leave further investigation of this interesting structure to further work.

Of the 61,539 toric bases, only 17,961 appear as the resolution of a singular base in a genus-one fibration. The most common base is base 417, a non-weak-Fano base with $h^{1,1}(B) = 8$ and which appears as (the resolution of) the base in 3.3% (372,445 total, 370,503 inequivalent) of such fibrations. The most common overall base, MT base 72 or equivalently the fiber F_{12}, appears as a singular base in only 1% (116,300 total, 115,138 inequivalent) of such fibrations. In spite of this shift, the statistical preference for small $h^{1,1}(B)$ remains; the largest singular base has $h^{1,1}(B) = 92$, and 97.7% (10,929,212 total, 10,882,539) of such fibrations have $h^{1,1}(B) \leq 25$.

4.4 Rank increase

One useful way of quantifying

the structure of a fibration is through the number of divisors that arise in the (tuned or non-Higgsable) gauge group, which by Shioda-Tate-Wazir is the difference between $h^{1,1}(X)$ and $h^{1,1}(B)$. We define two closely related notions of rank increase, the total rank increase

$$\delta_{\text{total}} := h^{1,1}(X) - h^{1,1}(B) - 1\,, \tag{4.2}$$

and the tuned rank increase

$$\delta_{\text{tuned}} := h^{1,1}(X) - \left[h^{1,1}(B) + \mathrm{rk}\,(\mathrm{NHC})\right] - 1. \tag{4.3}$$

We have the obvious bound

$$\delta_{\text{tuned}} \leq \delta_{\text{total}}, \tag{4.4}$$

with $\delta_{\text{tuned}} = \delta_{\text{total}}$ only for fibrations over a weak Fano base, and $\delta_{\text{tuned}} = 0$ for the generic elliptic fibration over a given base.

While for a weak Fano base these two notions coincide, for a non-weak-Fano base the tuned rank increase more closely quantifies how much tuning the fibration has by subtracting out a universal contribution from the NHC; we therefore find it to be a more useful definition. We have computed both the total and tuned rank increase for each fibration, but for the remainder of this section we will comment only on the tuned rank increases; for brevity, we will refer to the tuned rank increase simply as the rank increase in what follows.

Note that, for elliptic fibrations, the rank increase is nonnegative by Shioda-Tate Wazir. Nevertheless, we find fibrations with negative rank increase; this occurs only in genus-one fibrations, and is relatively rare, occurring in a total of only 3,868,168 fibrations (3,829,298 inequivalent). The appearance of negative rank increase reflects the fact that the Hodge numbers of the Jacobian fibration of a genus-one fibration are generally not equal to those of the genus-one fibered threefold [60, 61]. To avoid this complication, in what follows we will consider only genuine elliptic fibrations.

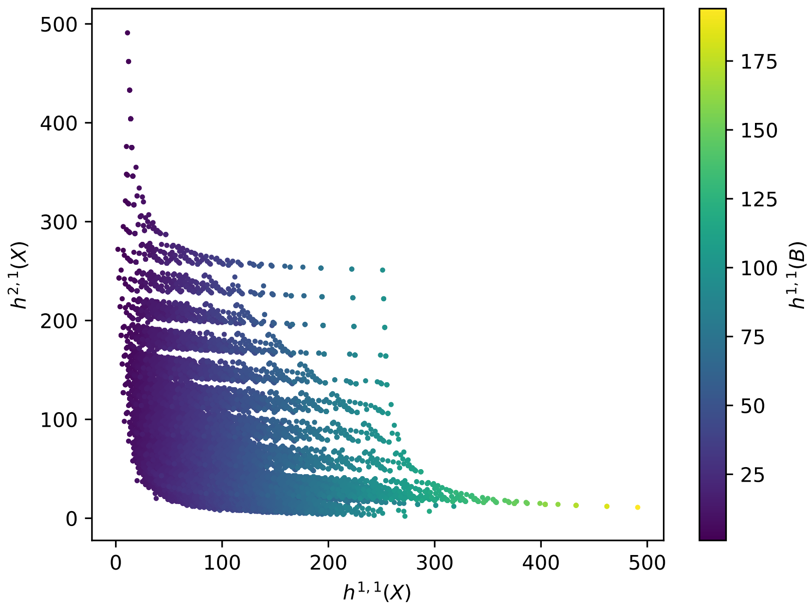

Figure 9: The Hodge numbers of the generic elliptic fibration over each base in the the MT list. For each Hodge pair, $h^{1,1}(B)$ is indicated by the color. 7,524 of the 30,108 unique Hodge pairs in the Kreuzer-Skarke list are realized in this way.

In the context of elliptic fibrations, we find a total of 630,778 (630,291 inequivalent) fibrations with rank increase zero, all of which have fiber F_{10}; we find at least one such fibration over each of the 61,539 bases in the MT list. A total of 10,558 bases appear as the base for only a single rank-increase zero elliptic fibration; in particular, each of the sixteen weak Fano bases appears only once. The remaining 50,981 bases appear more than once; moreover, all fibrations over a fixed base with $\delta_{\text{tuned}} = 0$ are found in polytopes with the same Hodge pair, as expected from Shioda-Tate-Wazir. For instance, the most common base for fibrations with rank increase zero is MT base 3868, which appears as the base in 2,865 such fibrations; all of these fibrations originate in polytopes with $h^{1,1} = h^{2,1} = 39$. We have plotted the Hodge numbers of the generic elliptic fibration over each base in the MT list in Figure 9.

The remaining 1,828,049,985 elliptic fibrations (1,817,131,593 inequivalent) have positive rank increase. We have plotted the number of inequivalent elliptic fibrations of each rank increase in Figure 10. The largest bases that appear with positive rank increase are bases 61,521 and 61,523, each of which has $h^{1,1}(B) = 150$ and appears as the base for a single fibration with $\delta_{\text{tuned}} = 1$. The most common rank increase is $\delta_{\text{tuned}} = 15$, which occurs in 101,205,632 elliptic fibrations (100,589,846 inequivalent). We find that large rank increases are extremely rare; only 3,933 (3,931 inequivalent) fibrations have $\delta_{\text{tuned}} \geq 200$.

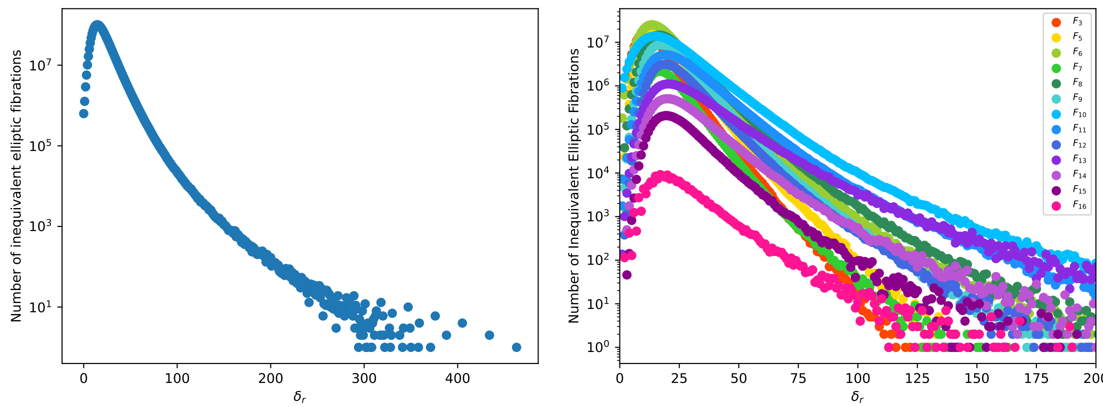

(a) (b)

Figure 10: The number of inequivalent elliptic fibrations as a function of rank increase. In Figure (a), we have combined all fiber types; in Figure (b), we split the fibrations by fiber type and have zoomed in to the window $0 \leq \delta_r \leq 200$.

We have plotted the relative density of each of the thirteen fiber types of elliptic fibrations in Figure 11; from this figure, it is clear that fibrations by fiber F_{13} dominate at large δ_r. The largest rank increase is $\delta_r = 463$, found in an F_{13} fibration over base 680 in polytope v05-393, the unique polytope with $h^{1,1}(X) = 491$; we discuss this polytope and its fibrations in §5.6. Indeed, this fiber-base pair is universal at large δ_r; the largest rank increase that does not come from an F_{13} fibration over base 680 is 350, found in an F_{13} fibration over base 679 in a polytope v06-2907, which has $h^{1,1}(10) = 376$, $h^{2,1}(X) = 10$. By Eq. 2.14c, given an elliptic fibration in a CY3 with Hodge numbers $h^{1,1}, h^{2,1}$, we can sometimes trade one unit of $h^{1,1}$ for 29 units of $h^{2,1}$. The prevalence of fibrations of F_{13} over base 680 at large δ_r can (at least in part) be explained by the mirror of this process (which will also be described further in [67]): their Hodge numbers are given by $h^{1,1}(X) = 491 - 29n$, $h^{2,1}(X) = 11 + n$, as expected for the images of the F_{13} fibration in the $h^{1,1} = 491$ polytope under the mirror of these $\Delta T = 1$ transitions. Indeed, in Figure 6 it is clear that fibrations over base 680 dominate the large $h^{1,1}(X)$ regime.

Finally, we note a curious fact: each polytope hosting one of these large rank-increase fibrations of fiber F_{13} over base 680 also possesses a second fibration, namely the generic elliptic fibration over a base with very large $h^{1,1}(B)$. For instance, as discussed in §5.6, the polytope with $h^{1,1}(X) = 491$ also hosts the generic elliptic fibration over the largest toric base. Although we currently cannot explain this empirical phenomenon, we hope that the ideas of [9] can be applied to these pairs of fibrations.

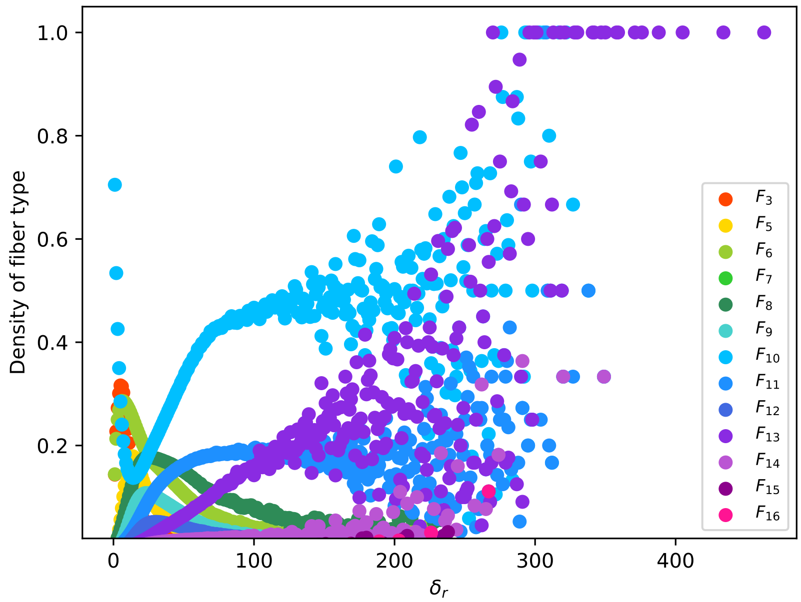

Figure 11: The relative density of each fiber type as a function of rank increase. Note that at large δ_r, fibrations by fiber F_{13} dominate.

5 Examples

In the previous section, we discussed properties of the entire ensemble of fibrations. In this section, we take the opposite approach, and analyze a small number of explicit fibrations and their description in F-theory, focusing primarily on those that either exhibit exotic features or connect to the existing literature. In general, F-theory compactifications on genuine elliptic fibrations are much better understood than those on genus-one fibrations, and so in this section we will focus on elliptic fibrations. Our goal in this section is twofold: to use the F-theory description of elliptic Calabi-Yaus as a way of understanding geometric structure, and to understand what kinds of F-theory models are realized through these constructions.

5.1 Fibrations with base $\mathbb{P}^2$

In §4.3.1, we enumerated fibrations over the sixteen weak Fano bases. Note that one of the Fano bases, MT ID 1, is simply $\mathbb{P}^2$. Automorphism-inequivalent toric fibrations over $\mathbb{P}^2$ were enumerated in [21]; our count of 102,581 such fibrations exactly matches with the count in that work.[9] In the following subsections, and in particular 5.3, we will re-analyze some specific examples discussed in [21] and provide a new perspective on their physics and geometry.

[9]We thank V. Braun for helpful discussions on this comparison.

5.2 Gauge groups over non-toric divisors; Examples: SU(N) on $\mathbb{P}^2$

One interesting feature of the fibrations found in the KS database is that, in many cases, nonabelian groups are tuned over non-toric divisors in a toric base. This can occur with a variety of fiber types, and even with the fiber F_{10} with non-standard stackings. This can occur for any fiber type when the divisor associated to one of the "generic" nonabelian gauge factors appearing in the appropriate line of Table 2 is not simply a single toric divisor.[10] Inspecting Table 2, we see that the only nonabelian gauge factors we can hope to realize in this way are those with algebras $\mathfrak{su}(2)$, $\mathfrak{su}(3)$, and $\mathfrak{su}(4)$. In this subsection, we demonstrate that all three of these types of gauge group can be realized on nontoric divisors in elliptic fibrations over $\mathbb{P}^2$.

5.2.1 SU(2) on non-toric divisors

As a specific example of this kind of construction, one can realize $SU(2)$ gauge groups on divisors of degree up to the maximum allowed degree of twelve. Consider the family of polytopes whose vertices are given by the columns of the matrix

$$\begin{pmatrix} 1 & 0 & -2 & 0 & 0 & -6+n \\ 0 & 1 & -3 & 0 & 0 & -9+n \\ 0 & 0 & 0 & 1 & 0 & -1 \\ 0 & 0 & 0 & 0 & 1 & -1 \end{pmatrix} \tag{5.1}$$

for $1 \leq n \leq 12$; these polytopes are summarized in Table 8.

The cases $9 \leq n \leq 11$ are subtle, so we begin with the remaining nine cases. These polytopes all have $h^{1,1} = 3$, and $h^{2,1}$ is determined by n via

$$h^{2,1}(n) = 3n^2 - 45n + 273. \tag{5.2}$$

Each of these polytopes has a single fibration, a nonstandard stacking of base $\mathbb{P}^2$ over fiber F_{10}. The total gauge group has rank 1 in each case, and we thus expect the $SU(3)$ factors must be absent; this implies that α must consist of a single monomial in each example, and this is in fact the case. However, the $SU(2)$ factor can be present, and explicit analysis of the Weierstrass model shows that such a factor indeed is present in each of these eight polytopes. In each case, β consists of

$$n_\beta = \frac{(n+1)(n+2)}{2} \tag{5.3}$$

monomials, forming a generic homogeneous polynomial of degree n on $\mathbb{P}^2$. (As discussed in § 2.6, monomials in β correspond to points $(2, -1; m)$ in the dual polytope, which are easily

[10] While these are the simplest examples of gauge groups hosted on nontoric divisors, they are not the only type; in the next subsection, we will encounter examples where the nontoric divisors hosting nonabelian gauge groups are absent in the toric description in the base, and only appear after resolving loci of the base where the fibration is "too singular", i.e. after resolving (4,6) points in the base, generally producing a new base which is itself non-toric.

ID	$(h^{1,1}, h^{2,1})$	n_β	deg(β)
v07-192	(3,231)	3	1
v07-190	(3,195)	6	2
v07-189	(3,165)	10	3
v07-187	(3,141)	15	4
v07-176	(3,123)	21	5
v07-147	(3,111)	28	6
v07-134	(3,105)	36	7
v07-136	(3,105)	45	8
v05-64	(4, 112)	55	9
v07-748	(4, 126)	66	10
v07-771	(4, 144)	78	11
v05-48	(3, 165)	91	12

Table 8: Polytopes with fibrations over $\mathbb{P}^2$ exhibiting an $\mathfrak{su}(2)$ gauge algebra tuned on the nontoric divisor nH for $1 \leq n \leq 12$. For each polytope, we give its ID, its Hodge numbers, the number of monomials in β, and the degree of β as a divisor in the base, so that $SU(2)$ is tuned on $\deg(\beta)H$.

enumerated.) Thus the fibrations of these polytopes contain an $SU(2)$ gauge group that has been tuned over a degree-n curve in the base, or equivalently on the nontoric divisor nH. From anomaly cancellation (see e.g. Table 7 in [56]), we know that the massless matter spectrum charged under such an SU(2) consists of $6n^2 + 16(1-g)$ fields in the fundamental representation and g fields in the adjoint representation, where $g = (n-1)(n-2)/2$ is the genus of the generic degree-n curve. Recalling that the Cartan elements of the adjoint do not contribute to H_{charged}, we see that this matter spectrum nicely matches with (2.14c) and the above formula for $h^{2,1}$.

Next, we consider the case $n = 9$, for which Eq. 5.1 once again furnishes a reflexive polytope, with Hodge numbers $h^{1,1}(X) = 4$, $h^{2,1}(X) = 112$. As before, this polytope has a single fibration, a nonstandard stacking of $\mathbb{P}^2$ over of F_{10}, and for $n = 9$, we find that β consists of 55 monomials, as expected for $\mathfrak{su}(2)$ hosted on a degree-nine curve. From the above discussion, for $\mathfrak{su}(2)$ on a nonic curve we expect 28 adjoints and 54 fundamentals, which would yield $h^{2,1}(X) = 111$. To satisfy Eq. 2.13, we require an additional gauge factor; since no toric divisors host nonabelian gauge groups and α consists of a single monomial, we conclude that the missing gauge factor is a $U(1)$. Furthermore, since the discrepancies in the Hodge numbers in the model without the U(1) factor are the same, all matter charged under this abelian gauge factor must also be charged under the SU(2). These constraints are nicely satisfied by the theory with gauge group $(SU(2) \times U(1))/\mathbb{Z}_2$, in which there are 27 fields in each of the representations $(\mathbf{2}, \pm\mathbf{1})$. This theory illustrates two general principles that have been identified in 6D F-theory models, and are hypothesized to hold in general but have not yet been fully proven. First, the global structure of the gauge group is fixed by the *massless charge completeness* hypothesis [68], which suggests that the gauge group does not contain any central elements under which the massless spectrum is invariant; this spectrum is invariant under the $\mathbb{Z}_2$ diagonal central element of $SU(2)\times U(1)$, so we select the quotient to project out this element. Second, the *automatic enhancement conjecture* [69] states that the additional U(1) factor here is a necessary consequence of the SU(2) spectrum; that is, since the U(1) factor cannot be broken through a Higgs mechanism while preserving the SU(2) symmetry, any Weierstrass model over $\mathbb{P}^2$ with an SU(2) tuned over a degree 9 curve will automatically force the presence of an additional U(1) factor of this form that enhances the Mordell-Weil group of the associated threefold. Indeed, precisely this example (as well as the cases with $n = 10, 11, 12$) is discussed in [69].

Next, we consider the cases $n = 10, 11$, for which Eq. 5.1 does not furnish a reflexive polytope. Instead, we employ the "dual of the dual" construction described above to find the polytopes whose vertices are given by the columns of the matrix

$$\begin{pmatrix} 2 & 0 & -2 & 0 & 0 & -6+n \\ 1 & 1 & -3 & 0 & 0 & -9+n \\ 0 & 0 & 0 & 1 & 0 & -1 \\ 0 & 0 & 0 & 0 & 1 & -1 \end{pmatrix}. \tag{5.4}$$

These are reflexive polytopes with $h^{1,1}(X) = 4$ and

$$h^{2,1}(X) = \begin{cases} 126, & n = 10 \\ 144, & n = 11 \end{cases} = 3n^2 - 45n + 276. \tag{5.5}$$

These polytopes each have a single fiber, with vertices given by the columns of the matrix

$$\begin{pmatrix} 2 & 0 & -2 \\ 1 & 1 & -3 \\ 0 & 0 & 0 \\ 0 & 0 & 0 \end{pmatrix}. \tag{5.6}$$

These subpolytopes have three vertices and seven total points each, and so we see that the effect of the "dual of the dual" procedure is to replace the F_{10} fiber in Eq. 5.1 with an F_{13} fiber. The generic gauge group associated to F_{13} fibrations was determined in [40] to be $(SU(4) \times SU(2)^2)/\mathbb{Z}_2$; in terms of the Weierstrass coefficients in Eq. 2.9, the $\mathfrak{su}(4)$ is hosted on α, one $\mathfrak{su}(2)$ is hosted on β as in F_{10} fibrations, and the other $\mathfrak{su}(2)$ is hosted on a_4. In these polytopes, the $\mathfrak{su}(4)$ is not turned on, but both $\mathfrak{su}(2)$ factors are. As above, β consists of $(n + 1)(n + 2)/2$ monomials, and so for $n = 10, 11$, we have an $\mathfrak{su}(2)$ tuned on divisors of degree 10 and 11, respectively, as desired. On the other hand, a_4 consists of $(13-n)(14-n)/2$ monomials, and so the other $\mathfrak{su}(2)$ is tuned on divisors of degrees 2 and 1, respectively. These cases exactly match the expectation from the automatic enhancement conjecture. Tuning SU(2) on a degree 10 or 11 curve forces a gauge group $(SU(2) \times SU(2))/\mathbb{Z}_2$, where all matter charged under the second SU(2) is also charged under the first SU(2) factor. For degree 10, there are 36 adjoints under the first SU(2) and 20 bifundamental fields $(\mathbf{2}, \mathbf{2})$, and in degree 11 there are 45 adjoints under the first SU(2) and 11 bifundamental fields. Note that in both cases the global structure of the gauge group is also compatible with the massless charge completeness conjecture.

It is also worth noting that for the degree 12 case, the spectrum consists of 55 adjoints, and the gauge group is actually $SO(3) = SU(2)/\mathbb{Z}_2$. This matches the massless charge completeness hypothesis and is shown explicitly by constructing the explicit torsion section in this case in [68].

Finally, it is worth noting that this set of polytopes thus includes every single possible elliptic Calabi-Yau threefold with a $\mathbb{P}^2$ base and the minimal gauge group and matter compatible with tuning only a nonabelian SU(2) factor. For $n = 13$, the anomaly cancellation conditions cannot be satisfied for any SU(2) matter content. Furthermore, this set of polytopes includes all possible elliptic Calabi-Yau threefolds with $h^{1,1}(X) = 3$ and only a nonabelian gauge group in the F-theory picture, for similar reasons to the above.

5.2.2 SU(4) on a non-toric divisor

Using this general mechanism, we expect a variety of realizations of SU(2), SU(3), and SU(4) gauge factors over non-toric divisors, often in combination with U(1) and other gauge factors. We have not identified cases with any other gauge factors over non-toric divisors in purely toric bases, although as mentioned above, there are gauge groups that can be tuned over non-toric divisors in more general non-toric resolved bases.

We also provide some simple but interesting examples where $SU(3)$ and $SU(4)$ are realized in this way in fibrations over $\mathbb{P}^2$. We begin with the SU(4) case, which is conceptually slightly more straightforward. To realize $SU(4)$ on a non-toric divisor in $\mathbb{P}^2$, we consider the polytope v05-110, whose vertices are given by the columns of the matrix

$$\begin{pmatrix} -1 & -1 & 1 & 1 & 1 \\ -2 & 2 & 0 & 0 & 0 \\ 0 & 0 & 1 & 0 & -1 \\ 0 & 0 & 0 & 1 & -1 \end{pmatrix}. \tag{5.7}$$

This polytope has $h^{1,1} = 6$, $h^{2,1} = 60$, and is a stacking of $\mathbb{P}^2$ over the vertex $(1, 0)$ of the fiber F_{13}. The analysis of [40] indicates that $SU(4)$ is tuned on the vanishing locus of the coefficient a_{012} in the cubic; in this geometry, a_{012} contains 28 monomials, as expected for a generic polynomial of degree 6, so we conclude that this fibration has an $SU(4)$ gauge group on a sextic in $\mathbb{P}^2$. From anomaly cancellation, we can ascertain that the massless spectrum for such an SU(4) factor will consist of no fields in the fundamental, 18 fields in the antisymmetric $(\mathbf{6})$ representation, and 10 fields in the adjoint $(\mathbf{15})$ representation. If this was the only gauge group and matter, we would expect to have a Calabi-Yau threefold with $h^{1,1} = 5, h^{2,1} = 59$. Thus, there is an additional hidden gauge factor. Since there are no other nonabelian factors manifest in the Weierstrass model, this must again be an abelian factor. Furthermore, since the discrepancies in the Hodge numbers are the same, again, all matter charged under this abelian gauge factor must also be charged under the nonabelian factor SU(4). These constraints are nicely satisfied by the theory with gauge group

$$G = (SU(4) \times U(1))/\mathbb{Z}_2 \,, \tag{5.8}$$

in which there are 9 fields in each of the representations $(\mathbf{6}, \pm\mathbf{1})$. This theory provides another nice example of both the massless charge completeness hypothesis and the automatic enhancement conjecture, which suggests that the additional U(1) factor here is a necessary consequence of the SU(4) spectrum; that is, since the U(1) factor cannot be broken through a Higgs mechanism while preserving the SU(4) symmetry, it seems that any Weierstrass model over $\mathbb{P}^2$ with an SU(4) tuned over a sextic curve will automatically force the presence of an additional U(1) factor of this form that enhances the Mordell-Weil group of the associated threefold. We have not checked this explicitly but leave confirmation of this as an interesting calculation for further work.

5.2.3 SU(3) on a non-toric curve

To realize SU(3), we consider polytope v05-108, a nonstandard stacking of a $\mathbb{P}^2$ base over fiber F_{10} whose vertices are given by the columns of the matrix

$$\begin{pmatrix} 1 & 0 & 0 & 0 & -2 \\ 0 & 1 & 1 & 1 & -3 \\ 0 & 1 & 0 & -1 & 0 \\ 0 & 0 & 1 & -1 & 0 \end{pmatrix} . \tag{5.9}$$

This polytope has $h^{1,1} = 6$, $h^{2,1} = 60$, and is a stacking of $\mathbb{P}^2$ over the vertex of F_{10} corresponding to the Weierstrass variable y in Eq. A.8. As discussed in 2.6, we expect the divisor α sitting in front of the y^2 term in the generalized long Weierstrass form to host an SU(3) gauge group whenever it consists of more than one monomial. In this polytope, α consists of 28 monomials, and so we realize an SU(3) gauge group on a generic sextic curve in $\mathbb{P}^2$. Anomaly cancellation again allows us to identify the spectrum of massless charged fields, which consists of 54 fields in the fundamental and 10 fields in the adjoint. If this was the only gauge group and matter, we would expect to have a Calabi-Yau threefold with $h^{1,1} = 4, h^{2,1} = 58$. Thus, there must be a hidden gauge group. Again, in this case there is no manifest nonabelian factor so we must have two U(1) factors, and again all matter charged under the U(1) factors must be also charged under the SU(3). A solution to this set of constraints is given by a theory with gauge group

$$G = (SU(3) \times U(1) \times U(1))/\mathbb{Z}_3 \,, \tag{5.10}$$

containing 18 fields in each of the representations $(\mathbf{3}, \mathbf{1}, \mathbf{1}), (\mathbf{3}, -\mathbf{1}, \mathbf{0}), (\mathbf{3}, \mathbf{0}, -\mathbf{1})$. This spectrum again manifests the principles of massless charge completeness and automatic enhancement; it seems that any tuning of SU(3) on a degree 6 curve in $\mathbb{P}^2$ will automatically have these extra U(1) factors in this form. Note that this spectrum can also be understood as arising from a Higgsing of a theory with gauge group $(SU(3) \times SU(3))/\mathbb{Z}_3$, with the SU(3) factors respectively living on a sextic and a cubic, where Higgsing is carried out on the single adjoint representation of the second SU(3) factor. This construction of the above $U(1) \times U(1)$ spectrum was realized in [32].

5.3 SCFTs and non-toric bases; Example: Maximum rank increase over $\mathbb{P}^2$

It is interesting to consider the example of the fibration over $\mathbb{P}^2$ with the largest $h^{1,1}(X)$. This Calabi Yau was identified in [21], where it was noted that the apparent gauge group is $SU(27)$, supported on the divisor H, and there are an additional 84 divisors encoded in non-flat fibers, giving a total of $h^{1,1}(X) = 112$. The polytope, whose ID is v05-65, has $h^{2,1} = 4$, and the fiber type in this fibration is F_{16}. We can understand this geometry in terms of an interesting SCFT with a natural geometric resolution.

Simply from the structure of the gauge group and an analysis of the F-theory and Weierstrass models, it is known that the gauge group SU(27) cannot be realized on the base $\mathbb{P}^2$ in a straightforward way. Anomaly cancellation considerations show that with only the gauge group SU(N), for $N > 24$ the number of fundamental matter representations would go negative, and SU(24) is the largest SU(N) group that can be tuned in an F-theory Weierstrass model without singularities outside the Kodaira classification of Table 1 [70].

Indeed, as pointed out in [21], in this model, there are three points on the base where the orders of vanishing of the Weierstrass coefficient f, g reach (4, 6), signaling a non-flat fiber, which can be interpreted as an SCFT coupled to the gravity theory [35, 36].

To analyze this geometry in more detail, we consider the explicit Weierstrass model for this fibration. Since the fiber is F_{16}, the monomials live in the dual fiber F_1, and we can think of this as a specialized Tate-form Weierstrass model as in Eq. 2.5, where the only non-vanishing a_i coefficients are a_1, a_3. More explicitly, we can put the polytope into (fiber; base) coordinates where the vertices are the columns of the matrix

$$\text{vertices}(\nabla) = \begin{pmatrix} 0 & 0 & 6 & -3 & -3 \\ 0 & 0 & -3 & 6 & -3 \\ 1 & 0 & -1 & -1 & -1 \\ 0 & 1 & -1 & -1 & -1 \end{pmatrix}. \tag{5.11}$$

so the vertices of the dual polytope are

$$\text{vertices}(\nabla^\circ) = \begin{pmatrix} 1 & 0 & 0 & 0 & -1 \\ 0 & 1 & 0 & 0 & -1 \\ -1 & -1 & 2 & -1 & -1 \\ -1 & -1 & -1 & 2 & -1 \end{pmatrix}, \tag{5.12}$$

or after a linear transformation

$$\text{vertices}(\nabla^\circ) = \begin{pmatrix} 1 & 0 & 0 & 0 & -1 \\ 0 & 1 & 0 & 0 & -1 \\ 0 & 0 & 2 & -1 & -3 \\ 0 & 0 & -1 & 2 & -3 \end{pmatrix}. \tag{5.13}$$

This corresponds to a Tate form Weierstrass model with a_1 a general cubic and a_3 of the form w^9.

The coefficients f, g and the discriminant can be written in local coordinates (x, w) on the base, where $x = 0$ is a (generically non-toric) root of $a_1 = x\tilde{g}(x, w) = 0$, as

$$f = -(a_1^4 - 24a_1a_3)/48 \sim x(x^3\tilde{g}(x, w)^3 + w^9)\tilde{g}(x, w)\,, \tag{5.14}$$

$$g = -(a_1^6 + 36a_1^3a_3 - 216a_3^2)/864 \sim (x^6\tilde{g}(x, w)^6 + x^3\tilde{g}(x, w)^3w^9 + w^{18})\,, \tag{5.15}$$

and

$$\Delta = a_3^3(a_1^3 - 27a_3) \sim w^{27}(w^9 + x^3\tilde{g}(x, w)^3)\,, \tag{5.16}$$

where $\sim$ means that we have dropped constant coefficients. There is a (4, 6) locus at the non-toric point $x = w = 0$. We blow up at this point by making the new local chart $(x, w) \to (u\hat{x}, u)$. We then have

$$f \to u^4[\hat{x}^4\tilde{g}^4 + u^5\tilde{g}] \tag{5.17}$$

$$g \to u^6[\hat{x}^6\tilde{g}^6 + \hat{x}^3\tilde{g}^3u^6 + u^{15}] \tag{5.18}$$

$$\Delta \to u^{12}[u^{15}(u^9 + u^3x^3\tilde{g}^3)]\,, \tag{5.19}$$

where $\tilde{g}$ is a nonzero constant plus higher order terms in u, x. Dropping the factor of u^{12} from Δ to take the proper transform, we get

$$\Delta \to u^{18}(u^6 + \hat{x}^3\tilde{g}^3)\,. \tag{5.20}$$

We thus see an SU(18) factor on $u = 0$, which is now a -1 curve, while $w = 0$ becomes a -2 curve after blowing up the (4, 6) point at each of the three roots of a_1. Following this branch further, there is another (4, 6) locus at the (non-toric) point where $\hat{x} = 0$ on $u = 0$. Blowing that up, a similar analysis shows that we get an SU(9) factor and one more point we must blow up, giving a chain of curves of self-intersections -2, -2, and -1, with the -2 curves carrying SU(18) and SU(9) gauge factors, respectively. There are three points like this on the original SU(27) locus, so the final geometry is as shown in Figure 12.

In the final resolved geometry, we have a non-toric (but semi-toric [37]) base with $h^{1,1}(B) = 10$. The gauge group is SU(27) $\times$ (SU(18) $\times$ SU(9))^3, and all seven SU(N) factors live on curves of self-intersection -2. In general, the matter content for an SU(N) gauge factor on a -2 curve is $2N$ fundamental matter fields. At each intersection between SU(N) $\times$ SU(N') a bifundamental matter field is supported. It is easy to check that these bifundamentals exactly saturate the anomaly cancellation condition for each SU(N) factor. The total number of charged matter fields is $3 \times 18 \times (9 + 27) = 1944$. We have $T = 9$, and there are $V = 1937$ vector multiplets, from which it is easy to confirm that all anomaly cancellation conditions are properly satisfied with $h^{2,1} = 4$.

This example illustrates a general feature of many fibrations in the database: in the elliptically fibered phase, there are non-flat fibers associated with (4, 6) fibration singularities in the Weierstrass model, corresponding in the F-theory picture to local strongly coupled

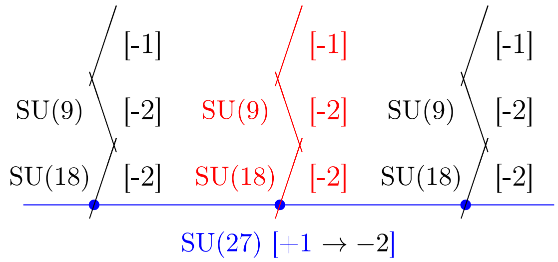

Figure 12: The elliptic fibration over $\mathbb{P}^2$ with largest $h^{1,1}(X)$ $(= 112)$, was identified by Braun, and has an apparently anomalous gauge group of SU(27) tuned on a $+1$ curve H. This is explained by the presence of three SCFT factors associated with (4, 6) loci on H. Resolving the geometry by going out on the tensor branch of these SCFTs gives a theory on a non-toric base with $h^{1,1}(B) = 10$ and a gauge group $\mathrm{SU}(27) \times (\mathrm{SU}(18) \times \mathrm{SU}(9))^3$. The figure depicts the final arrangement of negative self-intersection curves on the non-toric blown-up base.

superconformal field theory sectors. There is a resolved (non-toric) phase for such Calabi-Yau threefolds in which points on the base are blown up, giving generically a non-toric base, often with an enhanced gauge group. [11] This is a much more dramatic version of the familiar presence of (4, 6) loci on -9, -10, and -11 curves in a toric base. The structures of this kind that arise in the toric hypersurface database seem to describe elliptic fibrations over a wide range of non-toric bases. We have not explored this in any depth, but leave for further study the range of non-toric bases that are realized in this fashion in the database. It would be interesting to compare the set of bases realized in this way with previous partial analyses of the full set of non-toric bases [37, 38].

5.4 The most common base (base 72) and fiber (F_6)

As described in §4, the base that supports the most fibrations is base 72, and the most common fiber is fiber F_6. Thus, we may think of this base and fiber as characteristic of the structure of a "typical" Calabi-Yau threefold chosen by taking a random sample from the KS database. We explore here the structure of fibrations with this fiber and base in more detail.

We found that the most common fiber is F_6, so clearly that fiber merits special attention. The generic elliptic curve in F_6 takes the form

$$a_{300}u^3 + a_{210}u^2v + a_{120}uv^2 + a_{030}v^3 + a_{201}u^2w + a_{111}uvw + a_{021}v^2w + a_{102}uw^2 = 0, \quad (5.21)$$

which is a specialization of the generic cubic in $\mathbb{P}^2$. Passing to Weierstrass form as described

[11] Note that similar things can happen for different flop phases/triangulations of a CY where both bases are toric; for example, for a specific triangulation of the generic elliptic fibration (simple stacking) over Hirzebruch $\mathbb{F}_1$, the resulting CY3 is elliptically fibered over $\mathbb{P}^2$ with a non-flat fiber over the toric point that would be blown up to form $\mathbb{F}_1$ [71]; we expect that many examples of this that connect to a non-toric base phase similarly can be associated with flop transitions in the extended Kähler cone.

in Appendix A, we find that the Weierstrass coefficients f, g are given in terms of the a_{ijk} as

$$\begin{aligned} f = &-\frac{1}{48}a_{111}^4 + \frac{1}{6}a_{201}a_{111}^2a_{021} - \frac{1}{3}a_{201}^2a_{021}^2 - \frac{1}{2}a_{030}a_{201}a_{111}a_{102} + \frac{1}{6}a_{120}a_{111}^2a_{102} \\ &+ \frac{1}{3}a_{120}a_{201}a_{021}a_{102} - \frac{1}{2}a_{210}a_{111}a_{021}a_{102} + a_{300}a_{021}^2a_{102} - \frac{1}{3}a_{120}^2a_{102}^2 + a_{210}a_{030}a_{102}^2, \end{aligned} \tag{5.22a}$$

$$\begin{aligned} g = &\frac{1}{864}a_{111}^6 - \frac{1}{72}a_{201}a_{111}^4a_{021} + \frac{1}{18}a_{201}^2a_{111}^2a_{021}^2 - \frac{2}{27}a_{201}^3a_{021}^3 + \frac{1}{24}a_{030}a_{201}a_{111}^3a_{102} - \frac{1}{72}a_{120}a_{111}^4a_{102} \\ &- \frac{1}{6}a_{030}a_{201}^2a_{111}a_{021}a_{102} + \frac{1}{36}a_{120}a_{201}a_{111}^2a_{021}a_{102} + \frac{1}{24}a_{210}a_{111}^3a_{021}a_{102} + \frac{1}{9}a_{120}a_{201}^2a_{021}^2a_{102} \\ &- \frac{1}{6}a_{210}a_{201}a_{111}a_{021}^2a_{102} - \frac{1}{12}a_{300}a_{111}^2a_{021}^2a_{102} + \frac{1}{3}a_{300}a_{201}a_{021}^3a_{102} + \frac{1}{4}a_{030}^2a_{201}^2a_{102}^2 \\ &- \frac{1}{6}a_{120}a_{030}a_{201}a_{111}a_{102}^2 + \frac{1}{18}a_{120}^2a_{111}^2a_{102}^2 - \frac{1}{12}a_{210}a_{030}a_{111}^2a_{102}^2 + \frac{1}{9}a_{120}^2a_{201}a_{021}a_{102}^2 \\ &- \frac{1}{6}a_{210}a_{030}a_{201}a_{021}a_{102}^2 - \frac{1}{6}a_{210}a_{120}a_{111}a_{021}a_{102}^2 + a_{300}a_{030}a_{111}a_{021}a_{102}^2 + \frac{1}{4}a_{210}^2a_{021}^2a_{102}^2 \\ &- \frac{2}{3}a_{300}a_{120}a_{021}^2a_{102}^2 - \frac{2}{27}a_{120}^3a_{102}^3 + \frac{1}{3}a_{210}a_{120}a_{030}a_{102}^3 - a_{300}a_{030}^2a_{102}^3. \end{aligned} \tag{5.22b}$$

Note that these f, g do not generically factor. However, Δ does:

$$\Delta = -16\left(4f^3 + 27g^2\right) \sim -a_{102}^2\,(\text{ten-ic polynomial in the remaining } a_{ijk})\,. \tag{5.23}$$

Thus, whenever a_{102} consists of more than one monomial, we have a Tate-tuned $\mathfrak{su}(2)$ over the locus $a_{102} = 0$ [40]. Additionally, it was shown in [40] that F_6 fibrations always have at least a $U(1)$ abelian sector; whereas the "generic" $\mathfrak{su}(2)$ might or might not be realized in any particular example, this $U(1)$ always appears, regardless of whether any of the a_{ijk} consist of a single monomial. The presence of this extra Mordell-Weil section can also be seen immediately from the fact that the fiber F_6 contains two distinct -1 curves, as mentioned in Section 2.5

In this subsection, we will consider fibrations by F_6 over base 72, which is also fiber F_{12}. This base has seven toric divisors, whose intersection structure is indicated in Figure 13. This is a weak Fano base, and so it has no NHCs.

We will present three examples of (72,6) fibrations: a "generic" example, with Hodge numbers characteristic of the ensemble of such geometries, and two extreme examples, which have the largest $h^{1,1}$ and $h^{2,1}$ of any (72,6) fibration.

5.4.1 A Typical (72,6) Fibration

To illustrate a "typical" example of an F_6 fiber over base 72, consider polytope v07-64854, whose vertices are given by the columns of the matrix

$$\begin{pmatrix} -1 & 0 & 1 & -3 & 0 & 0 & 0 & 0 & 1 \\ -1 & 0 & 0 & -1 & -1 & 0 & 2 & 4 & 4 \\ 0 & 1 & 0 & 2 & -1 & 0 & -1 & -1 & -2 \\ 2 & 0 & 0 & 0 & 0 & 1 & 0 & -2 & -2 \end{pmatrix}. \tag{5.24}$$

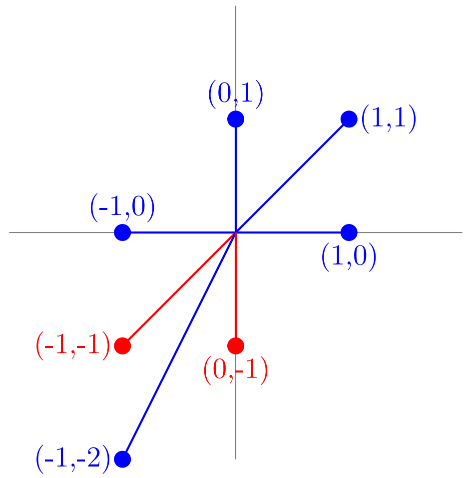

Figure 13: The seven toric divisors in base 72 and their intersection structure. Blue curves have self-intersection -1, and red curves have self-intersection -2.

This polytope has $h^{1,1} = 20, h^{2,1} = 26$, and contains four two-dimensional reflexive subpolytopes: an F_4 fiber with base 118, an F_6 fiber with base 72, an F_8 fiber with base 74, and an F_{10} fiber with base 392. We will analyze the F_6 fibration, and accordingly work in a basis where the subpolytope is in standard form, with vertices given by the columns of the matrix

$$\begin{pmatrix} 1 & 0 & -1 & -1 \\ 0 & 1 & 1 & -1 \\ 0 & 0 & 0 & 0 \\ 0 & 0 & 0 & 0 \end{pmatrix}. \tag{5.25}$$

Because base 72 has $h^{1,1}(B) = 5$, by STW we have a gauge group of total rank $20 - 5 - 1 = 14$. Moreover, by the analysis of [40], the abelian sector has rank at least one, so the total rank of the nonabelian sector of the gauge group is no larger than 13.

In this geometry, four of the eight coefficients a_{ijk}, namely a_{030}, a_{111}, a_{021}, and a_{102}, contain only a single monomial; we thus conclude that the "generic" SU(2) hosted on $a_{102} = 0$ is absent. Base 72 has seven toric divisors, and on these divisors we find three I_0^* singularities, one I_6 singularly, and one III singularity. We find that the toric divisors host a gauge algebra given by

$$\mathfrak{g}_2 \oplus \mathfrak{so}(7) \oplus \mathfrak{so}(8) \oplus \mathfrak{sp}(3) \oplus \mathfrak{su}(2), \tag{5.26}$$

as summarized in Table 9. This algebra has total rank $2+3+4+3+1 = 13$, and so we have completely identified the gauge group of this model (up to a possible discrete quotient) as

$$G = U(1) \times SU(2) \times SO(7) \times SO(8) \times Sp(3) \times G_2. \tag{5.27}$$

Base point	Self-intersection	#(points)	ord(f, g, Δ)	Kodaira type	Gauge algebra
(0,-1)	-2	2	(1,2,3)	III	$\mathfrak{su}(2)$
(1,0)	-1	3	(2,3,6)	I_0^*	$\mathfrak{so}(7)$
(1,1)	-1	1	(0,0,0)	Smooth	$\emptyset$
(0,1)	-1	3	(2,3,6)	I_0^*	$\mathfrak{so}(8)$
(-1,0)	-1	4	(0,0,6)	I_6	$\mathfrak{sp}(3)$
(-1,-1)	-2	2	(2,3,6)	I_0^*	$\mathfrak{g}_2$
(-1,-2)	-1	1	(0,0,0)	Smooth	$\emptyset$

Table 9: The toric gauge group of the F_6 fibration of the polytope in Eq. (5.24). For each of the seven toric divisors in base 72, we specify its self-intersection, the number of points in four-dimensional polytope that project to the base divisor, the orders to which the Weierstrass coefficients f and g and the discriminant Δ vanish on the divisor, the Kodaira singularity type inferred from these vanishings, and the gauge algebra picked out by the monodromies. From this table, we identify that the total nonabelian gauge algebra is $\mathfrak{su}(2)\oplus\mathfrak{so}(7)\oplus\mathfrak{so}(8)\oplus\mathfrak{sp}(3)\oplus\mathfrak{g}_2$, with no additional factors from nontoric divisors.

Now we consider the matter content of the compactification. As mentioned above, we have $h^{1,1}(B) = 5$, and hence

$$T = h^{1,1}(B) - 1 = 4 \tag{5.28}$$

tensor multiplets. From the gauge group G given in Eq. (5.27), we find that

$$V = 1 + 3 + 21 + 28 + 21 + 14 = 88. \tag{5.29}$$

Accordingly, from Eq. (2.14b), the spectrum contains

$$H = V + 273 - 29T = 245 \tag{5.30}$$

hypermultiplets, of which

$$H_{\text{neutral}} = h^{2,1}(X) + 1 = 27 \tag{5.31}$$

are neutral and

$$H_{\text{charged}} = H - H_{neutral} = 218 \tag{5.32}$$

are charged under the Cartan of the gauge group.

It is perhaps interesting to speculate on why it is natural that this kind of base + fiber structure is in some sense “typical”. One feature of base 72 is that it is a generalized del Pezzo surface, i.e. a weak Fano base with only -1 and -2 curves, and no curves of more negative self-intersection that would force a non-Higgsable/rigid gauge group. In some sense this gives the greatest flexibility for tuning gauge groups — for example, if a base has a curve of self-intersection -5 or below, that curve must support a non-Higgsable gauge factor, and no gauge groups can be supported on any curve that intersects that curve. Furthermore, this base has a relatively large number (5) of curves of self-intersection -1, and a relatively large $h^{1,1}(B)$ among weak Fano bases, so the number of places that gauge factors can be tuned and the flexibility in tuning these factors is relatively large. We see that the gauge group factors in this particular model all have relatively low rank (1–4); many of these factors can coexist on intersecting curves, giving a large combinatorial space for the set of possible tunings of low rank gauge factors on all the curves in this base. This makes it seem quite plausible that this kind of structure is indeed potentially typical not only for toric hypersurface Calabi-Yau threefolds, but also for general elliptic Calabi-Yau threefolds: we may expect many possibilities when the base is a generalized del Pezzo and the gauge group factors are relatively small and distributed on many different divisors.

5.4.2 The Largest $h^{2,1}$ (72,6) Fibration

The polytope (ID v12-6536) with the largest $h^{2,1}$ of any (72,6) fibration has vertices given by the columns of the matrix

$$\begin{pmatrix} 1 & -3 & -1 & -1 & -1 & 0 & 0 & 0 \\ 0 & 3 & -1 & 1 & 1 & 0 & 0 & 1 \\ 0 & -1 & 0 & -1 & 1 & 0 & 1 & 0 \\ 0 & -1 & 0 & 1 & -1 & 1 & 0 & 0 \end{pmatrix}. \tag{5.33}$$

This polytope has Hodge numbers $h^{1,1} = 7, h^{2,1} = 97$. Moreover, it contains a single two-dimensional reflexive subpolytope, namely the F_6 fiber; we again work in a basis where the vertices of the subpolytope are given by Eq. (5.25).

By Shioda-Tate-Wazir, we see that the total rank of the gauge group is $r = h^{1,1}(X) - h^{1,1}(B) - 1 = 1$. On the other hand, all F_6 fibrations have at least one $U(1)$ factor, so in this example the entire gauge group is the universal $U(1)$ identified in [40], with no nonabelian sector. Indeed, the Weierstrass coefficient a_{102} which gives rise to the universal $SU(2)$ factor consists of only a single monomial, and hence the $SU(2)$ factor does not appear; moreover, none of the a_{ijk} vanish on any toric divisor, and hence we have no toric Tate tunings, as expected.

We therefore have $V = 1$. As usual in fibrations with base 72, we have $T = 4$, and thus we have $H = 1 + 273 - 116 = 158$ hypers, of which $H_{\text{neutral}} = h^{2,1}(X) + 1 = 98$ are neutral; the remaining 60 hypers are charged under the $U(1)$ gauge group. We can check that this matches perfectly with anomaly cancellation. The anomaly coefficient b for the U(1) factor coming from the extra section associated with the fiber must be $-K$, with $b \cdot b = 5$. This U(1) carries exactly 60 charged fields (which can also be recognized as the number of fields coming from the 30 fundamentals of an SU(2) tuned on the genus-one anticanonical divisor after Higgsing on the single adjoint).

5.4.3 The Largest $h^{1,1}$ (72,6) Fibration

On the other hand, the polytope with the largest $h^{1,1}$ of any (72,6) fibration has vertices given by the columns of

$$\begin{pmatrix} -1 & -1 & -1 & -1 & -1 & -1 & -1 & -1 & 0 & 0 & 1 & 1 & 2 & 5 \\ 1 & 1 & -5 & -1 & -1 & 1 & 1 & 1 & 1 & 1 & 0 & 0 & 1 & -2 \\ 0 & 1 & -1 & -1 & 1 & -1 & -1 & 1 & -1 & 1 & -1 & 1 & -1 & -1 \\ 1 & 1 & -2 & 0 & 0 & -2 & 0 & 0 & 0 & 0 & 0 & 0 & -2 & -2 \end{pmatrix}. \tag{5.34}$$

This polytope (ID v08-22025) has Hodge numbers $h^{1,1}(X) = 68$, $h^{2,1}(X) = 8$, and has 25 two-dimensional reflexive subpolytopes; we will focus on the unique (72,6) fibration, and have again worked in a basis where the vertices of the subpolytope are given by the columns of the matrix in Eq. (5.25). By Shioda-Tate-Wazir, and including the universal $U(1)$ gauge group present in F_6 fibrations, we have $h^{1,1}(X) - 1 - 5 - 1 = 61$ total units of rank to identify in this geometry.

We begin by considering the gauge factors that can be determined by strictly toric information. The coefficient a_{102} consists of only a single monomial, so the univeral $\mathfrak{su}(2)$ is not present. As indicated in Table 10, the toric divisors host a

$$\mathfrak{G}_{\text{toric}} = \mathfrak{su}(15) \oplus \mathfrak{su}(10) \oplus \mathfrak{su}(10) \oplus \mathfrak{su}(5) \oplus \mathfrak{su}(5) \tag{5.35}$$

gauge algebra.

Base point	Self-intersection	#(points)	ord(f, g, Δ)	Kodaira type	Gauge algebra
(0,-1)	-2	10	(0,0,10)	I_{10}	$\mathfrak{su}(10)$
(1,0)	-1	6	(0,0,5)	I_5	$\mathfrak{su}(5)$
(1,1)	-1	1	(0,0,0)	Smooth	$\emptyset$
(0,1)	-1	1	(0,0,0)	Smooth	$\emptyset$
(-1,0)	-1	6	(0,0,5)	I_5	$\mathfrak{su}(5)$
(-1,-1)	-2	10	(0,0,10)	I_{10}	$\mathfrak{su}(10)$
(-1,-2)	-1	31	(0,0,15)	I_{15}	$\mathfrak{su}(15)$

Table 10: The toric gauge group of the F_6 fibration of the polytope in Eq. (5.34). For each of the seven toric divisors in base 72, we specify its self-intersection, the number of points in four-dimensional polytope that project to the base divisor, the orders to which the Weierstrass coefficients f and g and the discriminant Δ vanish on the divisor, the Kodaira singularity type inferred from these vanishings, and the gauge algebra picked out by the monodromies. From this table, we identify that the total nonabelian gauge algebra hosted on toric divisors is $\mathfrak{su}(15) \oplus \mathfrak{su}(10) \oplus \mathfrak{su}(10) \oplus \mathfrak{su}(5) \oplus \mathfrak{su}(5)$.

On each divisor D hosting a toric gauge group, the Weierstrass coefficients are given by

$$f = -\frac{1}{48} a_{111}^4 + \mathcal{O}(z^n), \; g = \frac{1}{846} a_{111}^6 + \mathcal{O}(z^m), \tag{5.36}$$

where $z = 0$ is a local description of the toric divisor and $n, m > 0$ depend on the particular divisor. Thus, if the divisor D intersects the zero locus of a_{111}, we then have a $(4,6)$ point, which must be blown up. a_{111} is a section of $-K$ [40], so it does not intersect the -2 curves, each of which hosts an $\mathfrak{su}(10)$ gauge algebra. Instead, we have $(4,6)$ points on the divisors $(-1,-2), (1,0)$ and $(-1,0)$, each of which must be blown up.

On the $\mathfrak{su}(5)$ curves $(1,0)$ and $(-1,0)$, we have

$$f = -\frac{1}{48}a_{111}^4 + \frac{a_{102}+a_{201}}{6}a_{111}^2 z^2 + \cdots \tag{5.37a}$$

$$g = \frac{1}{864}a_{111}^6 - \frac{a_{102}+a_{201}}{72}a_{111}^4 z^2 + \cdots \tag{5.37b}$$

$$\Delta = a_{102}^2 a_{111}^6 z^5 \left[-a_{300}a_{111} + (a_{300}+a_{201}+a_{300}a_{102})\, z\right] + \cdots \tag{5.37c}$$

We thus have a $(4,6)$ point on the nontoric point $a_{111} = z = 0$, which we resolve with the coordinate transformation

$$(a_{111}, z) \to (\hat{a}u, u) \tag{5.38}$$

at the cost of changing the toric divisor $z = 0$ from a -1 curve to a -2 curve; this yields

$$f = u^4\left(\frac{a_{102}+a_{201}}{6}\hat{a}^2 - \frac{1}{48}\hat{a}^4\right) \tag{5.39a}$$

$$g = u^6\left(-\frac{a_{102}+a_{201}}{72}\hat{a}^4 + \frac{1}{864}\hat{a}^6\right) \tag{5.39b}$$

$$\Delta = a_{102}^2\hat{a}^6 u^{12}\left(a_{300}+a_{201}+a_{300}a_{102}-a_{300}\hat{a}\right) \tag{5.39c}$$

Dropping the factor u^{12} as before, we find that

$$\Delta = a_{102}^2\hat{a}^6\left(a_{300}+a_{201}+a_{300}a_{102}-a_{300}\hat{a}\right), \tag{5.40}$$

and therefore we have no additional gauge algebra or $(4,6)$ points on the -1 curve $u = 0$.

Conversely, on the curve $(-1,-2)$, which hosts an $\mathfrak{su}(15)$ gauge algebra, we have

$$f = -\frac{1}{48}a_{111}^4 + \frac{a_{102}+a_{201}}{6}a_{111}^2 z^6 \tag{5.41a}$$

$$g = \frac{1}{864}a_{111}^4 - \frac{a_{102}+a_{201}}{72}a_{111}^4 z^6 \tag{5.41b}$$

$$\Delta = -a_{102}^2 a_{300}a_{111}^7 z^{15} + a_{102}^2\left(a_{201}+a_{300}+a_{102}a_{300}\right)a_{111}^6 z^{18} \tag{5.41c}$$

so that we have a $(4,6)$ point at $a_{111} = z = 0$,[12] which we can once again resolve by means of Eq. 5.38 to find

$$f = u^4\left(\frac{a_{102}+a_{201}}{6}\hat{a}^2u^4 - \frac{1}{48}\hat{a}^4\right) \tag{5.42a}$$

$$g = u^6\left(-\frac{a_{102}+a_{201}}{72}\hat{a}^4u^4 + \frac{1}{864}\hat{a}^6\right) \tag{5.42b}$$

$$\Delta = a_{102}^2\hat{a}^6u^{10}u^{12}\left[\left(a_{300}+a_{201}+a_{300}a_{102}\right)u^2 - a_{300}\hat{a}\right]. \tag{5.42c}$$

[12]Note that here $z = 0$ is a different divisor than above.

Thus, on the -1 curve $u = 0$, we have tuned an $\mathfrak{su}(10)$ gauge algebra, and we find an additional $(4, 6)$ point at $\hat{a} = u = 0$. Resolving this $(4, 6)$ point by blowing $u = 0$ up to a -2 curve, we obtain a -1 curve with an $\mathfrak{su}(5)$ gauge algebra and yet another $(4, 6)$ point; we must resolve this point as well, which introduces another -1 curve and no further gauge factors. Thus, in total, from blowing up $(4, 6)$ points, we find an additional gauge algebra

$$\mathfrak{G}_{(4,6)} = \mathfrak{su}(10) \oplus \mathfrak{su}(5). \tag{5.43}$$

Putting it all together, we find a compactification on a base B' which is a blowup of B at five points, and accordingly has

$$h^{1,1}(B') = h^{1,1}(B) + 5 = 10. \tag{5.44}$$

The nonabelian gauge algebra is given by

$$\mathfrak{G}_{\text{nonabelian}} = \mathfrak{G}_{\text{toric}} \oplus \mathfrak{G}_{(4,6)} = \mathfrak{su}(15) \oplus \mathfrak{su}(10)^3 \oplus \mathfrak{su}(5)^3, \tag{5.45}$$

and has rank

$$\text{rk}(\mathfrak{G}_{\text{nonabelian}}) = 14 + 27 + 12 = 53. \tag{5.46}$$

Note that the intersection structure of the curves of B' and the gauge groups they host is extremely reminiscent of the pattern in §5.3: a -2 curve hosts an $\mathfrak{su}(3N)$ gauge algebra and intersects three -2 curves, each of which hosts an $\mathfrak{su}(2N)$ gauge algebra and intersects an additional -2 curve hosting a $\mathfrak{su}(N)$ gauge group.

In addition to the nonabelian sector, there is at least one $U(1)$ gauge group. However, with the nonabelian gauge group in Eq. 5.45 and an abelian sector with only a single U(1) factor, the fibration over base B' does not satisfy STW:

$$h^{1,1}(B') + 1 + \text{rk}(\mathfrak{G}_{\text{nonabelian}}) + \text{rk}(U(1)) = 10 + 1 + 53 + 1 = 65 < h^{1,1}(X). \tag{5.47}$$

We conjecture that full abelian sector is $G_{\text{abelian}} = U(1)^4$, so that the entire gauge group is given, up to a possible discrete quotient (see below), by

$$G = G_{\text{abelian}} \times G_{\text{nonabelian}} \tag{5.48a}$$

$$= U(1)^4 \times SU(15) \times SU(10)^3 \times SU(5)^3, \tag{5.48b}$$

which satisfies STW. However, we emphasize that at this stage this is only a conjecture: we have not found an explicit coordinate representation for the missing three Mordell-Weil sections.

We now pass to anomaly cancellation, assuming that the gauge group is as in 5.48b. We have

$$V = 224 + 297 + 72 + 4 = 597. \tag{5.49}$$

We then have

$$H = V + 273 - 29T = 609 \tag{5.50}$$

hypers, of which

$$H_{\text{neutral}} = h^{2,1}(X) + 1 = 9 \tag{5.51}$$

are neutral under the Cartan and

$$H_{\text{charged}} = H - H_{\text{neutral}} = 600 \tag{5.52}$$

are charged. This precisely matches the complete matter content of the SU(N) gauge factors: an SU(N) gauge factor on a -2 curve has $2N$ fundamentals, and intersecting divisors carrying SU(N) gauge factors carry bifundamental matter. It is easy to check that all of the matter for each factor is taken care of by the bifundamentals, and the total number of fields is then just the number of fields charged under the SU(10) factors: $3 \times 20 = 60$ fundamentals, for 600 total charged fields.

This suggests that the U(1) factors must not have any charged matter. That is certainly true for the U(1) factor coming from the F_6 factor, since it has anomaly coefficient $b = -K$, and $-K \cdot -K = 0$ when $T = 10$, so there is no matter charged under this U(1). The only way to satisfy anomaly cancellation for the additional conjectured 3 U(1) factors would be for them to have the same anomaly coefficient. Given the dominant SU(5) structure in this geometry, it is tempting to speculate that these additional U(1) factors all are equivalent to what would arise from an SU(5) factor tuned on $-K$, which would have only a single adjoint and no fundamental matter, which was then broken to $U(1)^4$. Note that all the charged matter in this model is invariant under a central $\mathbb{Z}_5$, so that the massless charge completeness conjecture suggests that the global structure of the group is

$$G = (U(1)^4 \times SU(15) \times SU(10)^3 \times SU(5)^3)/\mathbb{Z}_5 \,, \tag{5.53}$$

which would fit nicely to the conjectured SU(5) structure of the abelian factors. This also has an interesting similarity to the structure identified in Eq. (5.10), suggesting some interesting as-yet unidentified structure for models with a certain global gauge group structure and multiple U(1) factors. We leave further investigation of this in similar models for future work.

5.5 Fiber F_{11} and the Standard Model

As indicated in Table 2, the generic gauge group for fibrations with fiber F_{11} is $(U(1) \times SU(2) \times SU(3))/\mathbb{Z}_6$, i.e. the Standard Model gauge group; this observation has generated significant interest in this fiber [40], and is the origin of, e.g., the quadrillion Standard Models of [72]. This arises because F_{11} can be realized by adding a vertex to F_{10} so that its defining polynomial is a specialization of Eq. 2.9, namely

$$\alpha y^2 + a_1 xyz + a_3 yz^2 = \beta x^3 + a_2 x^2 z^2 + a_4 xz^4. \tag{5.54}$$

In addition to the zero section and the $\mathfrak{su}(2)$ and $\mathfrak{su}(3)$ gauge algebras inherited from F_{10}, this polynomial has an additional Mordell-Weil section $(0 : 0 : 1)$, giving a rank-one Abelian sector and completing the Standard Model.

While we obviously do not live in six space-time dimensions, we expect that any special feature of this fiber type would likely be shared between Calabi-Yau threefolds and the elliptic Calabi-Yau fourfolds that are used for compactifications to 4D, and so it is natural to wonder whether this structure is in some way favored or special in the F-theory landscape. [13] Like the other fibers, F_{11} captures a particular slice of the moduli space of Weierstrass models, with certain specific tuned structures. The general form of the Weierstrass model with this tuned gauge group was described in [73, 74]. From this point of view, there is no *a priori* reason to expect this class of fibrations to be particularly favored, but it is certainly a good question to investigate.

As discussed above, any F_{11} fibration where α and β each contain more than one monomial contains at least the Standard Model gauge algebra, but in general such a fibration can also have a significantly larger gauge algebra. In this section, we classify those fibrations whose gauge algebra is exactly that of the Standard Model.

Any such fibration must have a topological rank increase (as defined in §4.4) of 4, which is the rank of the SM gauge group. Of the 112,327,098 total fibrations with fiber F_{11}, only 5,318 (5,317 inequivalent; one such polytope has two automorphism-equivalent F_{11} fibrations) meet this topological constraint, of which 5120 (5119 inequivalent) fibrations have weak Fano bases and 198 have non-weak-Fano bases. 1,186 fibrations (1,185 inequivalent) realize the Standard Model as described above, through the generic features of F_{11} fibrations; these are necessarily fibrations over weak Fano bases, as fibrations over non-weak-Fano bases will have other gauge factors from the NHCs.

The universal gauge group contribution is not the only way to realize an exact SM in F_{11} fibrations. Even if the nontoric divisors α, β do not host gauge factors in a given fibration, the missing gauge factors can be realized on toric divisors; in such examples, the F_{11} can effectively be thought of as providing the $U(1)$ factor, which is what makes it more useful than F_{10} in the context of the SM. Note, however that in this context the global structure of the gauge group will generally not include the $\mathbb{Z}_6$ quotient, which in the 4D context likely compromises any natural realization of Standard Model-like matter in such constructions [55].

For instance, consider F_{11} fibrations over the Hirzebruch surface $\mathbb{F}_3$, which has a single SU(3) NHC. Any such fibration has a gauge group no smaller than $U(1) \times SU(3)$, and hence we expect such fibrations to have $h^{1,1}(X) \geq 1 + h^{1,1}(\mathbb{F}_3) + 1 + \mathrm{rk}(SU(3)) = 6$. In fact, there is a single F_{11} fibration over $\mathbb{F}_3$ with $h^{1,1}(X) = 6$, with $h^{2,1}(X) = 152$; all other F_{11} fibrations over $\mathbb{F}_3$ have a larger gauge group.

There are seven F_{11} fibrations over $\mathbb{F}_3$ with $h^{1,1} = 7$, which is the correct rank increase to realize the SM. Because of the $SU(3)$ NHC, by STW we cannot activate the generic $\mathfrak{su}(3)$ on β; conversely, we can activate the generic $\mathfrak{su}(2)$ on α, and indeed whenever that occurs we will

[13] We would like to thank Damien Mayorga Pena for discussions on this issue.

have realized the full SM gauge algebra. This "hybrid" standard model gauge algebra (with potentially different global structure) occurs in five of the seven models mentioned above. One of the remaining two $h^{1,1} = 7$ models is actually yet another realization of the Standard Model, with $\mathfrak{su}(2)$ tuned on a toric divisor and $\mathfrak{su}(3)$ on the NHC; the final model has its NHC enhanced to $\mathfrak{so}(7)$ and no additional nontoric gauge algebras.

Thus, exact Standard Model gauge groups, i.e. those with no additional gauge factors, are rare, occurring in no more than 0.0023% of all fibrations.

5.6 Example: the largest $h^{1,1}(X)$ (polytope with $h^{1,1} = 491$)

It is naturally interesting to consider the polytopes with the largest values of the Hodge numbers. It has been known for many years that the largest values of the Hodge numbers $h^{1,1}, h^{2,1}$ for toric hypersurface Calabi-Yau threefolds are threefolds with $h^{1,1}(X) = 491, h^{2,1}(X) = 11$ and $h^{2,1}(X) = 491, h^{1,1} = 11$, respectively [44, 66]. There is a unique polytope (ID v05-394) with $h^{2,1}(X) = 491$, and it has a unique elliptic fibration, namely the standard stacking of fiber F_{10} over Hirzebruch $\mathbb{F}_{12}$; it is easily proven that this is in fact the largest $h^{2,1}(X)$ that can be realized in any elliptic Calabi-Yau threefold, and not just the largest possible in toric hypersurfaces [75].

It is much harder to prove rigorously that $h^{1,1}(X) = 491$ is a strict upper bound for general elliptic Calabi-Yau threefolds. It was shown long ago by studying dual heterotic instantons that there are two different F-theory models corresponding to an elliptic Calabi-Yau threefold with Hodge numbers $h^{2,1}(X) = 491, h^{1,1} = 11$ [66]. One of these corresponds to a 6D F-theory model with a large gauge group with many E_8 factors, related to the $E_8 \times E_8$ heterotic theory, and the other has a large gauge group with $Sp(N)$ and $SO(N)$ factors (and the largest gauge group rank known for any 6D supergravity model), related to the $\mathrm{Spin}(32)/\mathbb{Z}_2$ heterotic theory. In the intervening years these structures have been encountered in various ways in the literature. The Calabi-Yau threefold with these Hodge numbers and the large E_8-type gauge group was found in [34] to be a generic elliptic fibration over the maximal toric base, with $h^{1,1}(B) = 194$. From a rather different point of view, the authors of [76] argued (with some plausible physical assumptions) for the upper bound of $h^{1,1} = 491$ for an elliptic CY3, and argued that the two 6D $\mathcal{N} = (1, 0)$ theories associated with this Calabi-Yau are "extreme" in the sense that they have the largest possible number of tensor multiplets and the highest possible rank gauge sector, respectively for any 6D supergravity, not just those coming from toric hypersurface constructions.

Explicitly, the two theories associated with this Calabi-Yau are:

1. The theory with $T = 193$ tensor multiplets and gauge algebra

$$\mathfrak{e}_8^{17} \oplus \mathfrak{f}_4^{16} \oplus \mathfrak{g}_2^{32} \oplus \mathfrak{sp}_1^{32}. \tag{5.55}$$

2. A theory with $T = 9$ tensor multiplets and gauge algebra

$$\mathfrak{sp}(72) \oplus \mathfrak{sp}(56) \oplus \mathfrak{sp}(48) \oplus \mathfrak{so}(176) \oplus \mathfrak{sp}(24) \oplus \mathfrak{so}(128) \oplus \mathfrak{so}(80) \oplus \mathfrak{so}(64) \oplus \mathfrak{so}(32) \oplus \mathfrak{sp}(40), \tag{5.56}$$

which has rank 480.

In this section we summarize briefly how these theories can be understood in terms of the fiber structures analyzed in this paper.

There is a unique polytope (ID v05-393) with the Hodge numbers $h^{2,1}(X) = 491, h^{1,1} = 11$, the vertices of which are given by the columns of the matrix

$$\begin{pmatrix} 1 & 0 & 0 & 21 & -63 \\ 0 & 1 & 0 & 28 & -56 \\ 0 & 0 & 1 & 36 & -48 \\ 0 & 0 & 0 & 42 & -42 \end{pmatrix}. \tag{5.57}$$

This polytope has two subpolytopes, an F_{10} fiber and an F_{13} fiber. We will consider each of these in turn.

5.6.1 The F_{10} Fiber

We begin by analyzing the F_{10} fiber; to do so, it is as usual convenient to work in a basis where the fiber lives in the first two coordinates. In one such basis, the vertices of ∇ are given by the columns of

$$\begin{pmatrix} 1 & 0 & -2 & -2 & -2 \\ 0 & 1 & -3 & -3 & -3 \\ 0 & 0 & 42 & 0 & -42 \\ 0 & 0 & 36 & 1 & -48 \end{pmatrix}. \tag{5.58}$$

We see that we have a "standard stacking" of the base over the fiber vertex $(2, 3)$; in fact this is the generic elliptic fibration over the unique toric base with $h^{1,1}(B) = 194$, constructed in [34]. We therefore have

$$T = h^{1,1}(B) - 1 = 193 \tag{5.59}$$

tensor multiplets, in line with the upper bound proposed in [76].

Because this is the generic fibration over the $h^{1,1}(B) = 194$ base, the gauge group of the associated compactification is easy to compute: it is exactly the NHC associated to this base, as identified in [34], which straightforwardly reproduces the gauge algebra in Eq. 5.55.[14]

5.6.2 The F_{13} Fiber

This polytope also admits an elliptic fibration with an F_{13} fiber. As usual, we work in a basis where the F_{13} fiber occupies the first two coordinates; in one such basis, the vertices of the

[14]One can equally well identify this gauge algebra by identifying appropriate tops in the polytope, or by passing to Weierstrass form and applying the Kodaira classification; these three approaches all give the same gauge algebra, namely the one in 5.55.

Base point	Self-intersection	#(points)	ord(f,g,Δ)	Kodaira type	Gauge algebra
(1,0)	0	1	(0,0,0)	I_0	$\emptyset$
(0,1)	2	1	(0,0,0)	I_0	$\emptyset$
(-1,-2)	-4	4	(2,3,34)	I_{34}^*	$\mathfrak{so}(64)$
(-4,-9)	-1	57	(0,0,112)	I_{112}	$\mathfrak{sp}(56)$
(-3,-7)	-3	45	(2,3,90)	I_{90}^*	$\mathfrak{so}(176)$
(-5,-12)	-1	73	(0,0,144)	I_{144}	$\mathfrak{sp}(72)$
(-2,-5)	-4	4	(2,3,66)	I_{66}^*	$\mathfrak{so}(128)$
(-3, -8)	-1	49	(0,0,96)	I_{96}	$\mathfrak{sp}(48)$
(-1,-3)	-4	4	(2,3,42)	I_{42}^*	$\mathfrak{so}(80)$
(-1,-4)	-1	25	(0,0,48)	I_{48}	$\mathfrak{sp}(24)$
(0,-1)	-4	4	(2,3,18)	I_{18}^*	$\mathfrak{so}(32)$

Table 11: The toric gauge group of the F_{13} fibration of the polytope with $h^{1,1}(X) = 491$. For each of the eleven toric divisors in the base, we specify its self-intersection, the number of points in four-dimensional polytope that project to the base divisor, the orders to which the Weierstrass coefficients f and g and the discriminant Δ vanish on the divisor, the Kodaira singularity type inferred from these vanishings, and the gauge algebra picked out by the monodromies. From this table, we identify that the total nonabelian gauge group hosted on toric divisors is given by Eq. (5.62).

polytope are given by the columns of

$$\begin{pmatrix} 2 & 2 & 2 & 0 & -82 \\ 3 & 3 & 3 & -1 & -81 \\ -6 & 1 & 0 & 0 & -6 \\ -14 & 0 & 1 & 0 & -14 \end{pmatrix}. \tag{5.60}$$

In this basis we have arranged that the fiber coordinates are the first two, and the base coordinates are the last two coordinates. The base of the fibration is smooth, and has $h^{1,1}(B) = 9$. The base contains eleven curves; in our basis, they are given by

$$(0,1),\ (1,0),\ (-5,-12),\ (-4,-9),\ (-3,-8),\ (-3,-7), \tag{5.61}$$

$$(-1,-4),\ (-2,-5),\ (-1,-3),\ (-1,-2),\ \text{and}\ (0,-1), \tag{5.62}$$

and all but the first two host nontrivial gauge groups. In Table 11 we demonstrate that the gauge group hosted on toric divisors is given by

$$G_{\text{toric}} = \mathfrak{sp}(72) \oplus \mathfrak{sp}(56) \oplus \mathfrak{sp}(48) \oplus \mathfrak{so}(176) \oplus \mathfrak{sp}(24) \oplus \mathfrak{so}(128) \oplus \mathfrak{so}(80) \oplus \mathfrak{sp}(64) \oplus \mathfrak{sp}(32). \tag{5.63}$$

On all divisors hosting an $\mathfrak{so}(n)$ gauge algebra, the generic form of f, g is

$$f \sim a_{201}^2 z^2, \qquad g \sim a_{201}^3 z^3, \tag{5.64}$$

where $z = 0$ is a local description of the divisor. Thus, if any such divisor intersects a_{201}, the intersection furnishes a $(4, 6)$ point and must be blown up. This happens for only one divisor, the -3 curve $(-3, -7)$ hosting an $\mathfrak{so}(176)$ gauge algebra. We therefore blow up this -3 curve to obtain a -4 curve and a new -1 curve. The discriminant along the original -3 curve takes the form

$$\Delta \sim -a_{300}^2 z^{90} \left[a_{210}^2 + \mathcal{O}(z)\right], \tag{5.65}$$

and thus after implementing the blowup by the coordinate transformation $(a_{210}, z) \to (u, uz)$, we find that the -1 curve hosts an $\mathfrak{sp}(40)$ gauge algebra, with no additional $(4, 6)$ points to resolve. We have therefore shown that the gauge algebra is exactly as in Eq. (5.56), and moreover the intersection numbers of the curves hosting each summand of the algebra are exactly as described in [76].

6 Conclusions

In this paper, we have carried out a systematic exploration of the fibration structure of the toric hypersurface Calabi-Yau threefolds in the Kreuzer-Skarke database. The results found here follow two main themes: firstly, the elliptic and genus-one fibered Calabi-Yau threefolds in this set provide a wide range of examples that illustrate many aspects of the geometry and physics of F-theory. Secondly, the ubiquity of fibration structures and the physical/geometric language of F-theory provide a powerful lens with which to understand and interpret this largest class of known Calabi-Yau threefolds.

In general, on this second theme, the analysis of this paper illustrates that the identification of fibration structures and the geometric/physical language of F-theory provides a powerful approach to understanding and organizing the otherwise potentially bewildering array of possible Calabi-Yau threefolds. Because almost all known Calabi-Yau threefolds are connected by flops to an elliptic or genus-one fibered phase, it appears that the geometric data (and the associated physical F-theory data) characterizing these fibrations, such as the base variety and the list of divisors hosting gauge algebras in the base, is a useful way of capturing the structure of families of threefolds with a common extended Kähler cone. In particular, since elliptically fibered CY threefolds are all connected in a single moduli space by various (tensor, Higgs, matter) transitions, this provides a way of placing the set of threefolds in the KS database into this broader context. A forthcoming work will show how even the small fraction of non-fibered polytopes can generally be connected into this network through a fairly minimal set of transitions [77]. Understanding the distribution of and complementarity between different fibration structures for CY threefolds in the same family, i.e. related by flops and flips in the extended Kähler cone, provides another interesting opportunity for further insight into this structure; some aspects of this will be described further in [71]. Fibration structure also promises to provide new insights into mirror symmetry [78, 67].

In terms of exploring the range of examples relevant for, e.g., 6D F-theory, one remarkable aspect of this study is that while toric geometry is *a priori* a limited framework in which to construct generic Calabi-Yau threefolds, in many aspects, the set of geometric structures found in the KS database is somewhat broader than might be expected. It is natural that toric hypersurfaces will capture elliptic fibrations with toric bases and gauge groups tuned over toric divisors in those bases. We find, however, also a rich array of examples in which gauge groups are tuned over non-toric divisors in toric bases, and SCFT structures encode complex non-toric base geometries for elliptic fibrations. We have also encountered in the course of this study a number of somewhat exotic constructions that illustrate many ideas explored over the last decade in the 6D F-theory literature, including SCFTs, multiple U(1) factors, automatic enhancement, where tuning of one gauge factor forces another complementary factor to appear, and the massive charge completeness principle, which governs the global structure of many F-theory gauge groups in terms of torsion Mordell-Weil sections in the geometry. It is worth noting that many of the structures found in the KS database have already been identified through independent reasoning in the F-theory context. We expect, however, that further exploration of some of the more exotic structures in the database will reveal further geometric and physical structure. For example, the examples analyzed in §5.2.3 and §5.4.3 seem to share an intriguing structure involving multiple U(1) factors with a discrete quotient as would be seen upon breaking an SU(N) factor with a single adjoint; this hints at some interesting structural framework that we are not yet aware of.

One interesting question to explore further is the extent to which toric hypersurfaces provide a representative sample of the set of possible elliptic fibrations. As discussed in the introduction, the finite set of topologically distinct elliptic Calabi-Yau threefolds can in principle more or less be systematically classified by first finding all bases, then considering the allowed rigid and tuned nonabelian gauge factors, then classifying abelian gauge groups and matter. While there is not yet a systematic understanding of abelian U(1) or discrete gauge structure, the global space of bases and nonabelian gauge factors is reasonably well understood. The KS hypersurface threefolds represent specific slices of the full available elliptic CY3 fold moduli space. We have found that toric hypersurfaces sample a surprisingly wide range of non-toric bases, through non-flat fibers and associated SCFTs. For the gauge groups SU(2), SU(3), SU(4), toric hypersurfaces provide a wide range of realizations, and at least for the base $\mathbb{P}^2$, all possible tunings of SU(2) on non-toric divisors are realized. However, we do not see tunings of any other gauge factors on non-toric divisors in the KS database. While many of the examples encountered here have multiple U(1) factors, we do not yet have a systematic understanding of which Mordell-Weil structures can and cannot be realized in this context.

For discrete gauge factors, it is worth noting that toric hypersurface constructions produce genus-one fibrations only with k-sections for $k = 2, 3$, since these are the only genus-one types associated with 2D toric reflexive fibers (F_1, F_2, F_4). An important open question is to identify an upper bound on k for more general Calabi-Yau threefold constructions. It is known that complete intersection fibers can give genus-one fibrations with a 4-section [79]. While it has been proven that larger values of $k \geq 5$ cannot be realized through toric constructions or complete intersections, $k = 5$ Calabi-Yau threefolds have been constructed using more sophisticated methods [80]. It has been conjectured [81] that the maximum value of k possible is $k = 6$. At the same time, in [82], F-theory models were found that appear to admit a physical Higgsing to $\mathbb{Z}_{21}$, in tension with the conjecture that $k \leq 6$. The class of genus-one fibered Calabi-Yau threefolds with $k > 4$ represents perhaps the least-understood corner of the space of elliptic and genus-one fibered Calabi-Yau threefolds, and presents important challenges for further research.

We have presented here a range of specific examples from the data provided from the full analysis of fibration structures in the KS database. We expect that there is much more that can be learned from this data. A natural next step would be to apply some similar analysis to fibration structures for complete intersections in toric varieties, which would use as fibers intersections in higher-dimensional reflexive subpolytopes, such as the intersection fibers analyzed in [79].

Acknowledgments

We would like to thank Lara Anderson, Volker Braun, James Gray, Shing Yan Li, Damien Mayorga Pena, and Paul Oehlmann for helpful discussions. This work was supported by the DOE under contract #DE-SC00012567. WT would like to thank the Santa Fe Institute, where some of this work was carried out. RN is a Pappalardo Postdoctoral Fellow in the MIT Department of Physics. FA was supported by the Margaret MacVicar UROP Memorial Fund for this project.

A Details of Weierstrass Models

In this appendix we review the Weierstrass forms associated with the 16 reflexive 2D polytope toric fibers, originally analyzed in [40]; see also [52]. In principle, the procedure is to plug the defining polynomials for each of the 16 reflexive polytopes into Nagell's algorithm to find their generic Weierstrass models. However, the defining polynomials of the 16 fibers are closely related, and so in practice this exercise would be highly redundant. For instance, from Figure 1 it is straightforward to see that F_6 can be obtained from F_1 by adding a vertex, namely the point $(-1, 1)$. Adding a point to a polytope removes points from its dual, and hence the defining polynomial of the Calabi-Yau hypersurface defined by F_6 can be obtained by removing monomials from the polynomial of F_1, i.e. by setting their coefficients to be zero. Actually, F_6 can be obtained in a second way, by adding the vertex $(0, 1)$ to F_4; this provides an alternative but equivalent way of deriving the Weierstrass form of the defining polynomial of F_6.

In this way, the Weierstrass forms of each of the sixteen 2D reflexive polytopes can be obtained from specializations of one of four[15] base cases. These are:

[15] In fact, this is still a slight overcounting. F_{10} itself, and therefore F_{13}, can be obtained from a generic cubic. Nevertheless, we find it instructive to treat F_{10}, and its close analogy to the long Weierstrass model in Eq. (2.5), by hand.

The cubic in $\mathbb{P}^2$. Applying Eq. (2.4) to F_1 and its dual polytope F_{16}, we see that the defining polynomial takes the form of a generic cubic in $\mathbb{P}^2$:

$$a_{300}u^3 + a_{210}u^2v + a_{120}uv^2 + a_{030}v^3 + a_{201}u^2w + a_{111}uvw + a_{021}v^2w + a_{102}uw^2 + a_{012}vw^2 + a_{003}w^3 = 0. \tag{A.1}$$

Note that, for generic a_{ijk}, this equation has no nonzero solutions, and hence the defining polynomial does not have a point in $\mathbb{P}^2$. Thus the Calabi-Yau hypersurface defined by F_1 is a genus-one curve, and correspondingly fibrations with F_1 fiber are genus-one fibrations. Nevertheless, we can apply Nagell's algorithm to find a Weierstrass model for the Jacobian of this curve; the Weierstrass coefficients f, g are given in terms of the a_{ijk} as

$$\begin{aligned}
f =& -\frac{1}{48}a_{111}^4 + \frac{1}{6}a_{201}a_{111}^2a_{021} - \frac{1}{3}a_{201}^2a_{021}^2 - \frac{1}{2}a_{030}a_{201}a_{111}a_{102} + \frac{1}{6}a_{120}a_{111}^2a_{102} \\
&+ \frac{1}{3}a_{120}a_{201}a_{021}a_{102} - \frac{1}{2}a_{210}a_{111}a_{021}a_{102} + a_{300}a_{021}^2a_{102} - \frac{1}{3}a_{120}^2a_{102}^2 + a_{210}a_{030}a_{102}^2 \\
&+ a_{120}^2a_{201}a_{003} - 3a_{210}a_{030}a_{201}a_{003} - \frac{1}{2}a_{210}a_{120}a_{111}a_{003} + \frac{9}{2}a_{300}a_{030}a_{111}a_{003} + a_{210}^2a_{021}a_{003} \\
&- 3a_{300}a_{120}a_{021}a_{003} + a_{030}a_{201}^2a_{012} - \frac{1}{2}a_{120}a_{201}a_{111}a_{012} + \frac{1}{6}a_{210}a_{111}^2a_{012} + \frac{1}{3}a_{210}a_{201}a_{021}a_{012} \\
&- \frac{1}{2}a_{300}a_{111}a_{021}a_{012} + \frac{1}{3}a_{210}a_{120}a_{102}a_{012} - 3a_{300}a_{030}a_{102}a_{012} - \frac{1}{3}a_{210}^2a_{012}^2 + a_{300}a_{120}a_{012}^2 \\
g =& 1/864(a_{111}^6 - 12a_{111}^4(a_{102}a_{120} + a_{021}a_{201} + a_{012}a_{210}) + 36a_{111}^3(a_{030}a_{102}a_{201} + a_{012}a_{120}a_{201} + a_{021}a_{102}a_{210} \\
&+ a_{003}a_{120}a_{210} + a_{012}a_{021}a_{300} + 15a_{003}a_{030}a_{300}) + 24a_{111}^2(2a_{021}^2a_{201}^2 - 3a_{012}a_{030}a_{201}^2 + a_{012}a_{021}a_{201}a_{210} \\
&+ 2a_{012}^2a_{210}^2 + a_{102}a_{120}(a_{021}a_{201} + a_{012}a_{210}) + a_{102}^2(2a_{120}^2 - 3a_{030}a_{210}) - 3(a_{021}^2 + 9a_{012}a_{030})a_{102}a_{300} \\
&- 3a_{012}^2a_{120}a_{300} - 3a_{003}(a_{120}^2a_{201} + 9a_{030}a_{201}a_{210} + a_{021}a_{210}^2 + 9a_{021}a_{120}a_{300})) - 144a_{111}(a_{012}^2a_{210}(a_{120}a_{201} + a_{021}a_{300}) \\
&+ a_{210}(a_{003}a_{102}a_{120}^2 + a_{021}a_{120}(a_{102}^2 - 5a_{003}a_{201}) + a_{021}^2(a_{102}a_{201} - 6a_{003}a_{300})) + a_{012}(a_{021}a_{120}a_{201}^2 + a_{021}^2a_{201}a_{300} \\
&+ a_{003}a_{120}(a_{210}^2 - 6a_{120}a_{300}) + a_{102}(a_{120}^2a_{201} + a_{021}a_{210}^2 - 5a_{021}a_{120}a_{300})) + a_{030}(-6a_{012}^2a_{201}a_{300} \\
&+ a_{102}^2(a_{120}a_{201} - 6a_{021}a_{300}) + a_{102}(a_{021}a_{201}^2 - 5a_{012}a_{201}a_{210} - 6a_{003}a_{210}^2 + 9a_{003}a_{120}a_{300}) \\
&+ a_{003}(-6a_{120}a_{201}^2 + 9a_{021}a_{201}a_{300} + 9a_{012}a_{210}a_{300}))) + 8(-72a_{003}a_{021}a_{120}^2a_{201}^2 - 8a_{021}^3a_{201}^3 - 108a_{003}a_{030}^2a_{201}^3 \\
&+ 108a_{003}a_{021}a_{030}a_{201}^2a_{210} + 27a_{003}^2a_{120}^2a_{210}^2 - 72a_{003}a_{021}^2a_{201}a_{210}^2 - 108a_{003}^2a_{030}a_{210}^3 + 54a_{003}a_{120}(-2a_{003}a_{120}^2 \\
&+ 2a_{021}^2a_{201} + 9a_{003}a_{030}a_{210})a_{300} - 27a_{003}(4a_{021}^3 + 27a_{003}a_{030}^2)a_{300}^2 - 4a_{102}^3(2a_{120}^3 - 9a_{030}a_{120}a_{210} + 27a_{030}^2a_{300}) \\
&+ 3a_{012}^2(9a_{120}^2a_{201}^2 + 4a_{201}a_{210}(-6a_{030}a_{201} + a_{021}a_{210}) - 6a_{021}a_{120}a_{201}a_{300} + 9a_{021}^2a_{300}^2) - 4a_{012}^3(2a_{210}^3 - 9a_{120}a_{210}a_{300} \\
&+ 27a_{030}a_{300}^2) + 3a_{102}^2(4a_{012}a_{120}^2a_{210} + a_{021}(4a_{120}^2a_{201} - 6a_{030}a_{201}a_{210}) + 3a_{021}^2(3a_{210}^2 \\
&- 8a_{120}a_{300}) + 3a_{030}(3a_{030}a_{201}^2 - 8a_{012}a_{210}^2 + 12a_{012}a_{120}a_{300})) + 6a_{102}(a_{120}((2a_{021}^2 - 3a_{012}a_{030})a_{201}^2 + a_{012}a_{021}a_{201}a_{210} \\
&+ 2a_{012}^2a_{210}^2) + 6a_{021}^3a_{201}a_{300} - 3a_{012}(4a_{012}a_{120}^2 + 9a_{021}a_{030}a_{201} + a_{021}^2a_{210} - 6a_{012}a_{030}a_{210})a_{300} + 3a_{003}(2a_{120}^3a_{201} \\
&- a_{120}a_{210}(9a_{030}a_{201} + a_{021}a_{210}) + 6a_{021}a_{120}^2a_{300} + 9a_{030}(3a_{030}a_{201} - a_{021}a_{210})a_{300})) + 6a_{012}(2a_{021}^2a_{201}^2a_{210} \\
&- 3a_{003}a_{201}(a_{210}(a_{120}^2 - 6a_{030}a_{210}) + 9a_{030}a_{120}a_{300}) + 3a_{021}(2a_{030}a_{201}^3 + 2a_{003}a_{210}^3 - 9a_{003}a_{120}a_{210}a_{300} + 27a_{003}a_{030}a_{300}^2)))).
\end{aligned} \tag{A.2a}$$

While F_1 is only a genus-one curve, by specializing some of the coefficients a_{ijk} to vanish it is straightforward to obtain a defining polynomial with solutions, and therefore whose zero-locus is an elliptic curve. For instance, upon setting $a_{003} = 0$ we find that the point $(0 : 0 : 1)$ is a solution. The Jacobian of an elliptic curve is simply the curve itself, so Eq. (A.2) (with the appropriate coefficients set to zero) still gives the Weierstrass coefficients with specialized coefficients. In fact, the specialization $a_{003} = 0$ yields the defining polynomial of the polytope F_3.

The biquadric in $\mathbb{P}^1 \times \mathbb{P}^1$ The polytope F_2 describes $\mathbb{P}^1 \times \mathbb{P}^1$, and its defining polynomial is a general biquadric in four variables:

$$\begin{aligned} &a_{1111}tuvw + a_{2200}t^2u^2 + a_{2020}t^2v^2 + a_{0202}u^2w^2 + a_{0022}v^2w^2 \\ &+ a_{2110}t^2uv + a_{1201}tu^2w + a_{1021}tv^2w + a_{0112}uvw^2 = 0. \end{aligned} \tag{A.3}$$

Applying Nagell's algorithm to the Jacobian of this curve, we find the Weierstrass model

$$\begin{aligned} f =& -\frac{1}{48}a_{1111}^4 + \frac{1}{6}a_{1111}^2 a_{2020}a_{0202} - \frac{1}{3}a_{2020}^2 a_{0202}^2 + \frac{1}{6}a_{1111}^2 a_{2200}a_{0022} - \frac{14}{3}a_{2200}a_{2020}a_{0202}a_{0022} \\ & - \frac{1}{3}a_{2200}^2 a_{0022}^2 + a_{0202}a_{0022}a_{2110}^2 - \frac{1}{2}a_{1111}a_{0022}a_{2110}a_{1201} + a_{2020}a_{0022}a_{1201}^2 - \frac{1}{2}a_{1111}a_{0202}a_{2110}a_{1021} \\ & + \frac{1}{6}a_{1111}^2 a_{1201}a_{1021} + \frac{1}{3}a_{2020}a_{0202}a_{1201}a_{1021} + \frac{1}{3}a_{2200}a_{0022}a_{1201}a_{1021} + a_{2200}a_{0202}a_{1021}^2 - \frac{1}{3}a_{1201}^2 a_{1021}^2 \\ & + \frac{1}{6}a_{1111}^2 a_{2110}a_{0112} + \frac{1}{3}a_{2020}a_{0202}a_{2110}a_{0112} + \frac{1}{3}a_{2200}a_{0022}a_{2110}a_{0112} - \frac{1}{2}a_{1111}a_{2020}a_{1201}a_{0112} \\ & - \frac{1}{2}a_{1111}a_{2200}a_{1021}a_{0112} + \frac{1}{3}a_{2110}a_{1201}a_{1021}a_{0112} + a_{2200}a_{2020}a_{0112}^2 - \frac{1}{3}a_{2110}^2 a_{0112}^2 \end{aligned} \tag{A.4a}$$

$$\begin{aligned} g =& 1/864(a_{1111}^6 - 12a_{1111}^4(a_{1021}a_{1201} + a_{0202}a_{2020} + a_{0112}a_{2110} + a_{0022}a_{2200}) + 36a_{1111}^3(a_{0112}a_{1201}a_{2020} + a_{0202}a_{1021}a_{2110} \\ & + a_{0022}a_{1201}a_{2110} + a_{0112}a_{1021}a_{2200}) + 24a_{1111}^2(2a_{0202}^2 a_{2020}^2 + a_{0112}a_{0202}a_{2020}a_{2110} + 2a_{0112}^2 a_{2110}^2 - 3a_{0112}^2 a_{2020}a_{2200} \\ & + 2a_{0022}^2 a_{2200}^2 + a_{1021}a_{1201}(a_{0202}a_{2020} + a_{0112}a_{2110} + a_{0022}a_{2200}) + a_{1021}^2(2a_{1201}^2 - 3a_{0202}a_{2200}) + a_{0022}(-3a_{1201}^2 a_{2020} \\ & - 3a_{0202}a_{2110}^2 - 20a_{0202}a_{2020}a_{2200} + a_{0112}a_{2110}a_{2200})) + 8(-72a_{0022}a_{0202}a_{1201}^2 a_{2020}^2 - 8a_{0202}^3 a_{2020}^3 + 27a_{0022}^2 a_{1201}^2 a_{2110}^2 \\ & - 72a_{0022}a_{0202}^2 a_{2020}a_{2110}^2 - 24a_{0022}(-11a_{0202}^2 a_{2020}^2 + 3a_{0022}(a_{1201}^2 a_{2020} + a_{0202}a_{2110}^2))a_{2200} + 264a_{0022}^2 a_{0202}a_{2020}a_{2200}^2 \\ & - 8a_{0022}^3 a_{2200}^3 + a_{1021}^3(-8a_{1201}^3 + 36a_{0202}a_{1201}a_{2200}) + a_{0112}^3(-8a_{2110}^3 + 36a_{2020}a_{2110}a_{2200}) + 3a_{0112}^2(9a_{1201}^2 a_{2020}^2 - 4(a_{0202}a_{2020} \\ & + a_{0022}a_{2200})(-a_{2110}^2 + 6a_{2020}a_{2200})) - 3a_{1021}^2(-4a_{0202}a_{1201}^2 a_{2020} - 4a_{0112}a_{1201}^2 a_{2110} - 4a_{0022}a_{1201}^2 a_{2200} - 9a_{0112}^2 a_{2200}^2 \\ & + 6a_{0202}a_{2200}(a_{0112}a_{2110} + 4a_{0022}a_{2200}) + a_{0202}^2(-9a_{2110}^2 + 24a_{2020}a_{2200})) + 6a_{0112}a_{2110}(2a_{0202}^2 a_{2020}^2 + 2a_{0022}^2 a_{2200}^2 \\ & + a_{0022}(-3a_{1201}^2 a_{2020} + 6a_{0202}a_{2110}^2 - 20a_{0202}a_{2020}a_{2200})) + 6a_{1021}a_{1201}(2a_{0202}^2 a_{2020}^2 + a_{0112}a_{0202}a_{2020}a_{2110} + 2a_{0022}^2 a_{2200}^2 \\ & + a_{0112}^2(2a_{2110}^2 - 3a_{2020}a_{2200}) + a_{0022}(6a_{1201}^2 a_{2020} - 3a_{0202}a_{2110}^2 - 20a_{0202}a_{2020}a_{2200} + a_{0112}a_{2110}a_{2200}))) \\ & - 144a_{1111}(a_{0112}^2 a_{2110}(a_{1201}a_{2020} + a_{1021}a_{2200}) + a_{2110}(a_{0202}^2 a_{1021}a_{2020} + a_{0022}a_{1201}(a_{1021}a_{1201} + a_{0022}a_{2200}) + a_{0202}(a_{1021}^2 a_{1201} \\ & - 5a_{0022}a_{1201}a_{2020} - 5a_{0022}a_{1021}a_{2200})) + a_{0112}(a_{0202}a_{1201}a_{2020}^2 + a_{1021}^2 a_{1201}a_{2200} + a_{0022}a_{1201}(a_{2110}^2 - 5a_{2020}a_{2200}) \\ & + a_{1021}(a_{1201}^2 a_{2020} + a_{0022}a_{2200}^2 + a_{0202}(a_{2110}^2 - 5a_{2020}a_{2200}))))) \end{aligned} \tag{A.4b}$$

The quartic in $\mathbb{P}^{1,1,2}$ The polytope F_4 describes the weighted projective space $\mathbb{P}^{1,1,2}$, and so its defining polynomial is given by

$$a_{400}u^4 + a_{310}u^3v + a_{220}u^2v + a_{201}u^2w + a_{130}uv^3 + a_{111}uvw + a_{040}v^4 + a_{021}v^2w + a_{002}w^2 = 0. \tag{A.5}$$

This polynomial does not have a nonzero solution for generic a_{ijk}, and so we apply Nagell's algorithm to the Jacobian of this genus-one curve to find the Weierstrass model

$$f = -\frac{1}{48}a_{111}^4 + \frac{1}{6}a_{201}a_{111}^2a_{021} - \frac{1}{3}a_{201}^2a_{021}^2 - \frac{1}{2}a_{201}a_{130}a_{111}a_{002} + \frac{1}{6}a_{220}a_{111}^2a_{002} + a_{201}^2a_{040}a_{002}$$
$$+ \frac{1}{3}a_{220}a_{201}a_{021}a_{002} - \frac{1}{2}a_{310}a_{111}a_{021}a_{002} + a_{400}a_{021}^2a_{002} - \frac{1}{3}a_{220}^2a_{002}^2 + a_{310}a_{130}a_{002}^2 - 4a_{400}a_{040}a_{002}^2 \tag{A.6a}$$

$$g = \frac{1}{864}a_{111}^6 - \frac{1}{72}a_{201}a_{111}^4a_{021} + \frac{1}{18}a_{201}^2a_{111}^2a_{021}^2 - \frac{2}{27}a_{201}^3a_{021}^3 + \frac{1}{24}a_{201}a_{130}a_{111}^3a_{002}$$
$$- \frac{1}{72}a_{220}a_{111}^4a_{002} - \frac{1}{12}a_{201}^2a_{111}^2a_{040}a_{002} - \frac{1}{6}a_{201}^2a_{130}a_{111}a_{021}a_{002} + \frac{1}{36}a_{220}a_{201}a_{111}^2a_{021}a_{002}$$
$$+ \frac{1}{24}a_{310}a_{111}^3a_{021}a_{002} + \frac{1}{3}a_{201}^3a_{040}a_{021}a_{002} + \frac{1}{9}a_{220}a_{201}^2a_{021}^2a_{002} - \frac{1}{6}a_{310}a_{201}a_{111}a_{021}^2a_{002}$$
$$- \frac{1}{12}a_{400}a_{111}^2a_{021}^2a_{002} + \frac{1}{3}a_{400}a_{201}a_{021}^3a_{002} + \frac{1}{4}a_{201}^2a_{130}^2a_{002}^2 - \frac{1}{6}a_{220}a_{201}a_{130}a_{111}a_{002}^2$$
$$+ \frac{1}{18}a_{220}^2a_{111}^2a_{002}^2 - \frac{1}{12}a_{310}a_{130}a_{111}^2a_{002}^2 - \frac{2}{3}a_{220}a_{201}^2a_{040}a_{002}^2 + a_{310}a_{201}a_{111}a_{040}a_{002}^2$$
$$- \frac{2}{3}a_{400}a_{111}^2a_{040}a_{002}^2 + \frac{1}{9}a_{220}^2a_{201}a_{021}a_{002}^2 - \frac{1}{6}a_{310}a_{201}a_{130}a_{021}a_{002}^2 - \frac{1}{6}a_{310}a_{220}a_{111}a_{021}a_{002}^2$$
$$+ a_{400}a_{130}a_{111}a_{021}a_{002}^2 - \frac{4}{3}a_{400}a_{201}a_{040}a_{021}a_{002}^2 + \frac{1}{4}a_{310}^2a_{021}^2a_{002}^2 - \frac{2}{3}a_{400}a_{220}a_{021}^2a_{002}^2$$
$$- \frac{2}{27}a_{220}^3a_{002}^3 + \frac{1}{3}a_{310}a_{220}a_{130}a_{002}^3 - a_{400}a_{130}^2a_{002}^3 - a_{310}^2a_{040}a_{002}^3 + \frac{8}{3}a_{400}a_{220}a_{040}a_{002}^3. \tag{A.6b}$$

The generalized Weierstrass model in $\mathbb{P}^{1,2,3}$ The polytope F_{10} describes the weighted projective space $\mathbb{P}^{1,2,3}$, and so its defining polynomial is the most general sextic polynomial:

$$\alpha y^2 + a_1xyz + a_3yz^3 = \beta x^3 + a_2x^2z^2 + a_4xz^4 + a_6z^6\,. \tag{A.7}$$

We have suggestively chosen variable names to emphasize the close relationship between this polynomial and the long Weierstrass model in Eq. (2.5); while this has the same functional form as the long Weierstrass model in Eq. (2.5), because of the presence of α, β the short Weierstrass form of this model is no longer given by Eq. (2.7). However, Nagell's algorithm is still applicable in this more general context. We find that the short Weierstrass coefficients are given by

$$f = -\frac{1}{48}a_1^4 - \frac{1}{6}a_1^2a_2\alpha - \frac{1}{3}a_2^2\alpha^2 + \frac{1}{2}a_1a_3\alpha\beta + a_4\alpha^2\beta \tag{A.8a}$$
$$g = \frac{1}{864}a_1^6 + \frac{1}{72}a_1^4a_2\alpha + \frac{1}{18}a_1^2a_2^2\alpha^2 + \frac{2}{27}a_2^3\alpha^3 - \frac{1}{24}a_1^3a_3\alpha\beta$$
$$- \frac{1}{6}a_1a_2a_3\alpha^2\beta - \frac{1}{12}a_1^2a_4\alpha^2\beta - \frac{1}{3}a_2a_4\alpha^3\beta + \frac{1}{4}a_3^2\alpha^2\beta^2 + a_6\alpha^3\beta^2, \tag{A.8b}$$

Each of the sixteen reflexive polytopes can be realized in at least one way by adding points to one of F_1, F_2, F_4, and F_{10}, and therefore specializations of Eqs. A.2, A.4, A.6, and A.8 suffice to specify the defining polynomials of all 16 fiber types. The appropriate specializations have been worked out in e.g. [40], and are summarized for in Table 2. From the specializations, one can readily work out the generic gauge groups of [40] by plugging the forms of f, g into the formula for the discriminant Δ and factoring it, as described in the main text.

B Statistics of Polytope Automorphisms

In the course of our work, we enumerated the automorphisms of every polytope in the KS list, using the built-in capabilities of CYTools [62]; to the best of our knowledge, this is the first time that automorphisms have been exhaustively and systematically studied. While it is not the primary purpose of our work, we exhibit some statistics of those automorphisms in this Appendix.

Of the 473,800,776 polytopes, only 1.3% (6,095,530 total) have at least one nontrivial automorphism. The polytope with the largest automorphism group is the 24-cell, studied in e.g. [83, 84]. This polytope, which in our convention is labeled as v24-506398, is a self-dual polytope with Hodge numbers $h^{1,1}(X) = h^{2,1}(X) = 20$ and has an automorphism group of order 1,152. The symmetry group is the Weyl group of the F_4 root system, and can be given explicitly as

$$\Big(\Big(\big(\mathbb{Z}_2^3 \rtimes \mathbb{Z}_2^2\big) \rtimes \mathbb{Z}_3^2\Big) \rtimes \mathbb{Z}_2\Big) \rtimes \mathbb{Z}_2. \tag{B.1}$$

Large automorphism groups are the exception, rather than the rule. Of the polytopes with nontrivial automorphisms, 97.2% (5,925,190 total) have automorphism group $\mathbb{Z}_2$, and only 19 of the remaining 170,340 polytopes have $|\,\mathrm{Aut(X)}\,| \geq 100$. We have shown a histogram of the orders of the automorphism groups of the 6,095,511 polytopes with $1 < |\,\mathrm{Aut(X)}| < 100$ in Figure 14. A total of 35 finite groups appear as the automorphism group of a 4D reflexive polytope; we have listed these groups, and the number of times they appear, in Table 12.

Next we study the distribution of automorphism groups as a function of the number of vertices of the dual polytope. We observe, but have not attempted to explain, a curious trend: polytopes whose dual polytopes have either very many or very few vertices tend to have more automorphisms than polytopes whose dual polytopes are generic.[16] This can be seen in two ways, by considering either the fraction of polytopes admitting a nontrivial automorphism or by considering the average number of nontrivial automorphisms per polytope; these quantities are plotted as a function of the number of dual vertices in Figures 15a and 15b, respectively. We leave explaining this trend to future work.

References

[1] P. Candelas, G. T. Horowitz, A. Strominger and E. Witten, *Vacuum configurations for superstrings*, *Nucl. Phys. B* **258** (1985) 46.

[16] The average 4D reflexive polytope has 15.8 dual vertices.

Group	GAP ID [85]	Order	#(Polytopes)
$\mathbb{Z}_2$	[2,1]	2	5,925,190
$\mathbb{Z}_3$	[3,1]	3	1,080
$\mathbb{Z}_4$	[4, 1]	4	135
$\mathbb{Z}_2^2$	[4, 2]	4	151,281
S_3	[6, 1]	6	8,161
$\mathbb{Z}_6$	[6, 2]	6	57
D_8	[8, 3]	8	3,387
Z_2^4	[8, 5]	8	3,548
D_{10}	[10, 1]	10	4
D_{12}	[12, 4]	12	1,509
D_{16}	[16, 7]	16	2
$\mathbb{Z}_2 \times D_8$	[16, 11]	16	735
$\mathbb{Z}_2^4$	[16, 14]	16	19
$\mathbb{Z}_3 \times S_3$	[18, 3]	18	2
$\mathbb{Z}_5 \rtimes \mathbb{Z}_4$	[20, 3]	20	4
S_4	[24, 12]	24	106
$\mathbb{Z}_2^2 \times S_3$	[24, 14]	24	141
$\mathbb{Z}_2^4 \rtimes \mathbb{Z}_2$	[32, 27]	32	5
$\mathbb{Z}_2^2 \times D_8$	[32, 46]	32	18
S_3^2	[36, 10]	36	11
$D_8 \times S_3$	[48, 38]	48	8
$\mathbb{Z}_2 \times S_4$	[48, 48]	48	68
$\mathbb{Z}_2^3 \times S_3$	[48, 51]	48	3
D_8^2	[64, 226]	64	5
$S_3^2 \rtimes \mathbb{Z}_2$	[72, 40]	72	6
$\mathbb{Z}_2 \times S_3^2$	[72, 46]	72	4
$\mathbb{Z}_2 \times D_8 \times S_3$	[96, 209]	96	4
$\mathbb{Z}_2^2 \times S_4$	[96, 226]	96	18
S_5	[120, 34]	120	2
$D_8^2 \rtimes \mathbb{Z}_2$	[128, 928]	128	2
$\mathbb{Z}_2 \times (S_3^2 \rtimes \mathbb{Z}_2)$	[144, 186]	144	2
$\mathbb{Z}_2 \times S_5$	[240, 189]	240	4
$\mathbb{Z}_3^2 \rtimes \left(\mathbb{Z}_2^4 \rtimes \mathbb{Z}_2\right)$	[288, 889]	288	2
$\left(\left(\left(\mathbb{Z}_2^3 \rtimes \mathbb{Z}_2^2\right) \rtimes \mathbb{Z}_3\right) \rtimes \mathbb{Z}_2\right) \rtimes \mathbb{Z}_2$	[384, 5602]	384	6
$\left(\left(\left(\mathbb{Z}_2^3 \rtimes \mathbb{Z}_2^2\right) \rtimes \mathbb{Z}_3^2\right) \rtimes \mathbb{Z}_2\right) \rtimes \mathbb{Z}_2$	[1152, 157478]	1,152	1

Table 12: The 35 nontrivial groups that appear as the automorphism group of a 4D reflexive polytope. For each group, we list its order and the number of polytopes for which it is the automorphism group. "Gap ID" refers to the entry of the group in the online library of small groups, accessed through the GAP system [85].

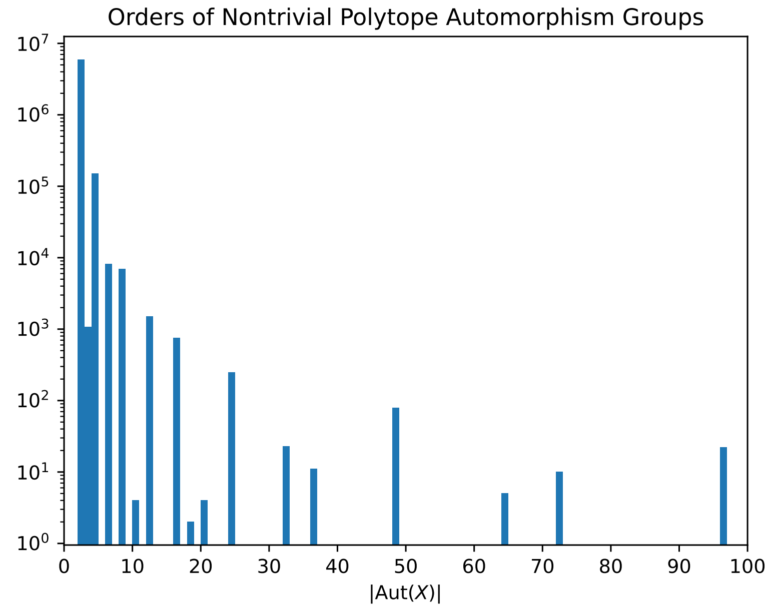

Figure 14: The orders of the automorphism groups of the 6,095,511 polytopes with $1 < |\operatorname{Aut}(X)| < 100$.

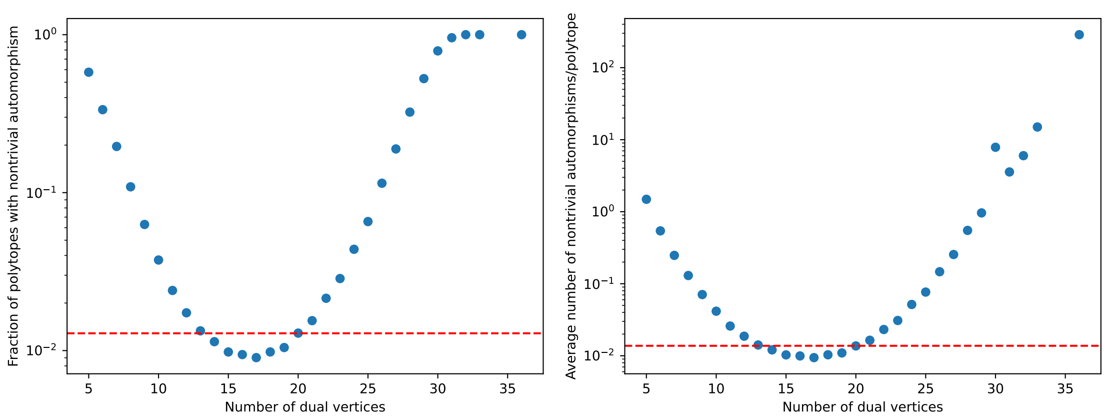

(a) (b)

Figure 15: (a) The fraction of polytopes with nontrivial automorphisms and (b) the average number of nontrivial automorphisms per polytope as a function of the number of dual vertices. The averages of both quantities are shown in red. We see in both figures that polytopes with either very many or very few dual vertices enjoy more automorphisms than generic polytopes.

[2] A. Grassi, *On minimal models of elliptic threefolds*, *Math. Ann.* **290** (1991) 287.

[3] M. Gross, *A finiteness theorem for elliptic calabi-yau threefolds*, *Duke Math. J.* **76** (1994) 271.

[4] C. Vafa, *Evidence for F theory*, *Nucl. Phys. B* **469** (1996) 403 [hep-th/9602022].

[5] D. R. Morrison and C. Vafa, *Compactifications of F theory on Calabi-Yau threefolds. 1*, *Nucl. Phys. B* **473** (1996) 74 [hep-th/9602114].

[6] D. R. Morrison and C. Vafa, *Compactifications of F theory on Calabi-Yau threefolds. 2.*, *Nucl. Phys. B* **476** (1996) 437 [hep-th/9603161].

[7] P. Candelas, A. Constantin and H. Skarke, *An Abundance of K3 Fibrations from Polyhedra with Interchangeable Parts*, *Commun. Math. Phys.* **324** (2013) 937 [1207.4792].

[8] J. Gray, A. S. Haupt and A. Lukas, *Topological Invariants and Fibration Structure of Complete Intersection Calabi-Yau Four-Folds*, *JHEP* **09** (2014) 093 [1405.2073].

[9] L. B. Anderson, X. Gao, J. Gray and S.-J. Lee, *Multiple Fibrations in Calabi-Yau Geometry and String Dualities*, *JHEP* **10** (2016) 105 [1608.07555].

[10] L. B. Anderson, X. Gao, J. Gray and S.-J. Lee, *Fibrations in CICY Threefolds*, *JHEP* **10** (2017) 077 [1708.07907].

[11] L. B. Anderson, J. Gray and B. Hammack, *Fibrations in Non-simply Connected Calabi-Yau Quotients*, *JHEP* **08** (2018) 128 [1805.05497].

[12] Y.-C. Huang and W. Taylor, *Comparing elliptic and toric hypersurface Calabi-Yau threefolds at large Hodge numbers*, *JHEP* **02** (2019) 087 [1805.05907].

[13] Y.-C. Huang and W. Taylor, *On the prevalence of elliptic and genus one fibrations among toric hypersurface Calabi-Yau threefolds*, *JHEP* **03** (2019) 014 [1809.05160].

[14] V. V. Batyrev, *Dual polyhedra and mirror symmetry for Calabi-Yau hypersurfaces in toric varieties*, *J. Alg. Geom.* **3** (1994) 493 [alg-geom/9310003].

[15] M. Kreuzer and H. Skarke, *Complete classification of reflexive polyhedra in four-dimensions*, *Adv. Theor. Math. Phys.* **4** (2000) 1209 [hep-th/0002240].

[16] M. Demirtas, L. McAllister and A. Rios-Tascon, *Bounding the Kreuzer-Skarke Landscape*, *Fortsch. Phys.* **68** (2020) 2000086 [2008.01730].

[17] N. Gendler, N. MacFadden, L. McAllister, J. Moritz, R. Nally, A. Schachner et al., *Counting Calabi-Yau Threefolds*, 2310.06820.

[18] A. Chandra, A. Constantin, C. S. Fraser-Taliente, T. R. Harvey and A. Lukas, *Enumerating Calabi-Yau Manifolds: Placing Bounds on the Number of Diffeomorphism Classes in the Kreuzer-Skarke List*, *Fortsch. Phys.* **72** (2024) 2300264 [2310.05909].

[19] N. MacFadden, *Efficient Algorithm for Generating Homotopy Inequivalent Calabi-Yaus*, 2309.10855.

[20] Y.-C. Huang and W. Taylor, *Fibration structure in toric hypersurface Calabi-Yau threefolds*, *JHEP* **03** (2020) 172 [1907.09482].

[21] V. Braun, *Toric Elliptic Fibrations and F-Theory Compactifications*, *JHEP* **01** (2013) 016 [1110.4883].

[22] "Zenodo archive with data and program files will be provided with a forthcoming version v2, hopefully by the end of november 2025. readers interested in getting their hands on the data immediately should contact the authors for a "beta" version.." [zenodo archive link to appear here].

[23] L. B. Anderson, J. Gray, N. Raghuram and W. Taylor, *Matter in transition*, *JHEP* **04** (2016) 080 [1512.05791].

[24] K. Kodaira, *On compact analytic surfaces: Ii*, *Annals of Mathematics* **77** (1963) 563.

[25] M. Bershadsky, K. A. Intriligator, S. Kachru, D. R. Morrison, V. Sadov and C. Vafa, *Geometric singularities and enhanced gauge symmetries*, *Nucl. Phys.* **B481** (1996) 215 [hep-th/9605200].

[26] V. Kumar, D. R. Morrison and W. Taylor, *Global aspects of the space of 6D $N = 1$ supergravities*, *JHEP* **11** (2010) 118 [1008.1062].

[27] T. Weigand, *F-theory*, *PoS* **TASI2017** (2018) 016 [1806.01854].

[28] D. R. Morrison and W. Taylor, *Classifying bases for 6D F-theory models*, *Central Eur. J. Phys.* **10** (2012) 1072 [1201.1943].

[29] S. H. Katz and C. Vafa, *Matter from geometry*, *Nucl. Phys. B* **497** (1997) 146 [hep-th/9606086].

[30] A. Grassi and D. R. Morrison, *Anomalies and the Euler characteristic of elliptic Calabi-Yau threefolds*, *Commun. Num. Theor. Phys.* **6** (2012) 51 [1109.0042].

[31] D. Klevers, D. R. Morrison, N. Raghuram and W. Taylor, *Exotic matter on singular divisors in F-theory*, *JHEP* **11** (2017) 124 [1706.08194].

[32] M. Cvetič, D. Klevers, H. Piragua and W. Taylor, *General $U(1)\times U(1)$ F-theory compactifications and beyond: geometry of unHiggsings and novel matter structure*, *JHEP* **11** (2015) 204 [1507.05954].

[33] B. Pioline and T. Schimannek, *Revisiting the Quantum Geometry of Torus-fibered Calabi-Yau Threefolds*, 2510.23722.

[34] D. R. Morrison and W. Taylor, *Toric bases for 6D F-theory models*, *Fortsch. Phys.* **60** (2012) 1187 [1204.0283].

[35] J. J. Heckman, D. R. Morrison and C. Vafa, *On the Classification of 6D SCFTs and Generalized ADE Orbifolds*, *JHEP* **05** (2014) 028 [1312.5746].

[36] J. J. Heckman, D. R. Morrison, T. Rudelius and C. Vafa, *Atomic Classification of 6D SCFTs*, *Fortsch. Phys.* **63** (2015) 468 [1502.05405].

[37] G. Martini and W. Taylor, *6D F-theory models and elliptically fibered Calabi–Yau threefolds over semi-toric base surfaces*, *JHEP* **06** (2015) 061 [1404.6300].

[38] W. Taylor and Y.-N. Wang, *Non-toric bases for elliptic Calabi-Yau threefolds and 6D F-theory vacua*, *Adv. Theor. Math. Phys.* **21** (2017) 1063 [1504.07689].

[39] H. Skarke, *String dualities and toric geometry: An Introduction*, *Chaos Solitons Fractals* **10** (1999) 543 [hep-th/9806059].

[40] D. Klevers, D. K. Mayorga Pena, P.-K. Oehlmann, H. Piragua and J. Reuter, *F-Theory on all Toric Hypersurface Fibrations and its Higgs Branches*, *JHEP* **01** (2015) 142 [1408.4808].

[41] A. C. Avram, M. Kreuzer, M. Mandelberg and H. Skarke, *Searching for K3 fibrations*, Nucl. Phys. B **494** (1997) 567 [hep-th/9610154].

[42] M. Kreuzer and H. Skarke, *Calabi-Yau four folds and toric fibrations*, J. Geom. Phys. **26** (1998) 272 [hep-th/9701175].

[43] P. Berglund and T. Hubsch, *A Generalized Construction of Calabi-Yau Models and Mirror Symmetry*, SciPost Phys. **4** (2018) 009 [1611.10300].

[44] P. Candelas, E. Perevalov and G. Rajesh, *Toric geometry and enhanced gauge symmetry of F theory / heterotic vacua*, Nucl. Phys. B **507** (1997) 445 [hep-th/9704097].

[45] V. Braun and D. R. Morrison, *F-theory on Genus-One Fibrations*, JHEP **08** (2014) 132 [1401.7844].

[46] D. R. Morrison and W. Taylor, *Sections, multisections, and U(1) fields in F-theory*, 1404.1527.

[47] P. Candelas, X. de la Ossa, M. Elmi and D. Van Straten, *A One Parameter Family of Calabi-Yau Manifolds with Attractor Points of Rank Two*, JHEP **10** (2020) 202 [1912.06146].

[48] S. Kachru, R. Nally and W. Yang, *Supersymmetric flux compactifications and Calabi-Yau modularity*, Commun. Num. Theor. Phys. **18** (2024) 653 [2001.06022].

[49] S. Kachru, R. Nally and W. Yang, *Flux Modularity, F-Theory, and Rational Models*, 2010.07285.

[50] P. Candelas, X. de la Ossa, P. Kuusela and J. McGovern, *Flux vacua and modularity for $\mathbb{Z}_2$ symmetric Calabi-Yau manifolds*, SciPost Phys. **15** (2023) 146 [2302.03047].

[51] The Sage Developers, *SageMath, the Sage Mathematics Software System (Version 10.5)*, 2024.

[52] S. Y. An, S. Y. Kim, D. C. Marshall, S. H. Marshall, W. G. McCallum and A. R. Perlis, *Jacobians of genus one curves*, *Journal of Number Theory* **90** (2001) 304.

[53] R. Wazir, *Arithmetic on elliptic threefolds*, *Compositio Mathematica* **140** (2004) 567.

[54] M. B. Green, J. H. Schwarz and P. C. West, *Anomaly Free Chiral Theories in Six-Dimensions*, Nucl. Phys. **B254** (1985) 327.

[55] W. Taylor and A. P. Turner, *Generic matter representations in 6D supergravity theories*, JHEP **05** (2019) 081 [1901.02012].

[56] S. B. Johnson and W. Taylor, *Enhanced gauge symmetry in 6D F-theory models and tuned elliptic Calabi-Yau threefolds*, Fortsch. Phys. **64** (2016) 581 [1605.08052].

[57] J. Erler, *Anomaly cancellation in six-dimensions*, J. Math. Phys. **35** (1994) 1819 [hep-th/9304104].

[58] D. S. Park and W. Taylor, *Constraints on 6D Supergravity Theories with Abelian Gauge Symmetry*, JHEP **01** (2012) 141 [1110.5916].

[59] D. S. Park, *Anomaly Equations and Intersection Theory*, JHEP **01** (2012) 093 [1111.2351].

[60] L. B. Anderson, J. Gray and P.-K. Oehlmann, *Twisted Fibrations in M/F-theory*, JHEP **01** (2024) 017 [2308.07364].

[61] L. B. Anderson, J. Gray and P.-K. Oehlmann, *Calabi-Yau Genus-One Fibrations and Twisted Dimensional Reductions of F-theory*, in *Nankai Symposium on Mathematical Dialogues: In celebration of S.S.Chern's 110th anniversary*, 8, 2023, 2308.12826.

[62] M. Demirtas, A. Rios-Tascon and L. McAllister, *CYTools: A Software Package for Analyzing Calabi-Yau Manifolds*, 2211.03823.

[63] J. Bezanson, A. Edelman, S. Karpinski and V. B. Shah, *Julia: A fresh approach to numerical computing*, *SIAM review* **59** (2017) 65.

[64] J. Bendavid et al., *SubMIT: A Physics Analysis Facility at MIT*, 2506.01958.

[65] M. "Kreuzer and H. Skarke, "Reflexive polyhedra in 4 dimensions." http://hep.itp.tuwien.ac.at/%7Ekreuzer/CY/CYcy.html.

[66] P. S. Aspinwall and D. R. Morrison, *Point - like instantons on K3 orbifolds*, *Nucl. Phys. B* **503** (1997) 533 [hep-th/9705104].

[67] P. Oehlmann and W. Taylor, *to appear*, .

[68] D. R. Morrison and W. Taylor, *Charge completeness and the massless charge lattice in F-theory models of supergravity*, *JHEP* **12** (2021) 040 [2108.02309].

[69] N. Raghuram, W. Taylor and A. P. Turner, *Automatic enhancement in 6D supergravity and F-theory models*, *JHEP* **07** (2021) 048 [2012.01437].

[70] D. R. Morrison and W. Taylor, *Matter and singularities*, *JHEP* **01** (2012) 022 [1106.3563].

[71] R. Nally and W. Taylor, *Work in progress*, .

[72] M. Cvetič, J. Halverson, L. Lin, M. Liu and J. Tian, *Quadrillion F-Theory Compactifications with the Exact Chiral Spectrum of the Standard Model*, *Phys. Rev. Lett.* **123** (2019) 101601 [1903.00009].

[73] W. Taylor and A. P. Turner, *Generic Construction of the Standard Model Gauge Group and Matter Representations in F-theory*, *Fortsch. Phys.* **68** (2020) 2000009 [1906.11092].

[74] N. Raghuram, W. Taylor and A. P. Turner, *General F-theory models with tuned* $(\mathrm{SU}(3) \times \mathrm{SU}(2) \times \mathrm{U}(1))/\mathbb{Z}_6$ *symmetry*, *JHEP* **04** (2020) 008 [1912.10991].

[75] W. Taylor, *On the Hodge structure of elliptically fibered Calabi-Yau threefolds*, *JHEP* **08** (2012) 032 [1205.0952].

[76] H.-C. Kim, C. Vafa and K. Xu, *Finite Landscape of 6d N=(1,0) Supergravity*, 2411.19155.

[77] L. Anderson, J. Gray, R. Nally and W. Taylor, *Work in progress*, .

[78] Y.-C. Huang and W. Taylor, *Mirror symmetry and elliptic Calabi-Yau manifolds*, *JHEP* **04** (2019) 083 [1811.04947].

[79] V. Braun, T. W. Grimm and J. Keitel, *Complete Intersection Fibers in F-Theory*, *JHEP* **03** (2015) 125 [1411.2615].

[80] J. Knapp, E. Scheidegger and T. Schimannek, *On genus one fibered Calabi-Yau threefolds with 5-sections*, 2107.05647.

[81] P.-K. Oehlmann, J. Reuter and T. Schimannek, *Mordell-Weil Torsion in the Mirror of Multi-Sections*, *JHEP* **12** (2016) 031 [1604.00011].

[82] N. Raghuram and W. Taylor, *Large U(1) charges in F-theory*, *JHEP* **10** (2018) 182 [1809.01666].

[83] V. Braun, *The 24-Cell and Calabi-Yau Threefolds with Hodge Numbers (1,1)*, *JHEP* **05** (2012) 101 [1102.4880].

[84] V. Braun, P. Candelas and X. de la Ossa, *Two One-Parameter Special Geometries*, 1512.08367.

[85] The GAP Group, *GAP – Groups, Algorithms, and Programming, Version 4.14.0*, 2024.